# The Effect of Lithology and Climate on the Morphology of Drainage Basins in Northwestern Colorado

**by**

**Sandra L. Eccker**

THE EFFECT OF LITHOLOGY AND CLIMATE
ON THE MORPHOLOGY OF DRAINAGE BASINS
IN NORTHWESTERN COLORADO


Project A-047-COLO

Agreement Nos. 14-34-0001-1106
                14-34-0001-2106

Sandra L. Eccker
Department of Earth Resources
Colorado State University

Research Project Technical Completion Report

Colorado Water Resources Research Institute
Colorado State University
Fort Collins, Colorado

Norman A. Evans, Director


June 1984

Contents of this publication do not necessarily reflect the views
and policies of the U.S. Department of the Interior nor does mention of
trade names or commercial products constitute their endorsement by
the U.S. Government.

ABSTRACT

## THE EFFECT OF LITHOLOGY AND CLIMATE ON THE MORPHOLOGY OF DRAINAGE BASINS IN NORTHWESTERN COLORADO

Mining and reclamation have had an impact on drainage-basin morphology. However, if mine operators can predict their effects on drainage development for a given lithology and climate, they can better design a stable post-mining watershed. The effects of changes in topography and vegetative cover can be evaluated by determining existing morphometric relationships for unimpacted drainage basins.

Fourteen headwater drainage basins in northwestern Colorado were chosen from three lithologies, the Mesa Verde Sandstone (5), the Browns Park Sandstone (4), and the Mancos Shale (5). For each lithology, the basins span a range of climate. For each basin, channel length and frequency, basin area, and drainage density were statistically related to select topographic, climatic, and vegetative variables. Regression equations were used to determine the effects of variability in topography and vegetative cover on drainage development for each lithology.

Drainage basins that develop on the resistant and permeable Mesa Verde Sandstone have steeper basin relief, slope (relief ratio), and channel gradient than those that

form on the less resistant Browns Park Sandstone and on the cohesive, but impermeable Mancos Shale. In addition, total channel length, total first-order channel length, and drainage-basin area are greater, and first-order channel frequency and density are less than on the other lithologies.

Conversely, the drainage basins which form on the Browns Park Sandstone and Mancos Shale are small and gently sloping with very fine textured stream networks. Although total channel length is less than on the Mesa Verde Sandstone, the higher channel frequency and smaller basin area result in a higher first-order channel density and drainage density.

For all the basins, as relief increases, basin slope and channel gradients also steepen. The steeper topography causes runoff to have greater potential energy. Consequently, more elongated and parallel streams develop, which result in narrower drainage basins. With steeper relief, channel length increases approximately equally among the first-order and higher order channels of the Mesa Verde Sandstone drainage basins. Conversely, for the Mancos Shale basins, the increase in channel length is predominantly among the first-order tributaries.

As climate becomes cooler and more moist, vegetative density increases. The greater surface resistance inhibits channel formation and elongation. Channel length and frequency decrease and drainage-basin

area increases. Over the range of climate studied,
vegetative cover is sufficiently dense to cause drainage
density to decrease with increasing precipitation and
decreasing temperature. This result confirms previously
described relationships between drainage density and the
climatic zones of the United States.

TABLE OF CONTENTS

LIST OF TABLES

Page

LIST OF FIGURES

# CHAPTER 1

## INTRODUCTION

In northwestern Colorado, coal mining has had an impact on many drainage networks. In accordance with the Federal Surface Mining Control and Reclamation Act, enacted in 1977, and the Colorado State Surface Coal Mining and Reclamation Act, approved by the Office of Surface Mining in 1980, coal companies are required to reclaim impacted drainage basins. Operators must reestablish stream channels and their floodplains so they can convey the 100 year flood and will maintain stability over the "long term." To reclaim successfully all or part of a watershed, one must know the relationships among watershed morphology and lithology, relief, climate, and vegetation.

In ideal mining situations, the Law requires the restoration of a stable post-mining topography that approximates the original pre-mining contour. However, if thick or thin overburden conditions exist, it may not be possible to design post-mining topography that will meet the above requirement. In addition, if the pre-mining topography is very steep, as it often is in Colorado, the mining company may have difficulty conforming to the Law. If the steep topography is reestablished, it may not be considered to be a stable landform. Therefore, changes in

drainage-basin topography, such as basin relief, slope, and shape, can result from mining and reclamation design.

In addition, reclaimed channels are designed to carry nonerodible streamflow velocities that have been defined as five feet or less per second for grass lined channels. Mining companies use empirical equations, such as Manning's Equation, to determine channel design. The streamflow velocity constraint results in the manipulation of channel gradient, width, and sinuosity to maintain the noneroding velocity. Such manipulation causes changes in the original channel character.

Likewise, the infiltration capacity and permeability of reclaimed spoils and topsoil are not the same as those of pre-mining soils and substrate. Mixing during the mining and reclamation processes causes the disruption of soil structure and horizontation. Consequently, reclaimed spoils usually have an infiltration rate that is lower than the pre-mining rate until vegetation becomes reestablished (Gifford, 1982). However, when native soils of low infiltration capacity are mixed with stony or sandy soils, the reclaimed spoils will have a higher infiltration rate.

Vegetative type and cover also may change as the result of mining and reclamation. More suitable species can be substituted for the native varieties, if they are of superior value for reclamation. In addition, shrubs are often very difficult to reestablish. Initially, the use of

special seed mixtures, fertilizers, and irrigation promotes rapid plant growth. However, the resulting vegetative cover is typically less than that which existed prior to mining.

The law requires mining companies to reclaim drainage basins and to reestablish stream networks so they are stable over the long term. If the mining operator restores the original drainage contour, the stream system may not be in equilibrium with the new or future conditions. However, according to Law, companies may vary channel length and frequency, basin area, and network density to provide for a stable landform. Therefore, if operators can predict the effects of changes in topography and vegetation on drainage development on a given lithology and within a given climate, they can improve their reclamation design of the stream system.

The following study is a morphometric analysis of the influence of lithology and climate on drainage-basin morphology. Several statistical relationships will be determined through the analysis of the environmental and morphometric characteristics of various study areas. These relationships will be used to predict the effects of changes in topography and vegetation on drainage development for three sedimentary lithologies.

Fourteen headwater drainage basins in northwestern Colorado were selected for morphometric analysis (Figure 1) on the basis of their accessibility, absence of structural control, and absence of man's influence. The basins are

4
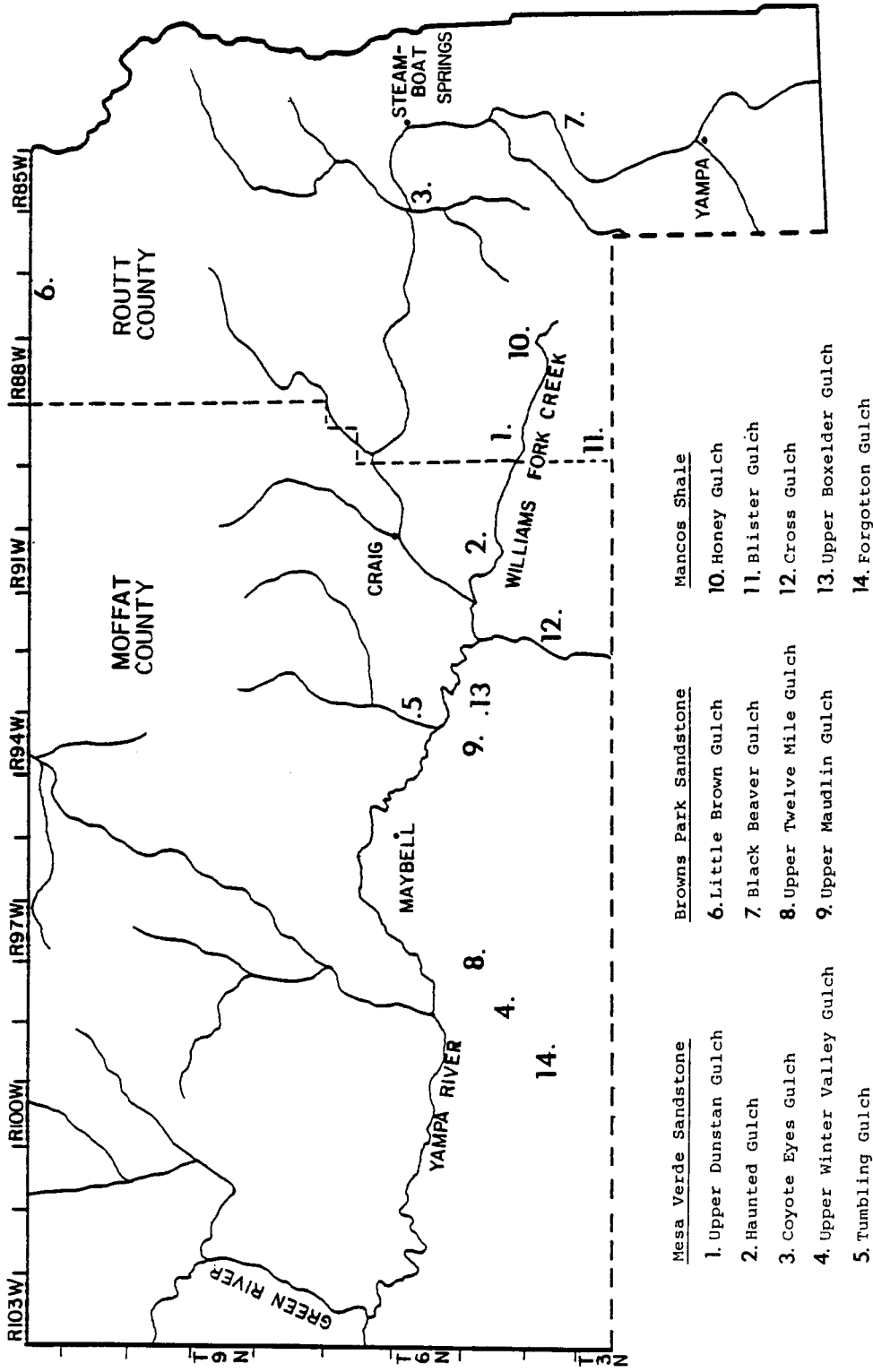


FIGURE 1. Index map of the study area.

Mesa Verde Sandstone

1. Upper Dunstan Gulch
2. Haunted Gulch
3. Coyote Eyes Gulch
4. Upper Winter Valley Gulch
5. Tumbling Gulch

Browns Park Sandstone

6. Little Brown Gulch
7. Black Beaver Gulch
8. Upper Twelve Mile Gulch
9. Upper Maudlin Gulch

Mancos Shale

10. Honey Gulch
11. Blister Gulch
12. Cross Gulch
13. Upper Boxelder Gulch
14. Forgotton Gulch

drained by ephemeral stream networks, which are
predominantly of dendritic pattern. The field sites were
selected from three lithologies, and they depict a wide
spectrum of climatic conditions in each lithology. The
lithologies are: the Mesa Verde Sandstone; the Browns Park
Sandstone; and the Mancos Shale. These and similar rock
types outcrop over much of the energy rich western United
States. Therefore, the procedures and findings may have
general application for mined-land reclamation throughout
the region.

In the field, channel longitudinal profiles and
cross sections were surveyed. Channel morphology was
described; and both channel sediment and bank soils were
sampled. Local vegetation was identified and the percentage
of ground cover was estimated. Morphometric measurements of
each field site were made from aerial photographs and
topographic maps. The measurements were compared
statistically, and the relationships between drainage-basin
morphology and lithology and climate were determined.
Finally, the effects of variability in topography and
vegetation on drainage-basin morphology were evaluated.

Although the study includes data on channel length
and frequency and basin area, it focuses on drainage
density, the total length of stream channel per unit area.
Drainage density is a morphometric variable that
characterizes the texture of a drainage network. It was
chosen as the primary variable, because it is extremely

sensitive to environmental conditions. The study also
discusses the variation in drainage density associated with
its measurement, and it presents a climatic evaluation of
northwestern Colorado, where limited meteorological
information exists.

## Variables Influencing Drainage Density
### Lithology

Lithology influences drainage density by affecting
the erosion process. The rate at which erosion proceeds
depends on the susceptibility of the surface to erosion and
the runoff intensity (Strahler, 1956). Typically, drainage
basins overlying resistant and permeable lithologies are
coarsely textured. Resistant lithologies with low runoff
intensity require more drainage area to accumulate runoff of
sufficient erosiveness to initiate a channel.

Wilson (1971) studied the relationship between
lithology and drainage density in several basins in the
central lowland of southern Connecticut. Although his field
sites are homogenous with respect to climate, vegetation,
and soil, they are underlaid with six contiguous
lithologies. Wilson found significantly lower drainage
densities among the basins overlying the more resistant
lithologies than among those overlying the weaker rock
types. Similarly, Morisawa (1959) found that even a more
resistant bed within a single lithologic unit can result in
a lower drainage density.

Strahler (1956) described contrasting drainage densities where rocks differing in erodibility and permeability are exposed side by side. He observed that resistant sandstones and limestones form large, coarsely dissected slopes whereas impervious clays and marls form very finely textured topography. Strahler described drainage densities ranging from as small as two to three in regions of massive sandstones to as high as 500 to 1,000 in badland areas comprised of weak clays. Likewise, other geomorphologists (Miller, 1953; Melton, 1957) have demonstrated that because of the difference in erodibility and permeability, mean drainage density is significantly less among stream networks that have formed in sandstone than among those that have formed in shale.

## Relief

In regions of steep topography, runoff has greater potential energy. Consequently, steep watersheds are subject to more intense rates of erosion and develop finer drainage networks than basins of low relief (Strahler, 1956). Chorley and Morgan (1962) determined that the fine drainage density of basins in the Unaka Mountains of Tennessee and North Carolina results from a high runoff intensity, caused by the steep basin relief and slope as well as the intense rainfall. Schumm (1956) found a similar relationship between drainage density and relief ratio. He presents graphically a direct power relationship between the variables.

## Climate

The influence of climate on drainage density also can be thought of in terms of its effect on runoff intensity and surface erodibility. As early as 1877, Gilbert recognized that, in dry regions, the rate of fluvial degradation is limited by the lack of available water. Increasing the amount and intensity of precipitation expedites both sediment erosion and its transport. More channels are formed and, therefore, drainage density increases. Gilbert also realized, however, that greater available moisture increases vegetative growth that, in turn, moderates runoff intensities, stabilizes sediment, and impairs its transport. The increase in vegetative cover lessens surface erodibility and causes drainage density to decrease (Melton, 1957).

In the absence of vegetation, runoff intensity and erosion are related directly to the amount and intensity of precipitation. Consequently, with increased precipitation, a greater total length of stream channel per unit area is needed to remove the additional water and sediment from the drainage basin. Many geomorphologists have related drainage density to mean annual precipitation (Chorley, 1957; Schumm, 1965; Stoddart, 1969; Abrahams, 1972; Gregory and Gardiner, 1974; Gregory, 1976; Morgan, 1976). Others have documented that rainfall intensity (Chorley, 1957; Melton, 1957; Chorley and Morgan, 1962; Seginer, 1966; Gregory and

Walling, 1968), seasonal distribution of precipitation (Gregory, 1976; Morgan, 1976), daily rainfall (Morgan, 1976), and storm frequency (Leopold, 1951) are important determinants of network density.

Rainfall intensity is strongly related to drainage density, because networks adjust to maximum rather than mean runoff (Carlston, 1966). During major precipitation events, the entire network flows and the runoff intensity is capable of overcoming surface resistance. Consequently, erosion takes place actively throughout the drainage system and results in the prevailing network and basin morphology.

Higher drainage density also often correlates with greater seasonality of precipitation (Gregory, 1976; Morgan, 1976). When annual precipitation occurs predominantly as spring and summer rainfall, it is likely to be associated with frequent and flashy thunderstorm events. Such rainfall conditions increase antecedent soil moisture and inhibit infiltration and evaporation during storms. Surface runoff is increased resulting in more erosion and higher drainage density.

Temperature, through evaporation, also influences drainage density (Abrahams, 1972; Morgan, 1976). As temperature increases, evaporation increases and more precipitation is required to produce comparable available moisture. In areas of high temperatures, rainfall evaporates rapidly from the air as well as from plant and soil surfaces. Any remaining moisture readily infiltrates

into the dessicated soils, where it is taken up by plants and transpired or it is left to evaporate. With increasing temperature, plants' consumptive water use and transpiration rates increase (Schumm, 1975). Thus, as temperature and evaporation rates increase, less precipitation is available for plant growth, although the vegetation's requirements for moisture are greater. Therefore, as temperature increases, vegetative cover decreases, resulting in enhanced surface erodibility and higher drainage density.

Vegetative Cover

The type and cover of vegetation is a very significant determinant of drainage density, especially in semiarid environments where plant growth varies markedly with differences in elevation, climate, and soil (Melton, 1957, 1958; Schumm, 1975). Vegetation lessens the amount of precipitation available for erosion by intercepting rainfall on its surfaces, where it can be evaporated, and by absorbing and transpiring water from the soil. In addition, it impedes water movement over the soil surface and provides drainage lines in the soil, thus, enhancing infiltration and permeability. Vegetation also decreases surface erodibility by protecting the soil from raindrop impact and by binding the upper horizons with its roots. Production of litter further protects the soil and retards surface runoff and erosion.

Variation of Drainage Density with Climate. The world pattern of drainage density conforms broadly to morphoclimatic zones and reflects the combined effect of climate and vegetation on network development (Figure 2). In the United States, drainage density progressively increases from areas of no precipitation through arid regions to a maximum in a semiarid environment. From its peak, drainage density successively decreases and reaches a minimum in temperate regions. Finally, in more humid areas, drainage density maintains a relatively steady value.

From arid to semiarid regions, the increase in precipitation increases surface runoff so that tributaries of ephemeral rivers incise and enlarge, and the frequency of channel segments increases. At the same time, runoff events become more frequent and less flashy. More sediment is flushed from tributary valleys during storms, resulting in aggradation in the main channels (Schumm, 1975). In the United States, drainage density reaches a maximum at approximately 11 inches of mean annual precipitation (Abrahams, 1972).

At approximately 12 inches of mean annual precipitation and 50°F mean annual temperature, a transition from desert shrubs to grass occurs. The more effective grass cover causes drainage density to decline (Schumm, 1965). As precipitation increases, vegetative cover increases further. Foliage encroaches and eliminates the smallest tributaries. Meanwhile, less sediment is eroded
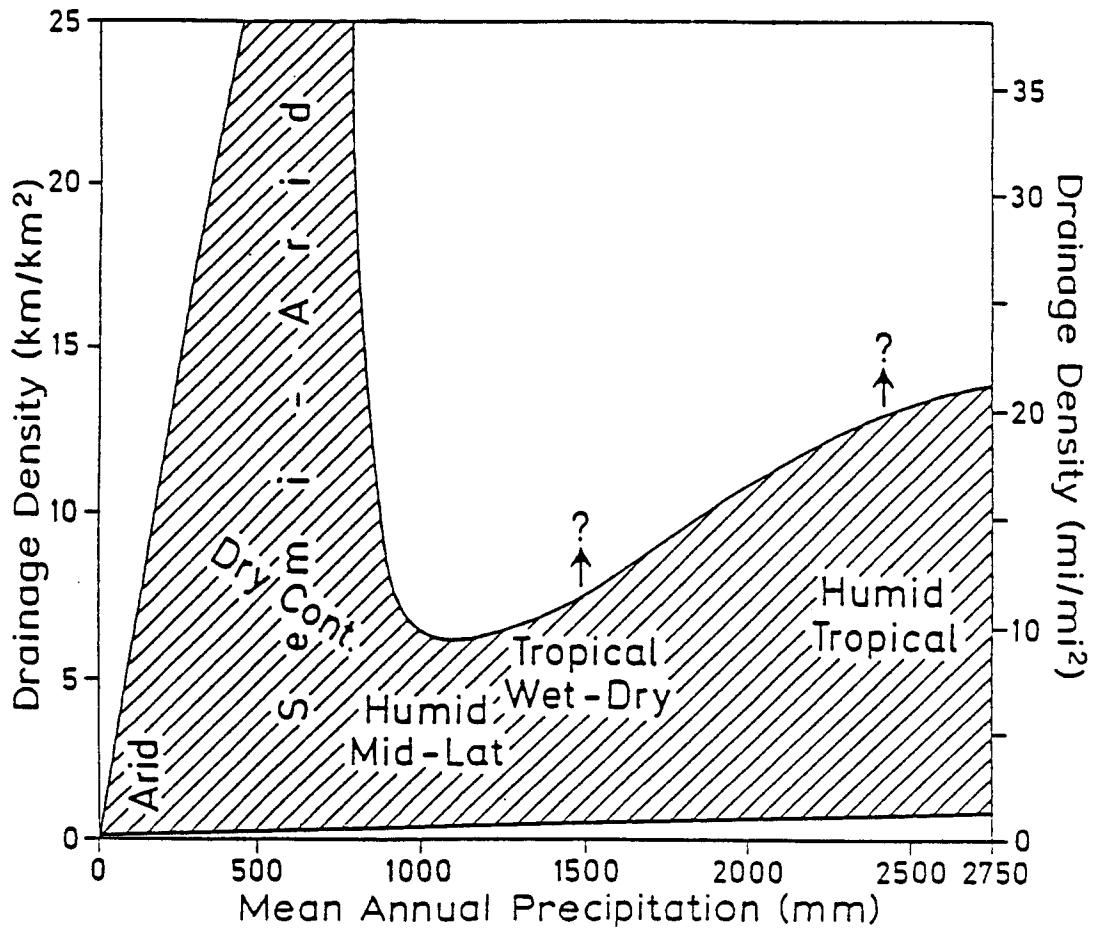
FIGURE 2. Relation between drainage density and mean annual precipitation (After Gregory, 1976).

and transported by the runoff. Lower sediment concentration in the runoff results in the enlargement of main channels (Schumm, 1975). In the United States, drainage density reaches a minimum at approximately 35 to 40 inches of mean annual precipitation (Abrahams, 1972). Above 40 inches, it remains relatively constant, even with an increase in available moisture (Abrahams, 1972).

**Conclusions**

The mechanism by which lithology and climate influence drainage density can be thought of in terms of the "critical area." Due to surface resistance, a minimum limiting area is required before flow can accumulate and become sufficiently erosive to initiate a channel (Schumm, 1956).

As runoff intensity increases, the critical area becomes smaller, because less area is required to accumulate runoff of adequate depth and velocity to start erosion (Carlston, 1963). A drainage basin that forms in a resistant lithology where there is a low runoff intensity will have a large critical area, fewer channels, and a low drainage density. On the other hand, a drainage basin that forms in an erodible lithology where there is a high runoff intensity will have a small critical area, more channels, and a high drainage density.

# CHAPTER 2

## REGIONAL DESCRIPTION OF
## NORTHWESTERN COLORADO

**Geological Setting**

## Location and Physiography

Most of the field sites are located in the Sand
Wash Basin of northwestern Colorado (Figure 1). This
shallow synclinal basin is bound on the east by the Sierra
Madre-Park Range Uplift, on the southwest by the White River
Uplift, and on the west by the Uinta Uplift (Figure 3). It
is separated from the Washakie Basin to the north, by the
Cherokee Ridge Arch and from the Piceance Basin, to the
southwest, by the Axial Basin Arch. The Sand Wash Basin is
completely occupied by the Yampa River watershed. Two of
the field sites are located just to the southwest of the
Sand Wash Basin, in the Piceance Basin. These drainages are
upper tributaries of the White River.

## Geology

The study focuses on three lithologic units: the
Mancos Shale Formation; the Mesa Verde Group; and the Browns
Park Formation, which are exposed intermittently throughout
northwestern Colorado (Figure 4). With development of the
region's coal, all three units will be disturbed by mining.

15
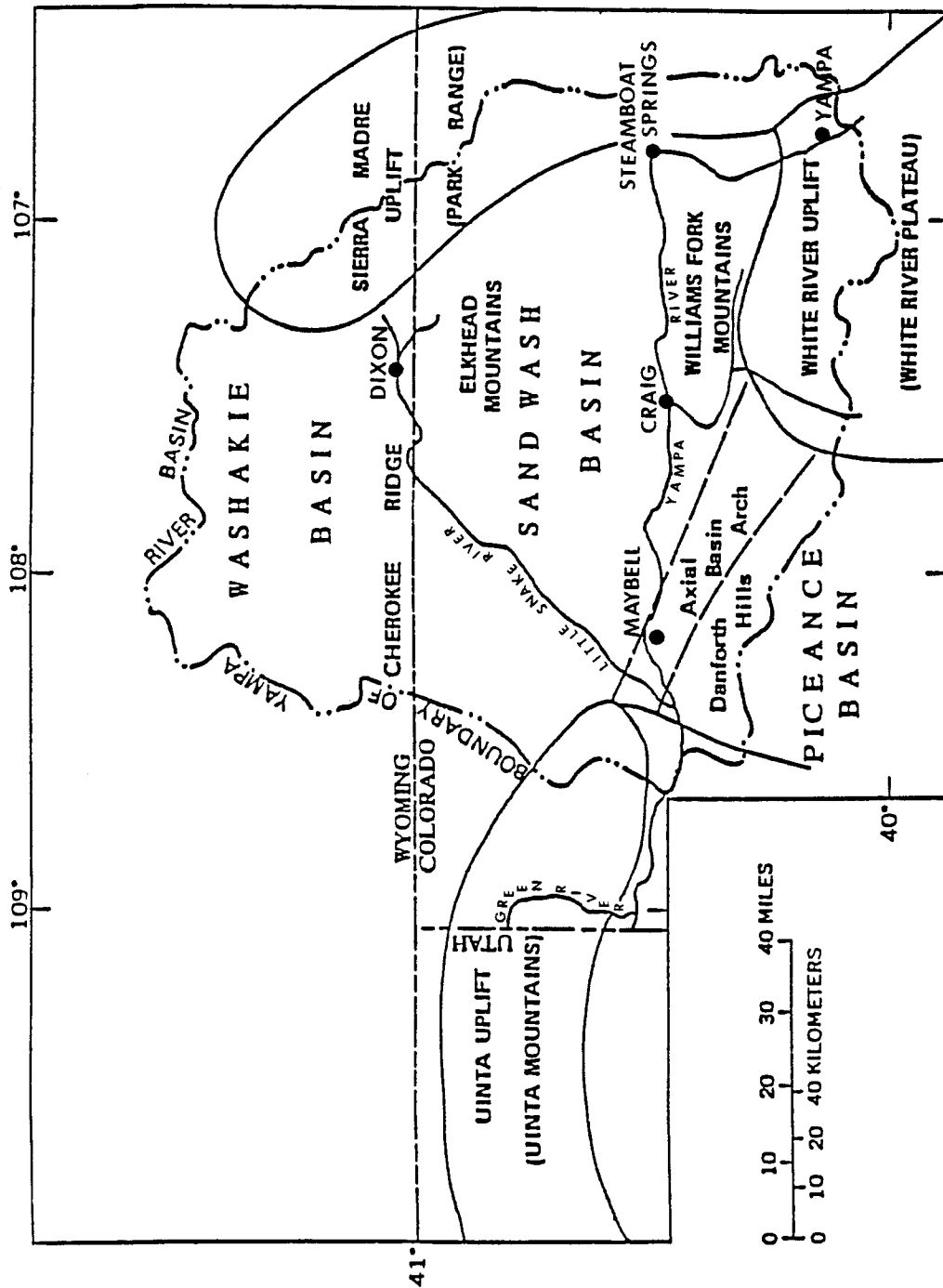


FIGURE 3. Major structural units and physiographic features of northwestern Colorado (Adapted from Steele et al., 1979).

**EXPLANATION**

QUATERNARY — Alluvium

TERTIARY
- Tbp — Browns Park Formation
- Tgw — Green River and Wasatch Formations
- Tfu — Fort Union Formation

CRETACEOUS
- Kla — Lance Formation
- Kls — Lewis Shale
- Kmv — Mesaverde Group
- Km — Mancos Shale

KЄr — Lower Cretaceous through Cambrian rocks, undivided

PЄr — Precambrian rocks, undivided

—— CONTACT

● FIELD SITES

Base from U.S. Geological Survey
1:500 000 State base map, 1969
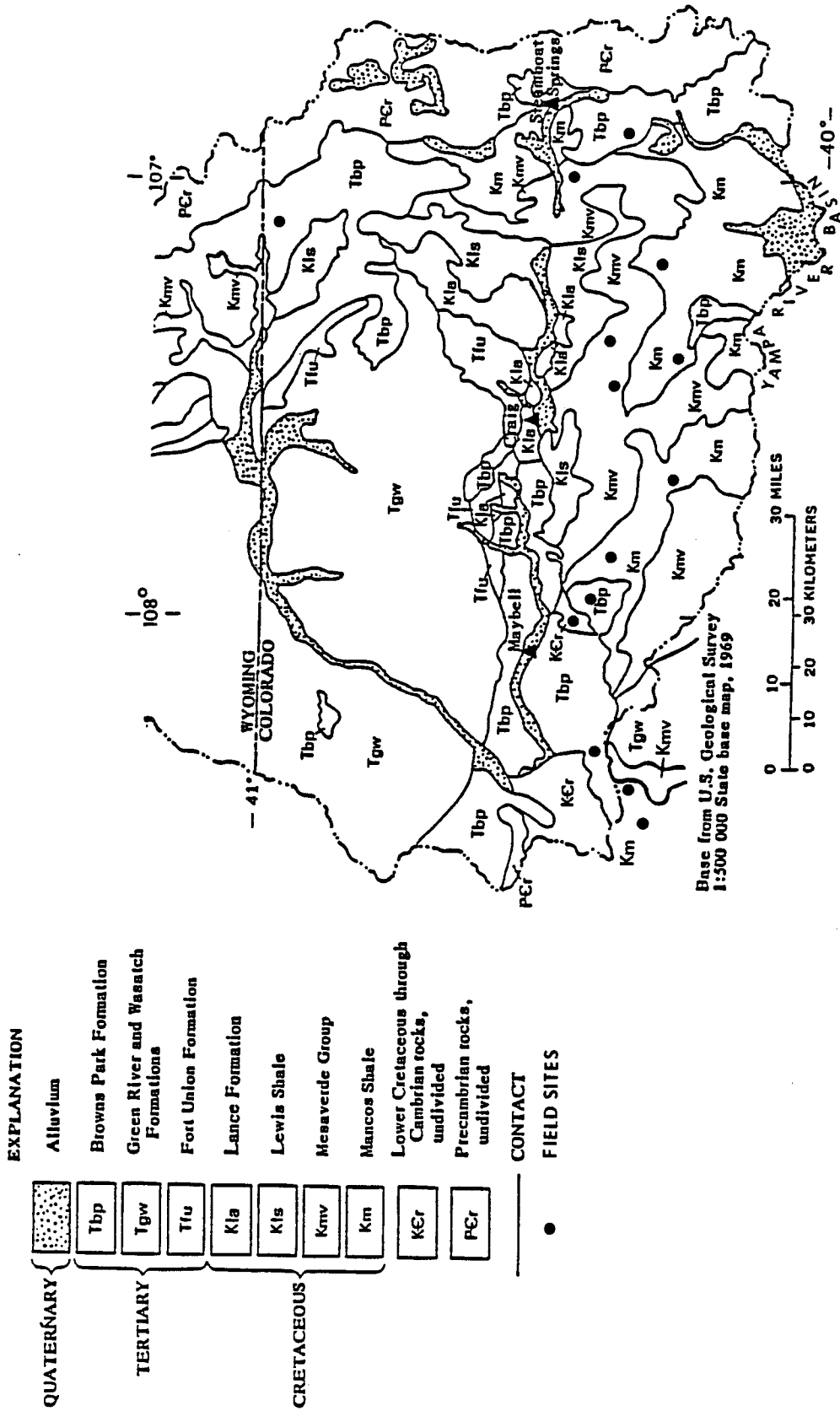
FIGURE 4. Generalized geology of northwestern Colorado (Adapted from Tweto, 1975, 1976, and Welder and McGreevey, 1966).

Mancos Shale Formation. The Mancos Shale Formation
was deposited during Upper Cretaceous time (Sears et al.,
1941). It is found over a large expanse of the western
interior, extending from central Utah to northern Colorado
to northeastern Arizona and to central New Mexico. The
Mancos Shale was deposited in a broad shallow geosyncline
that extended north and south for several thousand miles.
Throughout Upper Cretaceous time, the trough's middle,
deeper part was occupied by a shallow sea.

The Mancos Shale Formation is a distinctive
lithologic unit that is comprised predominantly of blue-gray
to dark gray sandy marine shale (Fisher et al., 1896;
Reeside, 1924). Where fresh cuts are exposed, the shale is
dark gray, limey, and bedded but lacking in pronounced
fissility. The Mancos Shale weathers to a powdery mass that
forms a sticky dark impervious clay when wet. Veinlets of
gypsum and calcite and lenses of limestone concretions are
common throughout the shale unit. In addition, beds of
sandstone and sandy zones occur. The upper limit of the
Mancos Shale Formation is bound by the Mesa Verde Group.
The contact is complicated by the intertonguing nature of
their marine and nearshore sediments.

Mesa Verde Group. The Mesa Verde Group, which
overlies the Mancos Shale Formation, was deposited during
Upper Cretaceous time (Hansen, 1975). By this time, the
Cretaceous Sea, which had dominated the region for so long,
was finally yielding to mountain building forces beginning

again in the west.  The Mesa Verde Group is comprised of marine, nearshore and terrestrial sediments, the stratigraphy of which reflects a gradually regressing intercontinental Cretaceous sea.

In northwestern Colorado, the Mesa Verde Group is divided into the lower Iles Formation and the upper Williams Fork Formation (Bass et al., 1955).

The Iles Formation is approximately 1500 feet thick.  Its basal unit is a massive yellow-gray-brown ledge-forming sandstone called the Tow Creek Sandstone Member.  The Tow Creek Sandstone is overlain by a sequence of interbedded light brown to yellowish gray fine to very fine grained sandstone, gray to light brown shale, brown carbonaceous shale, and, in the upper strata, thin coal beds.  The upper third of the Iles Formation is comprised of a shale sequence capped by a massive light brown to gray fine grained cliff-forming sandstone, known as the Trout Creek Sandstone Member.

The overlying Williams Fork Formation ranges in thickness from 1100 to nearly 5050 feet.  Its lower unit consists of approximately 1000 feet of gray sandy shale, brown carbonaceous shale, thin beds of gray-orange to yellow-gray fine grained lenticular sandstone, and several thick coal beds.  In many places, the coal bearing units form steep slopes above the Trout Creek Sandstone Member. Near the Williams Fork Mountains, these slopes are red due to the natural burning of the outcropping coal.  Above the

coal beds, interbedded thin sandstone and sandy shale units commonly form long dip slopes.

The middle unit of the Williams Fork Formation is comprised of the Twenty Mile Sandstone Member, a massive cliff forming sandstone approximately 100 to 200 feet thick. Above the Twenty Mile Sandstone, interbedded sandstone, sandy shale, dark gray shale, and coal form the Formation's upper unit.

The Mesa Verde Group thins westward and is overlain conformably by the Lewis Shale.

Browns Park Formation. The Browns Park Formation was deposited during the Oligocene and Pliocene Epochs of late Tertiary time (Buffler, 1967). It formed a vast sheet of sediment which extended from the Uinta Mountains to the Great Plains and filled the inter-montane basins of northern Colorado and southern Wyoming. At present, the Browns Park Formation is exposed throughout northwestern Colorado along the margins of post-Browns Park structural depressions and on the flanks of mountain ranges and volcanic intrusives. The Browns Park Formation lies unconformably on older rocks and generally consists of two distinct units, a basal conglomerate member and an overlying sandstone member.

In the vicinity of the field sites, the basal conglomerate member was derived from the adjacent Precambrian Park Range and was deposited in an alluvial fan environment. Conversely, the overlying sandstone member was brought from a distant southerly source by wind and streams. Its source had a complex and varied geology.

The basal conglomerate member of the Browns Park
Formation ranges in thickness from 0 to 300 feet (Buffler,
1967). Along the Park Range, it is comprised of poorly
sorted boulders, cobbles, gravel, and coarse sand. Moving
away from its source, the boulders and cobbles become less
frequent and the gravels become progressively more
rounded. The basal conglomerate member is moderately well
indurated. Calcite constitutes its primary cement with iron
oxide being the most common secondary cement. In addition,
the unit is generally poorly stratified with only occasional
crossbedding and channeling. Its upper contact with the
overlying sandstone member is sharp, except where locally
gradational.

The sandstone member is comprised of 1000 to 2000
feet of primarily eolian deposits (Buffler, 1967). It is
divided into a lower white sandstone facies and an upper
brown sandstone facies. The white sandstone facies is
comprised of well sorted subangular to subrounded, abraded,
frosted, pitted, and faceted sand grains. The unit contains
large steeply dipping crossbeds. The brown sandstone facies
consists of well sorted subangular to subrounded, abraded,
faceted sand and silt grains whose stratigraphy reflects
both floodplain and eolian environments.

## Climate of Northwestern Colorado

The climate of northwestern Colorado varies from
the arid desert basins in the west to the cool moist alpine

regions along the Continental Divide in the east. The
marked range in climate results from differences in
elevation, exposure, and topography. In addition,
microclimates of the region are influenced by local factors
such as slope, soil temperature and moisture, vegetation,
and air drainage (Marlatt, 1971)

Precipitation

Mean annual precipitation ranges from less than
nine inches in the west to more than fifty inches on the
Continental Divide (Figure 5). Several climatologists have
demonstrated that precipitation increases with elevation,
finding correlations between 0.30 (Russler and Spreen, 1947)
and 0.77 (Wymore, 1974). Other investigators have studied
the effect of site exposure and orientation, with respect to
prevailing storm paths, on precipitation (Richter, 1982;
Henry, 1919). In northwestern Colorado, winds prevail from
the west at high elevations and are largely dependent on
valley orientations at low elevations (U.S. Dept. of the
Interior, 1977). Generally, storms enter Colorado from the
southwest or west but turn southeast before reaching the
Continental Divide. The predominant storm direction in
northwestern Colorado is from the northwest (Striffler,
personal communication). However, the greatest
precipitation is not associated with a northwesterly wind
(Doesken, personal communication). The orientation of
mountain ranges is another important factor that influences
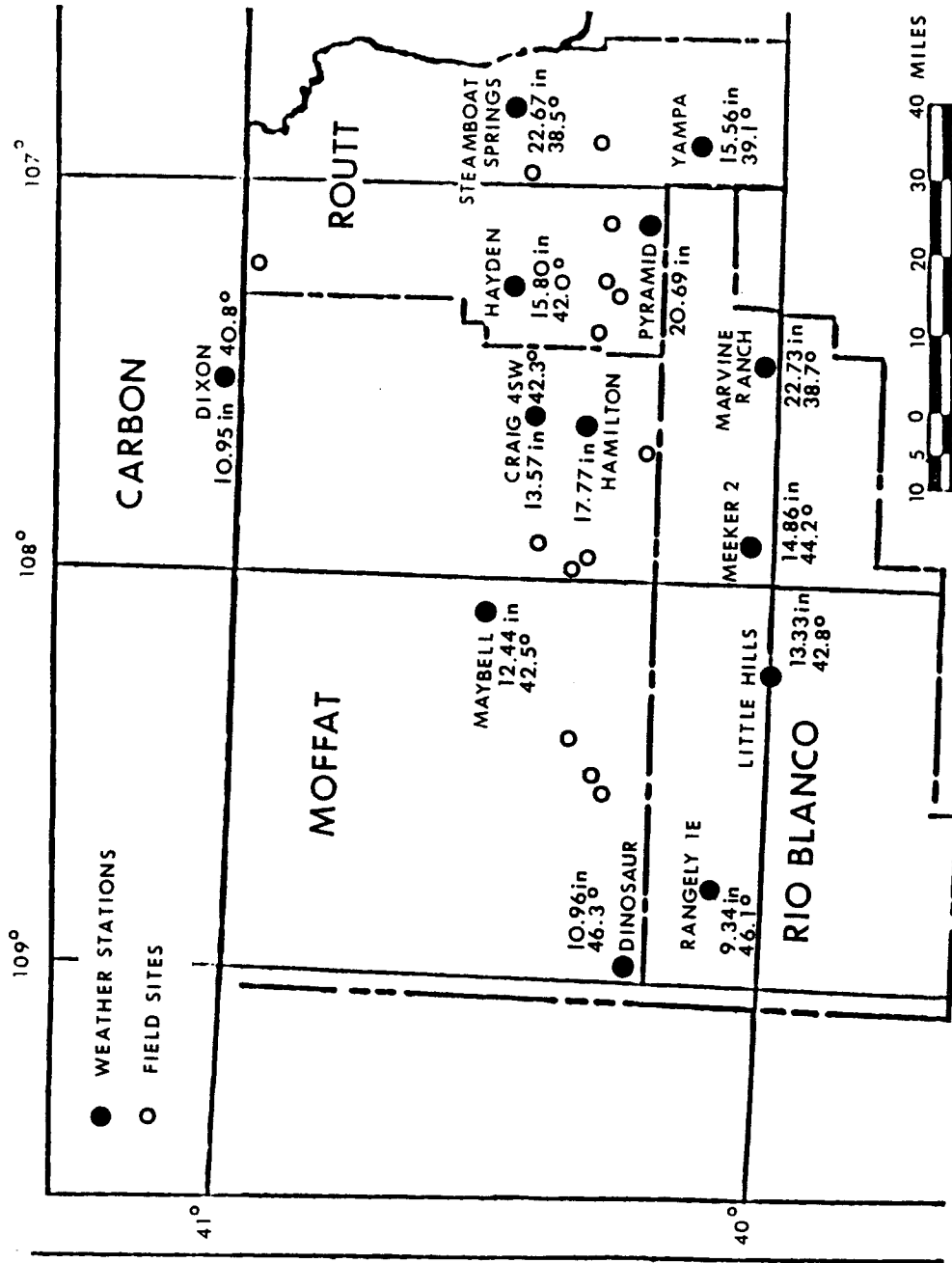
FIGURE 5. Index map of the weather stations used in the study and their twenty year (1960-1980) mean annual precipitation and temperature records.

precipitation. Barriers affect moisture flow and create rainshadows (Wymore, 1974). Finally, precipitation has been found to increase with steepening valley side slope (Smith, 1930; Maxwell, 1961; Katiyar, 1982).

Seasonal Precipitation. In northwestern Colorado, the annual distribution of precipitation is quite uniform. However, lower elevations receive a slightly larger percentage of precipitation during the summer months while higher elevations receive more precipitation during the winter months. Spring and summer rainfall occur almost entirely during cloudbursts and thunderstorms. These storms are often of high intensity with strong gusty winds, but they are usually of short duration. The overall amount of rainfall produced by each storm is generally small and localized. In the Piceance Basin nearly 80% of the storms produce less than one-quarter inch of precipitation (Richter, 1982). Generally, July and August have the greatest storm frequency and most rain falls in the afternoons.

The largest snow accumulation occurs from November through March. However, the beginning and ending of the snowfall season is not abrupt but is characterized by storms of both rain and snow. Measurable snow frequently falls as early as September and as late as June. At lower elevations, snow depth may reach two to three feet during midwinter. At higher elevations, snowpack can be expected to exceed six feet.

## Temperature

In northwestern Colorado, temperature varies on annual, seasonal, and daily time scales. The region is protected from severe cold fronts by the Continental Divide. The Divide deflects low pressure storm systems to the north and south of its mountains while holding high pressure systems over the region for days. The result is moderate temperatures, abundant sunshine, clear days, and large diurnal temperature variations.

Mean annual temperatures within the region range from over 46.5°F in the southwest to less than 39.0°F in the southeast. In the high mountainous areas, such as along the Continental Divide, mean annual temperatures generally are less than 32.0°F (Figure 5). The temperature of a given site is determined by several factors including latitude, elevation, local topography, and exposure. Latitude determines the intensity and duration of solar radiation along a given meridian. However, clouds, water vapor, dust, and turbidity will alter the solar flux within a region (Marlatt, 1971). A definite lapse rate or decrease in temperature with increasing elevation exists in northwestern Colorado. Calculated lapse rates vary seasonally from -2.34°F per 1000 feet elevation in the winter to -6.56°F per 1000 feet elevation in the summer (Wymore, 1974).

Surface temperatures are strongly influenced by local topography, especially with respect to exposure.

North facing slopes in narrow valleys may be shaded one to two hours longer each day. Consequently, adjacent to the surface, the temperature often differs by as much as 20 to 30°F between north and south facing slopes (Marlatt, 1971). In addition, wind is very sensitive to net radiation changes. The diurnal heating of mountain slopes causes an up valley air flow on sunny days, when the higher elevations heat more rapidly than the valleys, and a down valley air flow on clear nights, when the higher elevations cool more rapidly than the valleys. More pronounced valley circulation will be found on south facing slopes, because a sunny mountain slope is likely to have a wider daily temperature range than a shaded slope. Differences in the climatic conditions between northern and southern exposures are more marked at high elevations, where the sunlight is more intense, than at low elevations.

Seasonal Temperature. In northwestern Colorado, July is typically the warmest month, with mean temperatures ranging from the mid to upper 50's (°F) in the higher elevations to the mid 70's (°F) at lower elevations. Conversely, January is usually the coldest month with mean temperatures ranging from the mid teens to low 20's (°F), depending on the location.

The annual frost free period varies considerably within the region. Locations in the southwest experience the longest frost free period, over 125 days, while at high elevations, there may be only a few days between occurrences of freezing.

## Evapotranspiration

Evapotranspiration (ET) is the rate at which water is transferred into the atmosphere from vegetated land surfaces (Rosenberg, 1974). ET rates are controlled by meteorological factors such as radiation, wind, temperature, and humidity; soil factors such as soil moisture tension and soil moisture conditions; and plant physiological factors such as root range, stomatal aperture, and intersystem expediency of water movement.

In northwestern Colorado, evaporation and transpiration studies are scarce. However, National Weather Service data, from several locations along the Colorado River drainage, indicate that evaporation rates decrease with elevation, as temperatures become cooler. In addition, the data demonstrate that evaporation rates are greatest during June and July when mean monthly temperatures are highest and cloud cover is least. Evaporation losses from small ponds and reservoirs, within the region, range from 17 to 20 inches annually (Steele et al., 1979). Data from other areas within Colorado, with comparable climates, indicate that average evaporation rates within northwestern Colorado would range from 17 to 55 inches annually (Heil, 1976).

## Vegetative Cover

Plant communities vary from site to site, because of differences in topography, climate, and geology. Elevation, aspect, temperature, and the amount and timing of precipitation, as well as, soil depth and available moisture content influence the vegetative type and density of a given locality.

In semiarid regions, plant growth is often limited by the lack of moisture. As moisture increases, there is more opportunity for a greater number of plants, for each plant to reach maximum development, and for the growth of larger species (Langbein and Schumm, 1958). Tew (1969) related the consumptive water use of several species to their top-growth and root system production. Bennett et al. (1964) related the amount of available soil moisture directly to vegetative yields for forage species.

When adequate moisture is available, the rate of plant growth and the abundance of vegetation vary with temperature. Different species vary widely in their response to temperature, having their own conditions for minimum, optimum, and maximum growth. Generally, in the spring, if moisture isn't limiting, the period of maximum growth coincides with the period of maximum temperature (McGinnies et al., 1944).

Plant resistance to extremely low temperatures also varies. There are marked differences between species, between individuals of the same species, and even between

buds on the same branch. A plant's resistance depends on the climatic exposure it has had during its lifetime and the age of its tissue. Old plant tissues are more resistant than newly formed tissues (Robbins, 1917).

The close relationship between climate and vegetation produces distinct plant communities found throughout northwestern Colorado. The following description of the region's dominant vegetative types was adapted from the Bureau of Land Management Manuals 9160-9162 and Tiedeman (1978).

In northwestern Colorado, conifer grow in the highest elevations, especially on north and northwest facing slopes. These areas have the highest mean annual precipitation, coolest soils, and greatest snow accumulation. At slightly lower elevations, 7500 to 8500 feet, aspen communities develop. Aspen grow on more gentle and protected slopes than conifer, particularly on northwestern and eastern aspects. On lower elevation sites, aspen occur where the environment is locally mesic, such as in snowdrift areas. Typically, aspen grow where soils are deep. The smallest trees are found on the shallowest soils. Aspen communities often form a transition zone between conifer and mountain shrub vegetation.

Mountain shrub communities develop on moderately deep well drained soils, where moisture is adequate throughout the spring and early summer. Scrub oak, often associated with woods rose and columbine, grows extensively

on steep east facing slopes, where soils are relatively deep
and moist. On warmer drier sites scrub oak loses its
dominance to serviceberry. Serviceberry, in association
with snowberry, is found frequently along shallower slopes,
especially near stream valleys.

Sagebrush grows over a broad range of climatic
conditions. Tiedeman (1978) described big sagebrush
communities occurring from 5700 to 9000 feet elevation, and
encompassing a mean annual temperature range from 40.0 to
46.0°F and a mean annual precipitation range from 10 to 26
inches. Typically, sagebrush occurs on fairly level open
terrain and often on alluvial floodplains. Its soils are
fine grained, well drained, and always practically free of
alkali. As its soils become drier and shallower, sagebrush
becomes smaller.

Although sagebrush is more resistant to wind than
most of the mountain shrub species, it does not occur on
extremely windy ridgetops or where soils are rocky or
shallow. Wind accentuates climatic extremes by removing the
protective cover of snow, in the winter, and by creating a
more dessicative effect in the summer. When soils become
less then 20 inches deep, water holding capacity and rooting
depth cause stress on sagebrush growth.

On stony outcrops and where soils are shallow,
pinyon pine and juniper occur in place of sagebrush.
Generally, pinyon pine and juniper do not reach the high
elevations that sagebrush does, and when they are found at

high altitudes, they occur on southern exposures. Even
small patches of the trees are reliable indicators of
locally warm habitats. In addition to along ridgetops,
pinyon pine and juniper often occur in gullies where more
moisture is available.

At the lowest elevations and locations of least
precipitation, greasewood and saltbush communities
develop. Greasewood and saltbush grow extensively over
broad alluvial stream bottoms, on older stream terraces and
across alkaline flats. Frequently, their soils are more
finely textured and less well developed than those of
sagebrush. In addition, they are high in salt concentration
often because of a locally high watertable. Greasewood is
known to recycle salts to the soil surface by dropping
leaves high in alkaline. In this manner, the encroachment
of sagebrush is inhibited. Saltbush occurs on drier better
drained soils that are slightly less alkaline than those
supporting greasewood stands.

Grasslands develop on numerous sites, from wet
mountain meadows to dry rocky hillsides. The variety and
dominance of grass species depends substantially on the
site's elevation and exposure. Tew (1969) demonstrated that
timothy and orchard grasses grow best on cool north facing
slopes, at high elevations; tall oatgrass, on the other
hand, is better adapted to southeastern and eastern aspects,
at slightly lower elevations. On south facing slopes and at
the lowest elevations, he found wheat and smooth brome

grasses dominate.  Similarly, various sedge grasses are most abundant in wet areas and cheatgrass and winter annuals become better established following years of high autumn precipitation.

# CHAPTER 3

## COLLECTION OF DATA

### Procedure and Problems

For the study, fourteen headwater drainage basins were chosen in northwestern Colorado (Eccker, 1984). Each basin contains an ephemeral stream network, primarily of dendritic pattern. The field sites were selected to span a range of climate in three lithologies. Areas with marked structural control or which had been severely impacted by man's activities were avoided. Due to the prevalence of ranching within the region, it was also necessary to avoid sites where the native vegetation had been effected by overgrazing, the introduction of forage species, irrigation, and the elimination of brush and weeds through the use of pesticides and disking. In addition, stream networks dammed to provide stockponds and control sediment were excluded. Since most of the sites are located on private land, accessibility was also a major concern. In some cases, difficulty arose in finding a site meeting all of the above requirements.

After selecting the field sites, the drainage networks were delineated and several morphometric variables were calculated using enlarged aerial photographs and

topographic maps. The drainage networks could be delineated in detail using the enlarged aerial photographs. Probably the biggest advantage of aerial photography is that the network can be viewed in three dimension. Also, aerial photographs show subtleties of tone, texture, and vegetation, which indicate stream channels as well as simple changes in contour. In addition, aerial photographs allow one to determine if a change in contour is caused by a stream channel or reflects a structural feature. Finally, networks delineated from aerial photographs do not rely on a cartographer's interpretation and accuracy.

The delineations from the aerial photographs would have been improved if color infrared photography was used. Color infrared photography has better contrast between vegetated and bare ground and higher resolution of small channels. In addition, if the photographs had been taken in late spring or early fall, when snow is absent but vegetation is minimal, and at midday, when shadows are short but lighting is bright, the networks could have been delineated with greater accuracy. Also, photographic distortion would have been reduced if the photographs were taken while flying up the axis of the basin, with the center of the basin falling in the center of each aerial photograph. Finally, if the photographs were taken the year of the study and at larger scales, the delineations would have been improved.

In addition to drainage-basin morphology, the climate, soils, and vegetation at the field sites were characterized. Initially, the climate of the field sites was evaluated using an isohyetal map of northwestern Colorado. However, the map employed a limited number of weather stations and presented only a general portrayal of the regional climate. Therefore, a more precise method of extrapolating data from the weather stations to the field sites was devised. Although the method was successful, it resulted in a smaller range of climate than what was initially determined, especially among the Browns Park Sandstone basins. In the latter case, the small range caused poor results among several of the determined relationships.

In northwestern Colorado, information about soils and vegetation is very limited. The Soil Conservation Service has not finished the soil survey for either Routt or Moffat Counties. In addition, vegetation surveys were conducted at small scales and, consequently, vegetative type and cover data is very general.

Finally, morphometric variables for the field sites were compared using a standard student's t-test. In addition, simple and multivariate regression analyses were used to evaluate the effects of relief, climate, and vegetation on drainage-basin morphology. The statistical methods are limited, because the sites were not selected randomly. In addition, grouping the data became essential

to its correct interpretation. Consequently, the sample sizes are too small to give conclusive results.

Drainage network and basin dimensions vary with stream order (Horton, 1945; Morisawa, 1959; Fok, 1971, Gregory and Walling, 1973). Consequently, it was necessary to account for the variation created by Little Brown Gulch, which is not a fifth-order drainage basin. When the basin is included in regression analyses, order is included as as additional variable. Multivariate regression equations are used to determine and eliminate the amount of variation created by order from the relationships being investigated. In addition, sum of squares tables are described to indicate the influence of order on the relationships.

Although the selection of morphometric variables is limited, considerable information pertaining to drainage basin development and response to change is contained in these variables. Other variables that may have improved the analysis and that would have helped significantly in understanding the drainage basins' morphologies include 1) valley side slope; 2) the state of basin development, as measured by the hypsometric integral (Strahler, 1952); 3) hydraulic characteristics such as channel width and depth; and 4) hydrologic characteristics such as mean annual discharge and mean annual peak discharge.

**Field Measurements**

At each field site, the longitudinal profile and several cross sections were surveyed along the main channel and, the channel sinuosity and morphology were described. Tributaries, headcuts, slumps, and bars were located along the channel profile.

At each cross section, channel sediment and bank soil samples were taken. Later, the samples were sieved and their grain size distributions determined. The bank samples were used in conjunction with the U.S.D.A., Soil Conservation Service Range Site Descriptions and the Soils Map of Colorado (Heil, 1976 and Heil et al., 1977) to classify and to characterize qualitatively local soil depth, porosity, water holding capacity, available moisture, erodibility, potential for plant growth, and rates of infiltration, permeability, and drainage. In addition, the percentage of silt and clay in both the channel and bank samples was used as a measure of sediment cohesion.

Local vegetation was identified, and its height, dominance, and location were described. Grasses were identified with the aid of the Soil Conservation Service Range Site Descriptions. Although crown cover was estimated in the field, the percentages used throughout the study were determined by the Soil Conservation Service. At each site, the two values differed by less than 10%.

## Morphologic Measurements

The field site drainage networks were delineated from 1:24000 normal color aerial photographs using a Bausch and Lomb Stereo Zoom Transfer Scope. Each photograph was scaled precisely, using corresponding 1:24000 and 1:62500 topographic maps, and then enlarged approximately six times. Thus, the scales were increased to approximately 1:4000. The enlargement greatly improved resolution and enabled first-order stream channels to be seen on the photographs. All of the networks were mapped while viewing them stereoscopically. This helped to eliminate photographic error caused by parallax displacement (Lillesand et al., 1979).

Specific criteria for determining first-order stream channels were chosen to maintain consistency among the networks portrayed. A first-order stream, by definition, should be the smallest unbranched channel on the ground. However, when measuring drainage density from aerial photographs or maps, the interpreter must decide where first-order channels begin. When measuring drainage density from aerial photographs, first-order channels have been defined on the basis of permanency (Strahler, 1956; Melton, 1957), continuousness (Melton, 1957; Morisawa, 1959; Sotiriadis and Astaras, 1977), orientation and gradient (Melton, 1957; Abrahams, 1972; Sotiriadis and Astaras, 1977), cross sectional geometry (Melton, 1957; Maxwell, 1961; Sotiriadis and Astaras, 1977), and evidence of scour

(Morisawa, 1959; Sotiriadis and Astaras, 1977). When the criteria employed are not consistent, entirely different drainage densities are measured. For example, some interpreters require a first-order channel to be permanent and continuous with trapezoidal cross section and showing evidence of scour while others include steep grassy swales or ephemeral rills that may contain sheet flow after a storm event.

In semiarid regions, grassy swales often entrench and become active channels. Therefore, in this study, a first-order stream channel was defined as an unbranched linear depression with converging valley sides. It did not need to contain a distinct channel, but the gradient of its axis had to be less than the slope of the adjacent hillside. Grassy swales, where flow is concentrated after a precipitation event, and undulations between the active headcuts of discontinuous gullies, where there is no evidence of scour, were included. Rills, however, were not.

Basin order, channel length and number, and basin area were measured from the drainage networks delineated from the enlarged aerial photographs. The measurements were used to calculate the frequency and density of first-order channels, drainage density, and basin circularity.

Topographic maps were used to determine the elevation of the field sites. The elevations were calculated by weighting the mean elevation of two successive contour lines by the basin area between them. In addition,

basin relief and slope (relief ratio) and channel gradient were measured from the maps.

**Climatic Data**

Mean Annual Precipitation

The precipitation pattern of northwestern Colorado is influenced by elevation, exposure, and local topography. Consequently, interpolation between weather stations across diverse landscapes is likely to result in erroneous precipitation estimates. Unfortunately, there are few weather stations in this region and, consequently, they are located far apart. Therefore, to extrapolate precipitation data to the field sites, a multivariate regression analysis was used.

Variables that influence mean annual precipitation were regressed against the mean annual precipitation records of the proximal weather stations. Thirteen stations were included in the analysis (Figure 4). They are situated along large perennial rivers, either on the relatively flat bottom land or, a short distance up the surrounding mountain slopes, in areas of moderate steepness. A record length of twenty years, 1960 to 1980, was chosen to keep the time period approximately uniform for all of the stations, while including a complete weather cycle (Richter, 1982).

For the regression analysis the variables, elevation, exposure, and local topography, represented by the distance to the crest of the nearest barrier in the

storm direction and the distance to the crest of the Continental Divide, were employed.  They are defined as follows:

Elevation: Height above sea level, expressed in feet.

Exposure:  Direction of watershed exposure or aspect.  A basin with a northerly exposure opens towards a lower elevation in a northerly direction, i.e., faces north.  Expressed in number of degrees away from the predominant storm direction, N 45° W. Exposure may be measured clockwise or counterclockwise from N 45° W.  The maximum exposure possible is 180°.

Distance from a Northwestern Barrier:  The shortest distance in a northwesterly direction between the station and the crest of the nearest orographic barrier.  The latter is defined in terms of relative elevation with the station.  If the station is less than 8000 feet elevation, an orographic barrier must exceed the station by 725 feet in elevation.  If the station is greater than 8000 feet elevation, an orographic barrier must exceed the station by 600 feet elevation. The proceeding elevation limits were chosen subjectively, by determining the minimum elevation of significant orographic barriers within a reasonable distance of the weather stations.  Distance from a northwestern barrier is expressed in miles.

Distance from the Continental Divide: The shortest distance

between the station and the crest of the

Continental Divide, expressed in miles.

The data for the weather stations are presented in Table 1

and the determined regression equations are included in

Table 2.

Mean Annual Precipitation and Elevation. Mean

annual precipitation is most closely correlated with

elevation, having an $R^2$ of 0.53. In northwestern Colorado,

there is an increase of 3.90 inches of precipitation per

1000 feet rise (Table 2). This value agrees with the

observations of Henry (1919) who found an increase of

roughly 3.30 inches of precipitation per 1000 feet rise for

both Utah and Colorado. The linear relationship between

mean annual precipitation and elevation is strong at lower

elevations. Above 6770 feet elevation, variance may be

introduced by the existence of a maximum precipitation zone

above which precipitation decreases with increasing altitude

(Henry, 1919) or because other variables affecting

precipitation become relatively more influential. In

addition, departure from the linear relationship may be

attributable to difficulties in measuring snowfall (Wilson,

1954), which would be more important at higher elevations

where a larger percent of precipitation occurs as snow.

Mean Annual Precipitation and Exposure. The

relationship between exposure and mean annual precipitation

has an $R^2$ of only 0.15. Generally, as the exposure deviates

TABLE 1
Weather Station Data

| Weather Station | County | Latitude | Longitude | Elevation (feet) | Exposure (°) | Distance From A Northwestern Barrier (mi.) | Distance From The Continental Divide (mi.) | Mean Annual Precipitation (in.) | Mean Annual Temperature (°) |
|---|---|---|---|---|---|---|---|---|---|
| Pyramid | Routt | 40°14' | 107°05' | 8009 | 102 | 1.2 | 26.8 | 20.69 | ---- |
| Yampa | Routt | 40°09' | 106°54' | 7892 | 76 | 7.3 | 21.1 | 15.56 | 39.1* |
| Marvine Ranch | Rio Blanco | 40°02' | 107°28' | 7800 | 17 | 6.8 | 51.8 | 22.73 | 38.7 |
| Steamboat Springs | Routt | 40°30' | 106°50' | 6770 | 45 | 5.5 | 9.1 | 22.67 | 38.5 |
| Craig 4SW | Moffat | 40°27' | 107°36' | 6440 | 14 | 21.5 | 49.6 | 13.57 | 42.3 |
| Hayden | Routt | 40°29' | 107°15' | 6375 | 92 | 3.4 | 30.7 | 15.80 | 42.0 |
| Dixon, Wyo. | Carbon | 41°02' | 107°32' | 6360 | 126 | 51.6 | 29.5 | 10.95* | 40.8* |
| Meeker No. 2 | Rio Blanco | 40°02' | 107°55' | 6347 | 174 | 0.8 | 72.9 | 14.86 | 44.2 |
| Hamilton | Moffat | 40°22' | 107°37' | 6230 | 90 | 4.9 | 48.9 | 17.77 | ---- |
| Little Hills | Rio Blanco | 40°00' | 108°12' | 6140 | 119 | 40.4 | 87.9 | 13.33 | 42.8 |
| Dinosaur Natl. Monument | Moffat | 40°14' | 108°58' | 5921 | 94 | 11.9 | 125.7 | 10.96* | 46.3* |
| Maybell | Moffat | 40°31' | 108°05' | 5914 | 77 | 9.2 | 74.5 | 12.44* | 42.5 |
| Rangely IE | Rio Blanco | 40°03' | 108°46' | 5290 | 86 | 31.5 | 116.4 | 9.34 | 46.1 |
| $R^2$ | | | | 0.53 | 0.15 | 0.37 | 0.41 | 0.72 | |
| Sum of Squares (%) | | | | 74.2 | 5.1 | 14.3 | 6.4 | 100.0 | |
| $R^2$ | | | | 0.68 | 0.21 | | | | 0.71 |
| Sum of Squares (%) | | | | 97.0 | 3.0 | | | | 100.00 |

* The Weather Station Record Is Less Than 20 Years.

TABLE 2
Regression Equations Describing The Relationships
Between Climatic Variables And Mean Annual
And Mean Monthly Precipitation

| Mean Annual Precipitation | $R^2$ |
|---|---|
| M.A. PPT = -10.0 + 0.0039(E) | 0.53 |
| M.A. PPT = 18.8 - 0.0389(X) | 0.15 |
| M.A. PPT = 17.9 - 0.1630(NW) | 0.37 |
| M.A. PPT = 19.9 - 0.0779(CD) | 0.41 |
| M.A. PPT = 8.52 + 0.0018(E) - 0.0172(X) - 0.0986(NW) - 0.0350(CD) | 0.72 |

| Mean Monthly Precipitation | |
|---|---|
| January M.Mo. PPT = 1.78 + 0.0001(E) -0.0037(X) - 0.0122(NW) - 0.0091(CD) | 0.66 |
| February M.Mo. PPT = 0.314 + 0.0002(E) - 0.0032(X) - 0.0100(NW) - 0.0043(CD) | 0.64 |
| March M.Mo. PPT = 0.255 + 0.0002(E) - 0.0017(X) - 0.0123(NW) - 0.0006(CD) | 0.57 |
| April M.Mo. PPT = 1.69 + 0.0000(E) - 0.0011(X) - 0.0102(NW) - 0.0039(CD) | 0.50 |
| May M.Mo. PPT = 1.39 + 0.0001(E) - 0.0016(X) - 0.0065(NW) - 0.0016(CD) | 0.36 |
| June M.Mo. PPT = -0.0963 + 0.0002(E) + 0.0006(X) - 0.0049(NW) + 0.0006(CD) | 0.69 |
| July M.Mo. PPT = -0.707 + 0.0003(E) +0.0017(X) - 0.0020(NW) -0.0003(CD) | 0.64 |
| August M.Mo. PPT = 0.0242 + 0.0002(E) - 0.0005(X) - 0.0079(NW) - 0.0018(CD) | 0.71 |
| September M.Mo. PPT = 0.102 + 0.0002(E) - 0.0006(X) - 0.0018(NW) - 0.0008(CD) | 0.66 |
| October M.Mo PPT = 0.713 + 0.0001(E) - 0.0011(X) - 0.0089(NW) + 0.0005(CD) | 0.60 |
| November M.Mo. PPT = 1.44 + 0.0000(E) - 0.0017(X) - 0.0097(NW) - 0.0047(CD) | 0.67 |
| December M.Mo. PPT = 1.81 + 0.0001(E) - 0.0037(X) - 0.0123(NW) - 0.0080(CD) | 0.67 |

M.A. PPT = Mean Annual Precipitation
M. Mo. PPT = Mean Monthly Precipitation
E = Elevation
X = Exposure
NW = Distance From A Northwestern Barrier
CD = Distance From The Continental Divide

from the predominant storm direction, gage catch decreases
at a rate of approximately 0.20 inches per five degrees
(Table 2).

Mean Annual Precipitation and Local Topography.
The relationship between the distance from the nearest
northwestern barrier and mean annual precipitation has an $R^2$
of 0.37. As the distance between the station and barrier
increases, precipitation decreases at a rate of about 1.63
inches per 10.0 miles (Table 2).

Distance from the Continental Divide correlates
fairly well with mean annual precipitation, having an $R^2$ of
0.41. As the distance between the station and the
Continental Divide increases, precipitation decreases at a
rate of approximately 1.95 inches per 25.0 miles
(Table 2). Stations within fifty miles of the Continental
Divide showed the greatest variance. Generally, these are
also high elevation stations, which may explain some of
their deviation. Distance from the Continental Divide and
elevation have an inverse linear relationship with an $R^2$ of
0.44.

Mean Annual Precipitation and The Variables.
Regressing the four variables simultaneously with mean
annual precipitation resulted in a total $R^2$ of 0.72
(Table 2). The relative importance of each variable to the
correlation is indicated by the sum of squares analysis
(Table 1). Figure 6 is a plot of the measured mean annual
precipitation against the predicted mean annual
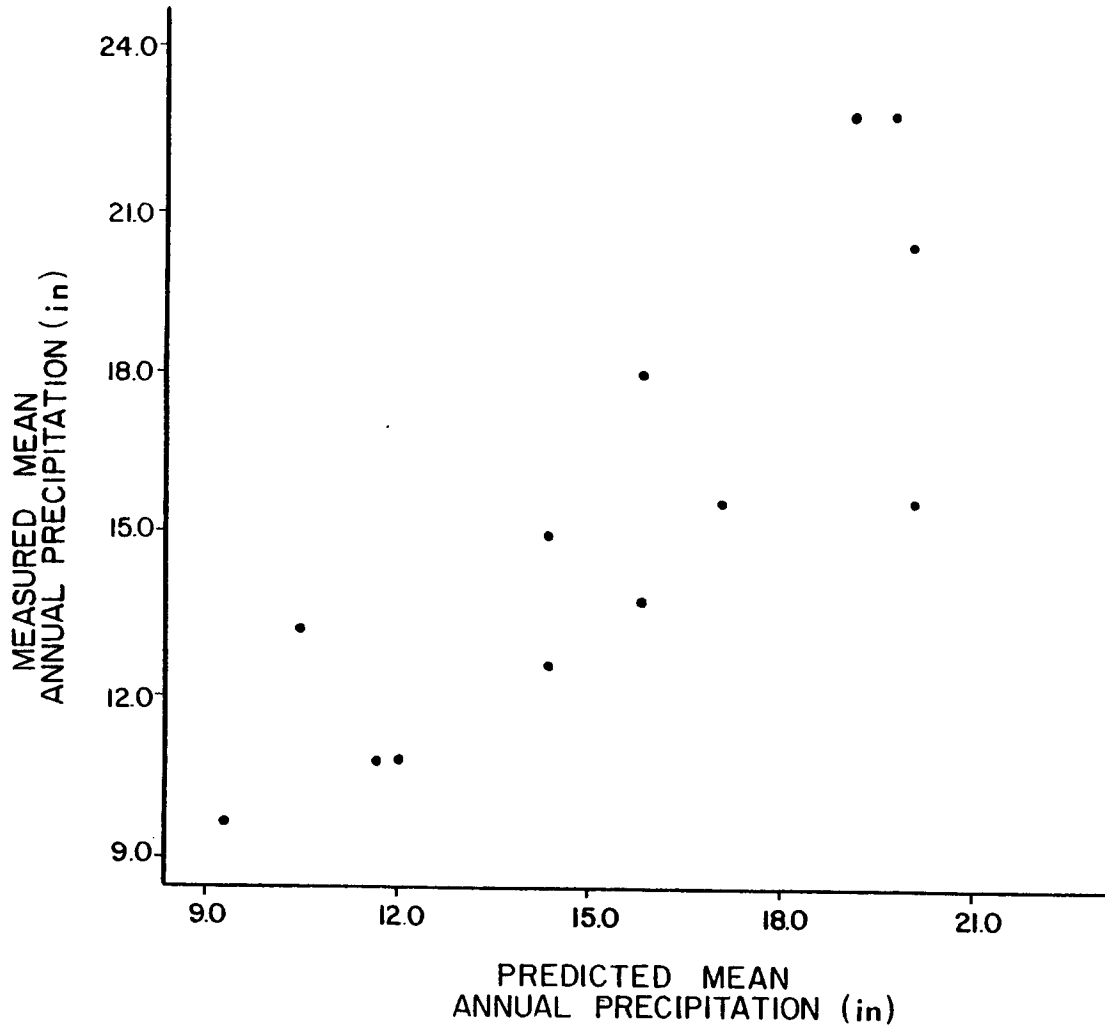
FIGURE 6. A plot of the measured mean annual precipitation against the predicted mean annual precipitation for each weather station.

precipitation for each station. Yampa is the greatest outlier with an actual mean annual precipitation of 15.56 inches and a predicted mean annual precipitation of 20.01 inches. Little Hills is a minor outlier with a gaged mean annual precipitation of 13.33 inches and a predicted mean annual precipitation of 10.47 inches.

The Yampa Station deficiency in mean annual precipitation can be analyzed by a plot of mean monthly precipitation for both Yampa and Steamboat Springs (Figure 7). Steamboat Springs receives approximately 22.67 inches of precipitation annually. As illustrated by the plot, the disparity in the Yampa Station's mean annual precipitation is largely attributable to a lack of snowfall. Yearly snowfall in Steamboat Springs is approximately 164 inches whereas, in Yampa, it is only 101 inches. The major reason for Yampa's snowfall deficit is that the station is located in a rainshadow created by the Flat Top Mountains and, therefore, is downwind of most major snowfall events.

In addition, some explanation may reside in the Yampa weather station's location. Wilson (1954) found that most variation in snowfall catch and water equivalent measurement is attributable to differences in local exposure of the observation site. Optimum stations are located where wind and snowfall interception are minimized, such as where shelter is provided by nearby trees and/or concave topography. The Yampa gage may be exposed to excessive
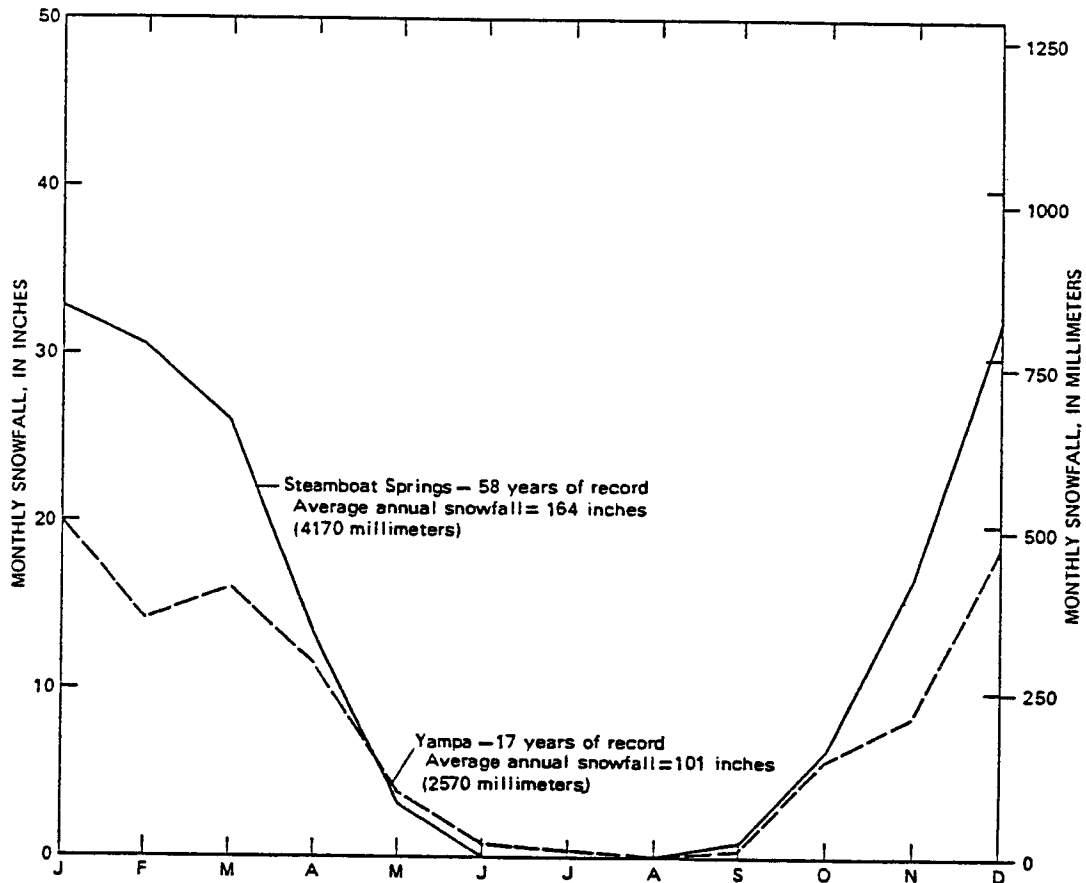
FIGURE 7.  Seasonal distribution of mean monthly snowfall, Steamboat Springs and Yampa, Colorado (Adapted from Steele et al., 1979).

wind, which would cause a significant reduction in snow catch.

## Seasonal Precipitation

To determine seasonal precipitation at the field sites, a similar multivariate regression analysis was used to correlate the variables with measured mean monthly precipitation totals. The weather station data are presented in Table 3.

Mean Monthly Precipitation and The Variables. The variables correlate well with mean monthly precipitation, except during the spring (March-May). For all months, elevation explains most of the variation in mean monthly precipitation whereas exposure accounts for the least variation. Elevation has more influence on mean monthly precipitation in the winter and summer than in the spring and fall (Table 2). When elevation becomes less important, both distance from a northwestern barrier and distance from the Continental Divide have better correlations. Of the two topographic variables, distance from a northwestern barrier has a better relationship with mean monthly precipitation during the spring and summer, when thunderstorm activity is common. During fall and winter, when there is more snowstorm activity, distance from the Continental Divide has stronger correlations. In this manner, both topographic variables work together to strengthen the annual relationship.

Table 3
Weather Station Mean Monthly Precipitation

| Weather Station | January (in) | February (in) | March (in) | April (in) | May (in) | June (in) | July (in) | August (in) | September (in) | October (in) | November (in) | December (in) | Sum of Monthly Precipitation (in) | Mean Annual Precipitation (in) |
|---|---|---|---|---|---|---|---|---|---|---|---|---|---|---|
| Pyramid | 1.99 | 1.79 | 2.19 | 1.93 | 1.44 | 1.42 | 1.38 | 1.67 | 1.54 | 1.67 | 1.65 | 2.00 | 20.67 | 20.69 |
| Yampa | 1.06 | 0.87 | 1.09 | 1.23 | 1.30 | 1.53 | 1.89 | 1.77 | 1.48 | 1.17 | 1.04 | 1.13 | 15.56 | 15.56 |
| Marvine Ranch | 2.07 | 2.20 | 2.05 | 2.00 | 1.88 | 1.40 | 1.21 | 1.96 | 1.91 | 1.93 | 1.65 | 2.46 | 22.72 | 22.73 |
| Steamboat Springs | 2.73 | 2.04 | 1.92 | 2.15 | 2.01 | 1.45 | 1.28 | 1.50 | 1.60 | 1.64 | 1.80 | 2.54 | 22.66 | 22.67 |
| Craig 4SW | 0.94 | 0.93 | 1.07 | 1.32 | 1.23 | 1.04 | 0.91 | 1.39 | 1.15 | 1.21 | 0.99 | 1.21 | 13.39 | 13.57 |
| Hayden | 1.49 | 1.15 | 1.18 | 1.49 | 1.28 | 1.22 | 1.08 | 1.49 | 1.21 | 1.34 | 1.24 | 1.65 | 15.82 | 15.80 |
| Dixon, Wyo.* | 0.90 | 0.69 | 0.69 | 1.03 | 1.02 | 1.01 | 0.91 | 0.81 | 1.18 | 1.04 | 0.78 | 1.05 | 11.11 | 10.95 |
| Meeker No. 2 | 0.87 | 1.00 | 1.22 | 1.48 | 1.36 | 1.26 | 1.25 | 1.49 | 1.38 | 1.38 | 1.02 | 1.17 | 14.88 | 14.86 |
| Hamilton | 1.27 | 1.19 | 1.71 | 1.96 | 1.74 | 1.14 | 1.11 | 1.67 | 1.36 | 1.59 | 1.36 | 1.67 | 17.77 | 17.77 |
| Little Hills | 0.66 | 0.69 | 1.08 | 1.49 | 1.53 | 1.13 | 1.10 | 1.34 | 1.22 | 1.11 | 0.98 | 0.98 | 13.31 | 13.33 |
| Dinosaur Natl. Monument* | 0.66 | 0.49 | 0.95 | 1.04 | 1.26 | 1.41 | 0.92 | 0.78 | 0.92 | 1.39 | 0.64 | 0.72 | 11.18 | 10.96 |
| Maybell* | 0.86 | 0.74 | 1.12 | 1.32 | 1.21 | 0.99 | 0.73 | 0.97 | 1.11 | 1.21 | 1.28 | 1.20 | 12.74 | 12.44 |
| Rangely IE | 0.53 | 0.49 | 0.95 | 0.94 | 0.91 | 0.73 | 0.94 | 0.81 | 1.09 | 0.95 | 0.63 | 0.55 | 9.52 | 9.34 |
| $R^2$ | 0.66 | 0.64 | 0.57 | 0.50 | 0.36 | 0.69 | 0.64 | 0.71 | 0.66 | 0.60 | 0.67 | 0.67 | --- | 0.72 |

* The Weather Station Record Is Less Than 20 Years.

## Results

The regression equations (Table 2) were used to extrapolate the weather records to each of the field sites. Both mean annual and mean monthly precipitation amounts were calculated (Tables 4 and 5).

Among the field sites, May and November are typically the months of maximum and minimum precipitation, respectively. At the higher elevation sites (>6371'), January and December also have notably high precipitation. In addition, July and February frequently have significantly high and low precipitation, respectively. In the latter case, rarely is one relationship observed, unaccompanied by the other. Generally, most precipitation occurs in the spring while the least occurs during fall. However, mean seasonal precipitation is very uniform. For the field sites, differences in mean seasonal precipitation range from 0.73 to 1.80 inches and average only 1.16 inches. Approximately 50 to 80 percent of mean annual precipitation falls when mean monthly temperatures are above freezing. Precipitation falling during this time will be designated "seasonal rainfall." With increasing elevation, annual variation in precipitation decreases. Also, as would be expected, the percent of seasonal rainfall decreases.

TABLE 4
Field Site Data

| | County | Elevation (feet) | Exposure (°) | Distance From A Northwestern Barrier (mi.) | Distance From The Continental Divide (mi.) | Mean Annual Precipitation (in.) | Mean Annual Temperature (°) |
|---|---|---|---|---|---|---|---|
| **Mesa Verde Sandstone** | | | | | | | |
| Upper Dunstan Gulch | Routt | 7907 | 140 | 0.5 | 37.4 | 18.98 | 38.6 |
| Haunted Gulch | Moffat | 7188 | 135 | 2.7 | 45.7 | 17.28 | 40.5 |
| Coyote Eyes Gulch | Routt | 7071 | 55 | 7.7 | 16.3 | 18.97 | 40.1 |
| Upper Winter Valley Gulch | Moffat | 6678 | 128 | 6.9 | 90.8 | 13.58 | 41.8 |
| Tumbling Gulch | Moffat | 6367 | 133 | 17.2 | 63.3 | 13.78 | 42.7 |
| **Browns Park Sandstone** | | | | | | | |
| Little Brown Gulch | Routt | 7353 | 60 | 11.5 | 13.6 | 19.12 | 39.4 |
| Black Beaver Gulch | Routt | 7261 | 60 | 11.3 | 17.2 | 18.85 | 39.6 |
| Upper Twelve Mile Gulch | Moffat | 6392 | 48 | 12.5 | 86.8 | 14.93 | 41.9 |
| Upper Maudlin Gulch | Moffat | 6294 | 2 | 5.7 | 67.8 | 16.88 | 41.7 |
| **Mancos Shale** | | | | | | | |
| Honey Gulch | Routt | 7294 | 176 | 1.6 | 29.8 | 17.43 | 40.6 |
| Blister Gulch | Routt | 7224 | 74 | 3.7 | 42.2 | 18.41 | 39.9 |
| Cross Gulch | Moffat | 6977 | 105 | 1.6 | 55.3 | 17.18 | 40.8 |
| Upper Boxelder Gulch | Moffat | 6227 | 163 | 8.7 | 64.5 | 13.81 | 43.4 |
| Forgotton Gulch | Moffat | 5824 | 145 | 4.4 | 98.0 | 12.65 | 44.3 |

Table 5
Field Site Mean Monthly Precipitation

| | January (in) | February (in) | March (in) | April (in) | May (in) | June (in) | July (in) | August (in) | September (in) | October (in) | November (in) | December (in) | Mean Monthly Precipitation Range (in) | Sum of Monthly Precipitation (in) | Mean Annual Precipitation (in) |
|---|---|---|---|---|---|---|---|---|---|---|---|---|---|---|---|
| **Mesa Verde Sandstone** | | | | | | | | | | | | | | | |
| Upper Dunstan Gulch | 1.71 | 1.28 | 1.57 | 1.38 | 1.89 | 1.59 | 1.89 | 1.46 | 1.57 | 1.36 | 1.02 | 1.78 | 0.87 | 18.50 | 18.98 |
| Haunted Gulch | 1.55 | 1.10 | 1.40 | 1.34 | 1.80 | 1.44 | 1.66 | 1.29 | 1.42 | 1.24 | 0.97 | 1.63 | 0.83 | 16.84 | 17.28 |
| Coyote Eyes Gulch | 2.04 | 1.41 | 1.47 | 1.49 | 1.93 | 1.32 | 1.49 | 1.32 | 1.46 | 1.30 | 1.20 | 2.09 | 0.89 | 18.52 | 18.97 |
| Upper Winter Valley Gulch | 0.95 | 0.69 | 1.12 | 1.03 | 1.60 | 1.29 | 1.45 | 1.01 | 1.26 | 1.14 | 0.64 | 1.08 | 0.96 | 13.26 | 13.58 |
| Tumbling Gulch | 1.14 | 0.72 | 1.05 | 1.12 | 1.60 | 1.21 | 1.38 | 0.98 | 1.21 | 1.08 | 0.75 | 1.24 | 0.88 | 13.48 | 13.78 |
| **Browns Park Sandstone** | | | | | | | | | | | | | | | |
| Little Brown Gulch | 2.03 | 1.42 | 1.47 | 1.45 | 1.93 | 1.36 | 1.57 | 1.35 | 1.51 | 1.29 | 1.16 | 2.07 | 0.91 | 18.61 | 19.12 |
| Black Beaver Gulch | 1.99 | 1.39 | 1.46 | 1.44 | 1.92 | 1.35 | 1.55 | 1.33 | 1.48 | 1.28 | 1.15 | 2.04 | 0.89 | 18.38 | 18.85 |
| Upper Twelve Mile Gulch | 1.30 | 0.94 | 1.25 | 1.17 | 1.73 | 1.20 | 1.24 | 1.02 | 1.26 | 1.23 | 0.83 | 1.42 | 0.90 | 14.59 | 14.93 |
| Upper Maudlin Gulch | 1.72 | 1.22 | 1.40 | 1.37 | 1.87 | 1.18 | 1.15 | 1.11 | 1.30 | 1.32 | 1.06 | 1.82 | 0.81 | 16.52 | 16.88 |
| **Mancos Shale** | | | | | | | | | | | | | | | |
| Honey Gulch | 1.57 | 1.07 | 1.38 | 1.36 | 1.78 | 1.48 | 1.77 | 1.33 | 1.43 | 1.25 | 0.99 | 1.63 | 0.79 | 17.04 | 17.43 |
| Blister Gulch | 1.80 | 1.30 | 1.50 | 1.41 | 1.90 | 1.40 | 1.57 | 1.33 | 1.46 | 1.34 | 1.08 | 1.88 | 0.82 | 17.97 | 18.41 |
| Cross Gulch | 1.57 | 1.12 | 1.42 | 1.34 | 1.82 | 1.39 | 1.54 | 1.25 | 1.39 | 1.31 | 0.99 | 1.66 | 0.83 | 16.80 | 17.18 |
| Upper Boxelder Gulch | 1.11 | 0.67 | 1.08 | 1.17 | 1.59 | 1.24 | 1.40 | 1.00 | 1.18 | 1.11 | 0.78 | 1.21 | 0.92 | 13.54 | 13.81 |
| Forgotten Gulch | 0.88 | 0.55 | 1.06 | 1.10 | 1.56 | 1.19 | 1.25 | 0.91 | 1.09 | 1.15 | 0.69 | 1.02 | 1.01 | 12.45 | 12.65 |

Mean Annual Temperature
====================

As in the case of precipitation, the temperature pattern of northwestern Colorado is influenced by topography. Therefore, to extrapolate mean annual temperature data from the weather stations to the field sites, a multivariate regression equation, similar to that used for precipitation, was developed. In this case, only eleven of the weather stations were employed, again using the twenty year record, 1960 to 1980. (Weather stations at Pyramid and Hamilton do not record temperature.) Since the distance to large orographic barriers is inapplicable, only the variables, elevation and exposure, are included in the analysis. These variables were evaluated according to the definitions described previously (Table 1).

Mean Annual Temperature and Elevation. Elevation is most important in explaining variation in mean annual temperature ($R^2$ = 0.68). The regression equation indicates an annual lapse rate of -2.9°F per 1000 feet elevation (Table 6). This value is slightly lower than the findings of Baker (1944) who observed an annual lapse rate of -3.5°F per 1000 feet elevation for the mountains of the western United States. Data for stations above 6770 feet elevation depart from the linear relationship between elevation and mean annual temperature. Their deviation may be partly attributable to the location of the weather stations. The stations are located along river valleys that lack of good air drainage. The measured temperatures, therefore, may underestimate the true temperature regime (Wymore, 1974).

TABLE 6
Regression Equations Describing The Relationships
Between Climatic Variables And Mean Annual
And Mean Monthly Temperature

| Mean Annual Temperature | $R^2$ |
|---|---|
| M.A. T = 60.9 − 0.0029(E) | 0.68 |
| M.A. T = 39.9 + 0.262(X) | 0.21 |
| M.A. T = 58.7 − 0.0027(E) + 0.0091(X) | 0.71 |
| | |
| Mean Monthly Temperature | |
| January M.Mo. T = 8.08 + 0.0011(E) + 0.0297(X) | 0.36 |
| February M.Mo. T = 25.7 − 0.0007(E) + 0.0269(X) | 0.43 |
| March M.Mo. T = 48.8 − 0.0030(E) + 0.0174(X) | 0.67 |
| April M.Mo. T = 65.4 − 0.0038(E) + 0.0048(X) | 0.88 |
| May M.Mo. T = 74.7 − 0.0037(E) + 0.0031(X) | 0.84 |
| June M.Mo. T = 86.8 − 0.0043(E) − 0.0001(X) | 0.76 |
| July M.Mo. T = 97.5 − 0.0048(E) − 0.0003(X) | 0.77 |
| August M.Mo. T = 92.6 − 0.0044(E) − 0.0007(X) | 0.76 |
| September M.Mo. T = 76.9 − 0.0034(E) + 0.0026(X) | 0.69 |
| October M.Mo. T = 59.0 − 0.0023(E) + 0.0032(X) | 0.57 |
| November M.Mo. T = 40.2 − 0.0015(E) + 0.0105(X) | 0.55 |
| December M.Mo. T = 14.0 + 0.0006(E) + 0.0282(X) | 0.37 |

---------------

M.A. T = Mean Annual Temperature

M. Mo. T = Mean Monthly Temperature

E = Elevation

X = Exposure

Mean Annual Temperature and Exposure. Mean annual temperature correlates weakly with exposure, having an $R^2$ of 0.21. As exposure becomes more southeasterly, mean annual temperature increases at a rate of 0.1 °F per five degrees (Table 6). If exposure were calculated as degrees from due north, rather than from N 45° W, the correlation may have been improved.

Mean Annual Temperature and The Variables. The multivariable regression analysis combining elevation and exposure resulted in a good correlation with mean annual temperature, having an $R^2$ of 0.71 (Table 6). The relative importance of each variable is indicated by the sum of squares analysis (Table 1). A plot of the measured mean annual temperature against the predicted mean annual temperature, for each station, is shown in Figure 8. The two highest stations, Yampa, at 7892 feet elevation, and Marvine Ranch, at 7899 feet elevation, are minor outliers. In both cases, the predicted temperatures are slightly lower, 0.8 and 0.7°F, respectively, than the actual temperatures measured at the stations. Again the differences may be attributable to the location of the weather stations, as described previously.

Seasonal Temperature

To determine seasonal trends in temperature for the field sites, the multivariate regression analysis was used to correlate the variables with average monthly temperature data from the weather stations (Table 7).
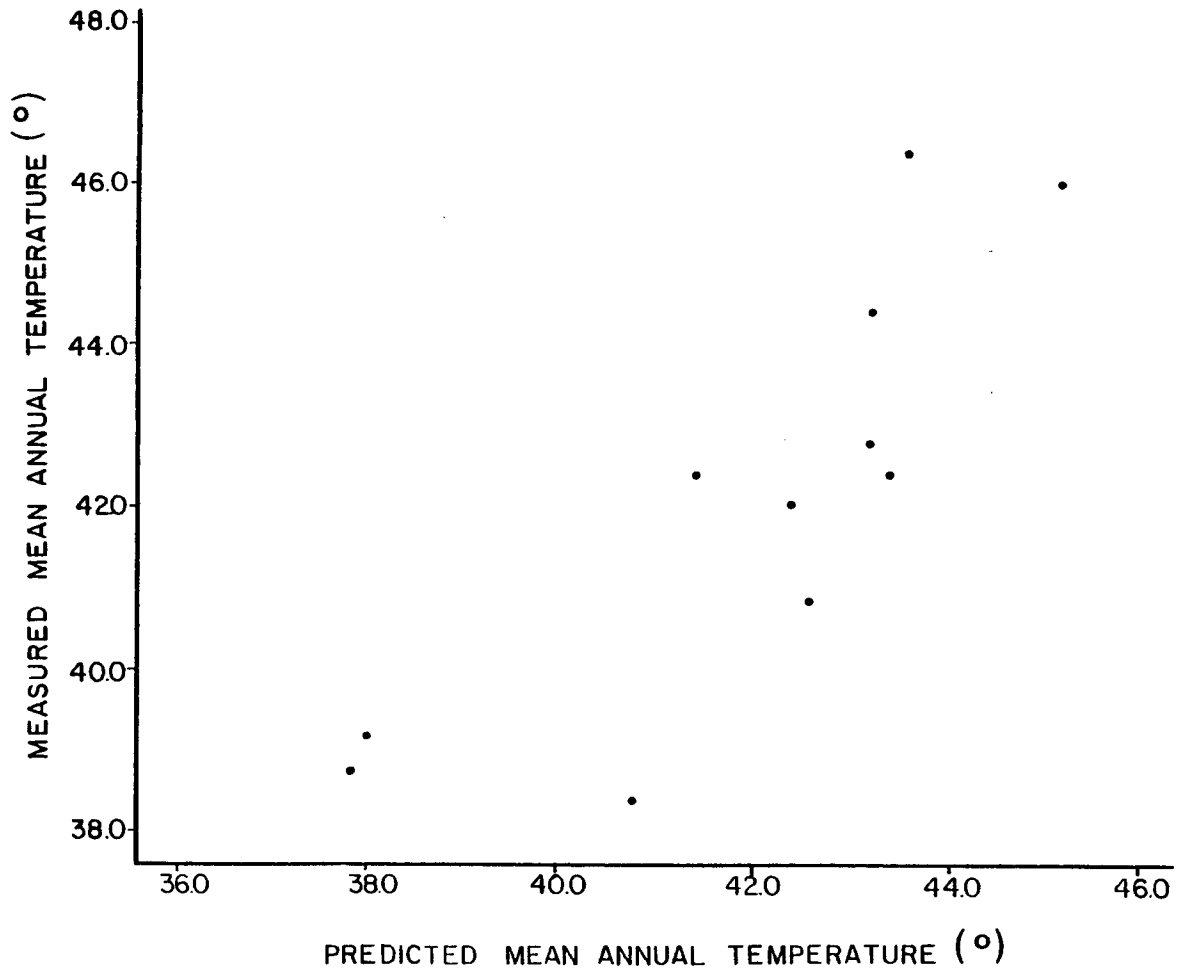
FIGURE 8.  A plot of the measured mean annual temperature
against the predicted mean annual temperature for
each weather station.

Table 7
Weather Station Mean Monthly Temperature

| Weather Station | January (°) | February (°) | March (°) | April (°) | May (°) | June (°) | July (°) | August (°) | September (°) | October (°) | November (°) | December (°) | Mean of Monthly Temperatures (°) | Mean Annual Temperature (°) |
|---|---|---|---|---|---|---|---|---|---|---|---|---|---|---|
| Yampa* | 18.9 | 21.7 | 27.1 | 36.5 | 46.9 | 54.9 | 61.3 | 59.3 | 51.8 | 42.2 | 29.4 | 20.8 | 39.2 | 39.1 |
| Marvine Ranch | 18.9 | 22.6 | 26.8 | 36.1 | 45.9 | 53.9 | 60.0 | 58.1 | 50.6 | 42.2 | 29.8 | 20.4 | 38.8 | 38.7 |
| Steamboat Springs | 14.5 | 19.5 | 25.9 | 38.0 | 47.5 | 54.8 | 61.6 | 59.6 | 51.6 | 41.9 | 28.9 | 17.2 | 38.4 | 38.5 |
| Craig 4SW | 17.2 | 22.2 | 30.1 | 41.3 | 51.3 | 60.1 | 67.3 | 65.0 | 55.8 | 45.0 | 32.1 | 20.1 | 42.3 | 42.3 |
| Hayden | 16.2 | 21.6 | 28.4 | 41.5 | 51.4 | 59.9 | 66.8 | 64.2 | 55.6 | 44.9 | 31.9 | 20.0 | 41.9 | 42.0 |
| Dixon, Wyo.* | 16.7 | 21.8 | 29.4 | 40.5 | 50.9 | 58.2 | 65.2 | 62.9 | 53.8 | 42.7 | 30.4 | 19.1 | 41.0 | 40.8 |
| Meeker No. 2 | 21.6 | 27.2 | 33.6 | 42.8 | 52.0 | 60.3 | 67.2 | 64.8 | 56.4 | 46.6 | 34.1 | 24.3 | 44.2 | 44.2 |
| Little Hills | 20.9 | 26.4 | 32.4 | 41.1 | 50.3 | 58.7 | 66.0 | 63.5 | 54.9 | 44.1 | 32.2 | 22.5 | 42.8 | 42.8 |
| Dinosaur Natl. Monument* | 19.8 | 26.1 | 35.9 | 44.7 | 55.1 | 64.6 | 72.8 | 70.3 | 60.6 | 48.5 | 34.3 | 22.5 | 46.3 | 46.3 |
| Maybell | 17.2 | 23.1 | 31.8 | 42.3 | 52.2 | 60.1 | 66.9 | 64.7 | 55.0 | 44.5 | 30.9 | 18.8 | 42.3 | 42.5 |
| Rangely IE | 15.6 | 24.3 | 35.0 | 46.8 | 56.4 | 65.8 | 73.3 | 70.0 | 60.3 | 48.5 | 33.7 | 19.2 | 45.7 | 46.1 |
| $R^2$ | 0.36 | 0.43 | 0.67 | 0.88 | 0.84 | 0.76 | 0.77 | 0.76 | 0.69 | 0.57 | 0.55 | 0.37 | --- | 0.71 |

* The Weather Station Record Is Less Than 20 Years.

Mean Monthly Temperature and The Variables. The variables correlate well with mean monthly temperature in the spring and summer, but explain progressively less variation in the fall and winter. Perhaps during the colder months, other variables, not included in the equation, are more significant.

During the year, elevation is always a much more important variable in determining mean monthly temperature than exposure (Table 6). Between April and October, exposure had no influence on the regressions. In winter, aspect becomes more important because the sun is lower in the sky and the influence of exposure on temperature is accentuated. In the summer, the sun is higher in the sky and is able to get more solar radiation to north facing slopes as well as to south facing slopes.

## Results

The determined regression equations (Table 6) were used to extrapolate both mean annual and mean monthly temperature data to the field sites. The results are presented in Tables 4 and 8.

Among the field sites, the monthly temperatures show a progression from a monthly minimum in January to a monthly maximum in July and successively decrease again through December. Winters are quite cold with mean monthly temperatures remaining relatively constant and below freezing. Rapid warming occurs through the spring until

Table 8
Field Site Mean Monthly Temperature

| | January (°) | February (°) | March (°) | April (°) | May (°) | June (°) | July (°) | August (°) | September (°) | October (°) | November (°) | December (°) | Mean Monthly Temperature Range (°) | Mean of Monthly Temperatures (°) | Mean Annual Temperature (°) |
|---|---|---|---|---|---|---|---|---|---|---|---|---|---|---|---|
| **Mesa Verde Sandstone** | | | | | | | | | | | | | | | |
| Upper Dunstan Gulch | 20.9 | 23.9 | 27.5 | 36.0 | 45.9 | 52.8 | 59.5 | 57.7 | 50.4 | 41.3 | 29.8 | 22.7 | 38.6 | 39.0 | 38.6 |
| Haunted Gulch | 20.0 | 24.3 | 29.6 | 38.7 | 48.5 | 55.9 | 63.0 | 60.9 | 52.8 | 42.9 | 30.8 | 22.1 | 43.0 | 40.8 | 40.5 |
| Coyote Eyes Gulch | 17.5 | 22.2 | 28.5 | 38.8 | 48.7 | 56.4 | 63.5 | 61.4 | 53.0 | 42.9 | 30.2 | 19.8 | 46.0 | 40.2 | 40.1 |
| Upper Winter Valley Gulch | 19.2 | 24.5 | 31.0 | 40.6 | 50.4 | 58.1 | 65.4 | 63.1 | 54.5 | 44.1 | 31.5 | 21.6 | 46.2 | 42.0 | 41.8 |
| Tumbling Gulch | 19.0 | 24.8 | 32.0 | 41.8 | 51.6 | 59.4 | 66.9 | 64.5 | 55.6 | 44.8 | 32.0 | 21.6 | 47.9 | 42.8 | 42.7 |
| **Browns Park Sandstone** | | | | | | | | | | | | | | | |
| Little Brown Gulch | 18.0 | 22.2 | 27.8 | 37.7 | 47.7 | 55.2 | 62.2 | 60.2 | 52.1 | 42.3 | 29.8 | 20.1 | 44.2 | 39.6 | 39.4 |
| Black Beaver Gulch | 17.8 | 22.2 | 28.1 | 38.1 | 48.0 | 55.6 | 62.6 | 60.6 | 52.4 | 42.5 | 29.9 | 20.0 | 44.8 | 39.8 | 39.6 |
| Upper Twelve Mile Gulch | 16.5 | 22.5 | 30.5 | 41.3 | 51.2 | 59.3 | 66.8 | 64.4 | 55.3 | 44.5 | 31.1 | 19.2 | 50.3 | 41.9 | 41.9 |
| Upper Maudlin Gulch | 15.1 | 21.3 | 30.0 | 41.5 | 51.4 | 59.7 | 67.3 | 64.9 | 55.5 | 44.5 | 30.8 | 17.8 | 52.2 | 41.7 | 41.7 |
| **Mancos Shale** | | | | | | | | | | | | | | | |
| Honey Gulch | 21.3 | 25.3 | 30.0 | 38.5 | 48.3 | 55.4 | 62.4 | 60.4 | 52.6 | 42.8 | 31.1 | 23.3 | 41.1 | 41.0 | 40.6 |
| Blister Gulch | 18.2 | 22.6 | 28.4 | 38.3 | 48.2 | 55.7 | 62.8 | 60.8 | 52.5 | 42.6 | 30.1 | 20.4 | 44.6 | 40.1 | 39.9 |
| Cross Gulch | 18.9 | 23.6 | 29.7 | 39.4 | 49.2 | 56.8 | 64.0 | 61.8 | 53.5 | 43.3 | 30.8 | 21.1 | 45.1 | 41.0 | 40.8 |
| Upper Boxelder Gulch | 19.8 | 25.7 | 33.0 | 42.5 | 52.2 | 60.0 | 67.6 | 65.1 | 56.2 | 45.2 | 32.6 | 22.3 | 47.8 | 43.5 | 43.4 |
| Forgotten Gulch | 18.8 | 25.5 | 33.9 | 44.0 | 53.6 | 61.7 | 69.5 | 66.9 | 57.5 | 46.1 | 33.0 | 21.6 | 50.7 | 44.3 | 44.3 |

summer, when mean monthly temperature changes are much less significant. Fall is the season of greatest temperature change. Mean monthly temperatures fall approximately 20°F over the course of three months. Average seasonal temperature increases from winter to spring to fall to summer. In winter and summer, the range of mean monthly temperatures is quite small, averaging only 4.6 and 7.2°F, respectively. On the other hand, in spring and fall, the range is much larger, averaging 19.5 and 22.7°F, respectively. The largest differences between mean monthly temperature occur from October to November and November to December. As elevation increases, both seasonal and annual temperature variation decrease.

## Evapotranspiration

Unfortunately, actual ET rates are difficult to measure directly and their calculation requires a detailed knowledge of meteorological factors, which are not available for the study region. Therefore, for the field sites, potential ET was determined using an empirical equation developed by Hamon (1963).

Hamon (1963) defines potential ET as "the rate at which water would be removed from an extended area covered by an actively growing green crop completely shading the soil, and with a nonlimiting supply of water." Kohler (1958) has suggested that evaporation from a large surface of water must be equivalent to potential ET.

Hamon derived his equation from several postulates: 1) when soil moisture is not limiting, potential ET almost depends entirely on the solar energy reaching the surface during daytime hours and the heat that it produces; 2) average potential ET may be considered proportional to the saturated water vapor density at the air temperature near the surface; and 3) percent error in potential ET due to wind is negligible in dry regions and, therefore, can be considered constant. Hamon's equation for potential ET is:

$$PE = CD^2P_t$$

where:

PE = average potential ET (in/day)
D  = possible hours of sunshine in units of 12 hours
$P_t$ = saturated water vapor density (absolute humidity) at the daily mean temperature ($g/m^3$ x $10^2$)
C  = 0.55, chosen to give appropriate yearly values of potential ET as indicated by observations in the literature

Results from Hamon's equation compare very well with other commonly used methods, over a wide range of climates. In addition, his equation corrects a short coming of the frequently used Thornthwaite method, which generally underestimates potential ET in the winter and overestimates potential ET in the summer (Hamon, 1963).

The calculated mean annual and mean monthly potential ET rates for the field sites (Table 9) are a direct function of temperature. Therefore, their relationships resemble those of temperature. Mean monthly potential ET rates progress from a minimum in January to a

Table 9
Field Site Mean Annual And Mean Monthly Potential Evapotranspiration

| | January (in) | February (in) | March (in) | April (in) | May (in) | June (in) | July (in) | August (in) | September (in) | October (in) | November (in) | December (in) | Mean Annual Potential Evapotranspiration (in) |
|---|---|---|---|---|---|---|---|---|---|---|---|---|---|
| **Mesa Verde Sandstone** | | | | | | | | | | | | | |
| Upper Dunstan Gulch | 0.38 | 0.38 | 0.74 | 1.15 | 2.13 | 2.66 | 3.59 | 2.92 | 1.70 | 1.08 | 0.51 | 0.38 | 17.62 |
| Haunted Gulch | 0.36 | 0.38 | 0.80 | 1.27 | 2.34 | 2.98 | 4.03 | 3.24 | 1.86 | 1.15 | 0.53 | 0.37 | 19.31 |
| Coyote Eyes Gulch | 0.33 | 0.35 | 0.77 | 1.28 | 2.36 | 3.02 | 4.10 | 3.32 | 1.87 | 1.15 | 0.51 | 0.33 | 19.39 |
| Upper Winter Valley Gulch | 0.35 | 0.38 | 0.84 | 1.37 | 2.50 | 3.21 | 4.38 | 3.50 | 1.96 | 1.19 | 0.54 | 0.36 | 20.58 |
| Tumbling Gulch | 0.35 | 0.39 | 0.88 | 1.43 | 2.61 | 3.35 | 4.59 | 3.67 | 2.04 | 1.22 | 0.55 | 0.36 | 21.44 |
| **Browns Park Sandstone** | | | | | | | | | | | | | |
| Little Brown Gulch | 0.33 | 0.35 | 0.75 | 1.22 | 2.30 | 2.95 | 3.93 | 3.23 | 1.80 | 1.12 | 0.50 | 0.33 | 18.81 |
| Black Beaver Gulch | 0.33 | 0.35 | 0.75 | 1.24 | 2.30 | 2.94 | 3.98 | 3.22 | 1.82 | 1.13 | 0.51 | 0.34 | 18.91 |
| Upper Twelve Mile Gulch | 0.32 | 0.35 | 0.82 | 1.40 | 2.58 | 3.35 | 4.57 | 3.65 | 2.01 | 1.21 | 0.53 | 0.33 | 21.12 |
| Upper Maudlin Gulch | 0.30 | 0.34 | 0.81 | 1.41 | 2.59 | 3.39 | 4.65 | 3.72 | 2.04 | 1.22 | 0.53 | 0.31 | 21.31 |
| **Mancos Shale** | | | | | | | | | | | | | |
| Honey Gulch | 0.38 | 0.40 | 0.81 | 1.26 | 2.31 | 2.93 | 3.96 | 3.20 | 1.83 | 1.14 | 0.53 | 0.39 | 19.14 |
| Blister Gulch | 0.34 | 0.36 | 0.76 | 1.25 | 2.31 | 2.96 | 4.01 | 3.24 | 1.83 | 1.13 | 0.51 | 0.34 | 19.04 |
| Cross Gulch | 0.35 | 0.37 | 0.80 | 1.30 | 2.40 | 3.07 | 4.18 | 3.36 | 1.89 | 1.16 | 0.53 | 0.35 | 19.76 |
| Upper Boxelder Gulch | 0.36 | 0.40 | 0.91 | 1.46 | 2.66 | 3.43 | 4.70 | 3.74 | 2.08 | 1.24 | 0.56 | 0.37 | 21.91 |
| Forgotten Gulch | 0.35 | 0.40 | 0.94 | 1.53 | 2.79 | 3.62 | 4.98 | 3.96 | 2.18 | 1.28 | 0.57 | 0.36 | 22.96 |

maximum in July and successively decrease again through December. Average seasonal potential ET is highest in the summer and decreases from spring to fall to winter. Although the mean seasonal temperature is lower in spring than in fall, the number of possible hours of sunshine is greater. The latter causes potential ET rates to be higher in spring than in fall. The range of mean monthly potential ET rates also are higher in spring, averaging 1.61 inches than in fall, averaging 1.38 inches, while they are much smaller in winter and summer, averaging 0.03 and 1.11 inches, respectively. The greatest differences in mean monthly potential ET rates occur between August and September, April and May, and June and July. As elevation increases, mean annual and mean seasonal variation in potential ET decrease.

## Net Precipitation

Evapotranspiration and precipitation are opposed with respect to water availability. Their combined effect can be estimated by taking the difference between precipitation and potential ET, thereby calculating "net precipitation."

Mean monthly net precipitation (Table 10) is highest in December, decreases to a minimum in July, and progressively increases again. Mean seasonal net precipitation is greatest in the winter, when potential ET rates are low, approximately the same in the spring and

Table 10

Field Site Mean Annual and Mean Monthly Net Precipitation

| | January (in) | February (in) | March (in) | April (in) | May (in) | June (in) | July (in) | August (in) | September (in) | October (in) | November (in) | December (in) | Sum of Mean Monthly Net Precipitation (in) | Mean Annual Net Precipitation (in) |
|---|---|---|---|---|---|---|---|---|---|---|---|---|---|---|
| **Mesa Verde Sandstone** | | | | | | | | | | | | | | |
| Upper Dunstan Gulch | 1.33 | 0.90 | 0.83 | 0.23 | -0.24 | -1.07 | -1.70 | -1.46 | -0.13 | 0.28 | 0.51 | 1.40 | 0.88 | 1.36 |
| Haunted Gulch | 1.19 | 0.72 | 0.60 | 0.07 | -0.54 | -1.54 | -2.37 | -1.95 | -0.44 | 0.09 | 0.44 | 1.26 | -2.47 | -2.03 |
| Coyote Eyes Gulch | 1.71 | 1.06 | 0.70 | 0.21 | -0.43 | -1.70 | -2.61 | -2.00 | -0.41 | 0.15 | 0.69 | 1.76 | -0.87 | -0.42 |
| Upper Winter Valley Gulch | 0.60 | 0.31 | 0.28 | -0.34 | -0.90 | -1.92 | -2.93 | -2.49 | -0.70 | -0.05 | 0.10 | 0.72 | -7.32 | -7.00 |
| Tumbling Gulch | 0.79 | 0.33 | 0.17 | -0.31 | -1.01 | -2.14 | -3.21 | -2.69 | -0.83 | -0.14 | 0.20 | 0.88 | -7.96 | -7.66 |
| **Browns Park Sandstone** | | | | | | | | | | | | | | |
| Little Brown Gulch | 1.70 | 1.07 | 0.72 | 0.23 | -0.37 | -1.59 | -2.36 | -1.88 | -0.29 | 0.17 | 0.66 | 1.74 | -0.20 | 0.31 |
| Black Beaver Gulch | 1.66 | 1.04 | 0.71 | 0.20 | -0.38 | -1.59 | -2.43 | -1.89 | -0.34 | 0.15 | 0.64 | 1.70 | -0.53 | -0.06 |
| Upper Twelve Mile Gulch | 0.98 | 0.59 | 0.43 | -0.23 | -0.85 | -2.15 | -3.33 | -2.63 | -0.75 | 0.02 | 0.30 | 1.09 | -6.53 | -6.19 |
| Upper Maudlin Gulch | 1.42 | 0.88 | 0.59 | -0.04 | -0.72 | -2.21 | -3.50 | -2.61 | -0.74 | 0.10 | 0.53 | 1.51 | -4.79 | -4.43 |
| **Mancos Shale** | | | | | | | | | | | | | | |
| Honey Gulch | 1.19 | 0.67 | 0.57 | 0.10 | -0.53 | -1.45 | -2.19 | -1.87 | -0.40 | 0.11 | 0.46 | 1.24 | -2.10 | -1.71 |
| Blister Gulch | 1.46 | 0.94 | 0.74 | 0.16 | -0.41 | -1.56 | -2.44 | -1.91 | -0.37 | 0.21 | 0.57 | 1.54 | -1.07 | -0.63 |
| Cross Gulch | 1.22 | 0.75 | 0.62 | 0.04 | -0.58 | -1.68 | -2.64 | -2.11 | -0.50 | 0.15 | 0.46 | 1.31 | -2.96 | -2.58 |
| Upper Boxelder Gulch | 0.75 | 0.27 | 0.17 | -0.29 | -1.07 | -2.19 | -3.30 | -2.74 | -0.90 | -0.13 | 0.22 | 0.84 | -8.37 | -8.10 |
| Forgotten Gulch | 0.53 | 0.15 | 0.12 | -0.43 | -1.23 | -2.43 | -3.73 | -3.05 | -1.09 | -0.13 | 0.12 | 0.66 | -10.51 | -10.31 |

fall, and the least in the summer, when potential ET rates are high. The range of mean monthly net precipitation is greatest in spring, averaging 1.17 inches, and successively decreases through fall, winter and summer, averaging 0.96, 0.57, and 0.42 inches, respectively. The greatest differences between mean monthly net precipitation occur between August and September and May and June. Among the lower elevation sites (<6678'), mean monthly net precipitation between April and October is negative. Among the higher elevation sites, the period of May through September experiences negative mean monthly net precipitation. As elevation increases, variation in mean annual and mean seasonal net precipitation decreases.

**Vegetative Measurements**

<u>Growing Season</u>

Grasses and most native shrubs of Northwestern Colorado are not seriously damaged until a threshold temperature of 24.0°F is reached. Below a mean daily temperature of 40.0°F, however, their growth is negligible (Siemer and Heermann, 1970). Weather Service gages measure air temperature five feet above the ground surface (Marlatt, 1971). Air temperature six inches above the surface is usually six to eight degrees lower (Robbins, 1917). Therefore, the frost free period or the number of consecutive days when the mean daily temperature is greater than 32.0°F is a reasonable measure of "growing season."

The growing season at each field site was determined through simple regression analysis. A linear relationship between length of growing season and mean annual temperature was developed for the weather stations (Table 11). Because growing season is defined by temperature, it was the only variable included in the analysis. However, it is important to realize that although the air temperature of opposing slopes may be identical, the difference in exposure also influences vegetation. The amount of direct sunlight received and the amount of heat generated by terrestrial radiation is extremely important, especially to the growth of young plants and seedlings (McGinnies et al., 1944). The correlation between growing season and temperature for the weather station data is 0.77. The regression equation (Table 11) was used to calculate growing seasons at the field sites. The results are included in Table 12.

## Precipitation Effectiveness

During the critical period for plant growth, evaporation rates exceed rainfall amounts. As previously indicated, field site net precipitation is lowest in July and highest in January, being negative throughout the late spring, summer, and early fall.

Precipitation in the form of snow is not available to plants until it melts. Snow, however, protects vegetation and supplies the soil with moisture that often is

Table 11
Weather Station Mean Annual Temperature
And Growing Season

| Weather Station | Mean Annual Temperature (°) | Growing Season (days) |
|---|---|---|
| Yampa* | 39.1 | 57 |
| Marvine Ranch | 38.7 | 41 |
| Steamboat Springs | 38.5 | 33 |
| Craig 45W | 42.3 | 96 |
| Hayden | 42.0 | 91 |
| Dixon, Wyo.* | 40.8 | 83 |
| Meeker No. 2 | 44.2 | 89 |
| Little Hills | 42.8 | 59 |
| Dinosaur National Monument* | 46.3 | 111 |
| Maybell | 42.5 | 83 |
| Rangely | 46.1 | 116 |

Growing Season = -292 + 8.78 (Mean Annual Temperature)

$R^2$ = 0.77

* The Weather Station Record Is Less Than 20 Years.

Table 12
Field Site Climatic And Vegetative Variables

| | Mean Annual Temperature (°) | Growing Season (days) | Mean Seasonal Rainfall (in) | Percent Mean Seasonal Rainfall (%) | Mean Seasonal Net Rainfall (in) | P-E Index | Vegetative Cover (%) |
|---|---|---|---|---|---|---|---|
| **Mesa Verde Sandstone** | | | | | | | |
| Upper Dunstan Gulch | 38.6 | 47 | 11.14 | 58.7 | -4.09 | 22.57 | 41 |
| Haunted Gulch | 40.5 | 64 | 10.19 | 59.0 | -6.68 | 20.15 | 55 |
| Coyote Eyes Gulch | 40.1 | 60 | 10.32 | 54.4 | -6.79 | 25.90 | 41 |
| Upper Winter Valley Gulch | 41.8 | 75 | 8.78 | 64.7 | -9.33 | 14.06 | 25 |
| Tumbling Gulch | 42.7 | 83 | 10.38 | 75.3 | -9.96 | 14.91 | 30 |
| **Browns Park Sandstone** | | | | | | | |
| Little Brown Gulch | 39.4 | 54 | 10.46 | 54.7 | -6.09 | 26.06 | 35 |
| Black Beaver Gulch | 39.6 | 56 | 10.35 | 54.9 | -6.28 | 25.41 | 60 |
| Upper Twelve Mile Gulch | 41.9 | 76 | 8.85 | 59.3 | -9.92 | 18.20 | 28 |
| Upper Maudlin Gulch | 41.7 | 74 | 9.30 | 55.1 | -9.72 | 23.23 | 18 |
| **Mancos Shale** | | | | | | | |
| Honey Gulch | 40.6 | 64 | 10.40 | 59.7 | -6.23 | 19.65 | 35 |
| Blister Gulch | 39.9 | 58 | 10.41 | 56.5 | -6.32 | 23.74 | 45 |
| Cross Gulch | 40.8 | 66 | 10.04 | 58.4 | -7.32 | 20.75 | 34 |
| Upper Boxelder Gulch | 43.4 | 89 | 10.55 | 76.4 | -10.23 | 14.40 | 20 |
| Forgotten Gulch | 44.3 | 97 | 10.00 | 79.1 | -11.85 | 12.55 | 21 |

not exhausted until midsummer (Robbins, 1917). In semiarid areas, where evaporation rates are very high, snow is essential for vegetation survival. At the field sites, the vegetative cover is directly related to the percentage of precipitation falling as snow.

Thornthwaite (1931) considered the amount and distribution of precipitation with respect to rates of evaporation in devising a Precipitation Effectiveness (P-E) Index. The P-E Index is a measure of the availability of moisture to vegetation. It indicates both the amount and type of plant growth that can be expected in a region. There is a direct relationship between the P-E Index and vegetative cover. The higher the index, the more favorable the area is for growth.

The P-E Index is equal to ten times the sum of the twelve monthly P-E ratios:

$$I = 10 \sum_{12} \frac{P}{E}$$

where P is equal to mean monthly precipitation and E is equal to mean monthly evaporation. The P-E Index was calculated for the field sites using the extrapolated monthly precipitation and potential evapotranspiration data (Table 12).

## Results

The vegetative cover on each lithology is most strongly influenced by different climatic variables. Among

the Mesa Verde Sandstone field sites, vegetative cover is most closely related to precipitation factors, including the mean monthly precipitation range. Conversely, among the Browns Park Sandstone field sites, vegetative cover correlates best with temperature factors, including the mean monthly temperature range. Vegetative cover, among the Mancos Shale field sites, depends largely on both climatic factors and variables indicating potential for plant growth, such as the percentage of seasonal rainfall. The vegetative cover on most of the field sites is related to elevation because it incorporates the climatic variables that directly affect plant growth. The correlations ($R^2$) between elevation and the percentage of vegetative cover range from 0.31 among the Mesa Verde Sandstone drainage basins to 0.81 among the Mancos Shale basins. Likewise, for most sites, vegetative cover relates to mean seasonal net rainfall, which also integrates precipitation, temperature, and evaporation rates. The latter correlations range from 0.39 among the Mesa Verde Sandstone sites to 0.81 among the Mancos Shale sites. Thornthwaite's P-E Index has slightly lower correlations with vegetative cover, ranging from 0.22 among the Brown Park Sandstone basins to 0.91 among the Mancos Shale basins.

# CHAPTER 4

## DRAINAGE BASIN MORPHOLOGY

### Lithology and Drainage Basin Morphology

The morphology of the field sites was evaluated (Table 13) and the average of each morphologic variable for each lithology was calculated (Table 14). Except for Little Brown Gulch, all of the field sites are fifth-order drainage basins.

### Mesa Verde Sandstone Field Sites

Drainage basins that form on the Mesa Verde Sandstone are large, circular, and steep with a few widely spaced streams (Table 14). Mean drainage-basin area is significantly greater than on the Browns Park Sandstone and Mancos Shale (Table 15). The high infiltration capacity and permeability of the Mesa Verde Sandstone minimizes runoff so that a drainage network of a given order occupies a larger watershed. Average basin relief, slope, and circularity also are greater on the resistant Mesa Verde Sandstone than on the other lithologies. Due to the steep topography, mean channel gradient is very steep. In addition, of all the lithologies studied, the Mesa Verde Sandstone drainage basins have the greatest average total length of stream

71

Table 13
Field Site Morphologic Variables
-Symbols Defined in Appendix A

| | Order | Elevation | M | R | Rc | Rr | s | $\Sigma_l$ | $\Sigma_{l_1}$ | $\Sigma_{l_1}/\Sigma_{l_{1-5}}$ | A | N₁/Basin | F₁ | D₁ | D |
|---|---|---|---|---|---|---|---|---|---|---|---|---|---|---|---|
| **Mesa Verde Sandstone** | | | | | | | | | | | | | | | |
| Upper Dunstan Gulch | 5 | 7907 | 0.09 | 790 | 0.64 | 0.25 | 0.20 | 8.06 | 4.44 | 1.23 | 0.24 | 137 | 574.9 | 18.6 | 33.8 |
| Haunted Gulch | 5 | 7188 | 0.08 | 1120 | 0.40 | 0.18 | 0.17 | 16.50 | 9.46 | 1.34 | 0.29 | 373 | 1301.9 | 33.0 | 57.6 |
| Coyote Eyes Gulch | 5 | 7071 | 0.13 | 690 | 0.66 | 0.16 | 0.15 | 11.31 | 6.11 | 1.18 | 0.28 | 247 | 868.3 | 21.5 | 39.8 |
| Upper Winter Valley Gulch | 5 | 6678 | 0.14 | 270 | 0.62 | 0.11 | 0.09 | 6.16 | 3.50 | 1.32 | 0.10 | 170 | 1647.5 | 33.9 | 59.7 |
| Tumbling Gulch | 5 | 6367 | 0.05 | 240 | 0.44 | 0.07 | 0.06 | 8.38 | 5.46 | 1.87 | 0.11 | 219 | 1971.2 | 49.2 | 75.5 |
| **Browns Park Sandstone** | | | | | | | | | | | | | | | |
| Little Brown Gulch | 4 | 7353 | 0.08 | 250 | 0.54 | 0.20 | 0.14 | 1.77 | 0.98 | 1.24 | 0.02 | 61 | 2786.1 | 44.8 | 81.0 |
| Black Beaver Gulch | 5 | 7261 | 0.14 | 710 | 0.26 | 0.18 | 0.14 | 6.52 | 3.69 | 1.30 | 0.09 | 224 | 2546.5 | 42.0 | 74.2 |
| Upper Twelve Mile Gulch | 5 | 6392 | 0.04 | 310 | 0.48 | 0.09 | 0.20 | 9.94 | 5.68 | 1.33 | 0.14 | 274 | 1996.0 | 41.4 | 72.4 |
| Upper Maudlin Gulch | 5 | 6294 | 0.02 | 145 | 0.66 | 0.08 | 0.06 | 8.42 | 5.01 | 1.47 | 0.11 | 245 | 2269.0 | 46.4 | 78.0 |
| **Mancos Shale** | | | | | | | | | | | | | | | |
| Honey Gulch | 5 | 7294 | 0.20 | 300 | 0.67 | 0.15 | 0.15 | 4.38 | 2.69 | 1.59 | 0.08 | 139 | 1782.1 | 34.5 | 56.2 |
| Blister Gulch | 5 | 7224 | 0.08 | 770 | 0.56 | 0.17 | 0.17 | 14.58 | 8.62 | 1.45 | 0.22 | 307 | 1384.8 | 38.9 | 65.8 |
| Cross Gulch | 5 | 6977 | 0.10 | 268 | 0.47 | 0.05 | 0.05 | 12.12 | 6.99 | 1.36 | 0.21 | 262 | 1252.4 | 33.4 | 57.9 |
| Upper Boxelder Gulch | 5 | 6227 | 0.24 | 250 | 0.43 | 0.07 | 0.06 | 11.33 | 6.61 | 1.40 | 0.13 | 398 | 3171.3 | 52.7 | 90.3 |
| Forgotten Gulch | 5 | 5824 | 0.22 | 130 | 0.58 | 0.09 | 0.07 | 3.48 | 2.04 | 1.42 | 0.04 | 94 | 2385.8 | 51.6 | 88.3 |

Table 14
Field Site Morphologic Variables' Averages For Each Lithology
—Symbols Defined in Appendix A

| | $\bar{M}$ | $\bar{R}$ | $\bar{R_c}$ | $\bar{R_r}$ | $\bar{S}$ | $\bar{\Sigma l}$ | $\bar{\Sigma l_1}$ | $\dfrac{\bar{\Sigma l_1}}{\Sigma l_{2-5}}$ | $\bar{A}$ | $\dfrac{\bar{N_1}}{Basin}$ | $\bar{F_1}$ | $\bar{D_1}$ | $\bar{D}$ | $\bar{D}$ Range |
|---|---|---|---|---|---|---|---|---|---|---|---|---|---|---|
| Mesa Verde Sandstone | 0.10 | 622 | 0.55 | 0.15 | 0.13 | 10.08 | 5.79 | 1.39 | 0.20 | 229 | 1272.8 | 31.2 | 53.3 | 41.7 |
| Browns Park Sandstone | 0.07 | 388 | 0.47 | 0.12 | 0.13 | 8.29 | 4.79 | 1.37 | 0.11 | 248 | 2270.5 | 43.2 | 74.8 | 5.6 |
| Mancos Shale | 0.17 | 344 | 0.54 | 0.11 | 0.10 | 9.18 | 5.39 | 1.44 | 0.14 | 240 | 1995.3 | 42.2 | 71.7 | 34.1 |

TABLE 15

Results of Student's T-Test Comparing Morphologic Variables for Each Lithology

-Symbols Defined in Appendix A

| | Significantly Greater Than: | Significantly Greater Than: | Significantly Less Than: | Significantly Greater Than: | Significantly Less Than: | Significantly Less Than: |
|---|---|---|---|---|---|---|
| R (ft) | MVS > OL $\alpha$= 0.10 | MVS > BPS $\alpha$= 0.25 | BPS < MVS $\alpha$= 0.25 | BPS > MS $\alpha$= * | MS < BPS $\alpha$= * | MS < OL $\alpha$= 0.10 |
| Rc | MVS > OL $\alpha$= * | MVS > MS $\alpha$= * | MS < MVS $\alpha$= * | MS > BPS $\alpha$= 0.10 | BPS < MS $\alpha$= * | BPS < OL $\alpha$= * |
| Rr | MVS > OL $\alpha$= 0.25 | MVS > BPS $\alpha$= 0.25 | BPS < MVS $\alpha$= 0.25 | BPS > MS $\alpha$= * | MS < BPS $\alpha$= * | MS < OL $\alpha$= 0.25 |
| s (ft/ft) | MVS > OL $\alpha$= 0.25 | MVS > BPS $\alpha$= * | BPS < MVS $\alpha$= * | BPS > MS $\alpha$= * | MS < BPS $\alpha$= 0.25 | MS < OL $\alpha$= 0.25 |
| $\Sigma_1$ (mi) | MVS > OL $\alpha$= * | MVS > MS $\alpha$= * | MS < MVS $\alpha$= * | MS > BPS $\alpha$= * | BPS < MS $\alpha$= 0.25 | BPS < OL $\alpha$= 0.25 |
| $\Sigma_{11}$ (mi) | MVS > OL $\alpha$= * | MVS > MS $\alpha$= * | MS < MVS $\alpha$= * | MS > BPS $\alpha$= * | BPS < MS $\alpha$= 0.25 | BPS < OL $\alpha$= 0.25 |
| A (mi$^2$) | MVS > OL $\alpha$= 0.10 | MVS > MS $\alpha$= 0.10 | MS < MVS $\alpha$= 0.25 | MS > BPS $\alpha$= * | BPS < MS $\alpha$= 0.25 | BPS < OL $\alpha$= 0.05 |
| N$_1$/Basin (Channels) | BPS > OL $\alpha$= 0.25 | BPS > MS $\alpha$= * | MS < BPS $\alpha$= * | MS > MVS $\alpha$= * | MVS < MS $\alpha$= * | MVS < OL $\alpha$= * |
| F$_1$ $\frac{(Channels)}{mi^2}$ | BPS > OL $\alpha$= 0.05 | BPS > MS $\alpha$= 0.25 | MS < BPS $\alpha$= 0.25 | MS > MVS $\alpha$= 0.10 | MVS < MS $\alpha$= 0.025 | MVS < OL $\alpha$= 0.025 |
| D$_1$ (mi/mi$^2$) | BPS > OL $\alpha$= 0.05 | BPS > MS $\alpha$= * | MS < BPS $\alpha$= * | MS > MVS $\alpha$= 0.05 | MVS < MS $\alpha$= 0.10 | MVS < OL $\alpha$= 0.10 |
| D (mi/mi$^2$) | BPS > OL $\alpha$= 0.01 | BPS > MS $\alpha$= 0.10 | MS < BPS $\alpha$= * | MS > MVS $\alpha$= 0.05 | MVS < MS $\alpha$= 0.05 | MVS < OL $\alpha$= 0.05 |

MVS = Mesa Verde Sandstone
BPS = Browns Park Sandstone
MS = Mancos Shale
OL = Other lithologies
* The Significance of the Test is Less than 0.25.

channel, and total length of first-order stream channels, and the least average number of first-order stream channels.

The relatively small average number of first-order channels and large mean basin area result in a significantly lower average first-order channel frequency and density than is found on either the Browns Park Sandstone or Mancos Shale. Mean drainage density on the Mesa Verde Sandstone also is significantly less than on the other lithologies. It averages 53.3 miles/mile$^2$ and ranges from 33.8 to 75.5 miles/mile$^2$.

Among the Mesa Verde Sandstone basins, total channel length and total first-order channel length correlate well with basin relief (Table 16): as the basin becomes steeper, channel length increases. On the other hand, channel gradient correlates directly with basin slope. Although there is a fairly strong direct relationship between basin relief and slope (Table 17), the differences in their correlation with the other morphologic variables are substantial. Drainage-basin area and first-order channel frequency and density and drainage density also correlate well with relief and relief ratio, respectively. However, these relationships are obscured by strong direct intercorrelations between basin relief and vegetative cover ($R^2$ = 0.95) and basin slope and elevation ($R^2$ = 0.98). As the basin topography steepens and elevation increases, vegetative cover increases, resulting in greater drainage-basin area and lower channel frequency and drainage

TABLE 16

The Effect of Topographic Variability on
Drainage-Basin Morphology For The Mesa Verde Sandstone
—Symbols Defined in Appendix A

| | Regression Equation | $R^2$ |
|---|---|---|
| **$S(ft/ft)$** | | |
| R | $S = 0.0517 + 0.0001(R)$ | 0.73 |
| Rr | $S = 0.0131 + 0.774(Rr)$ | 0.97 |
| Rc | $S = 0.0562 + 0.138(Rc)$ | 0.22 |
| **$\sum_1 (mi)$** | | |
| R | $\sum_1 = 4.47 + 0.0090(R)$ | 0.69 |
| Rr | $\sum_1 = 7.43 + 17.2(Rr)$ | 0.21 |
| Rc | $\sum_1 = 20.1 - 18.1(Rc)$ | 0.30 |
| **$\sum_{11} (mi)$** | | |
| R | $\sum_{11} = 2.91 + 0.0046(R)$ | 0.57 |
| Rr | $\sum_{11} = 4.86 + 6.09(Rr)$ | 0.28 |
| Rc | $\sum_{11} = 12.8 - 12.6(Rc)$ | 0.45 |
| **$A(mi^2)$** | | |
| R | $A = 0.0655 + 0.0002(R)$ | 0.83 |
| Rr | $A = 0.0566 + 0.963(Rr)$ | 0.57 |
| Rc | $A = 0.173 + 0.0581(Rc)$ | 0.33 |
| **$F_1 (Channels/mi^2)$** | | |
| R | $F_1 = 1870 - 0.960(R)$ | 0.40 |
| Rr | $F_1 = 2402 - 7340(Rr)$ | 0.86 |
| Rc | $F_1 = 2822 - 2819(Rc)$ | 0.36 |
| **$D_1 (mi/mi^2)$** | | |
| R | $D_1 = 42.2 - 0.0176(R)$ | 0.29 |
| Rr | $D_1 = 53.6 - 145(Rr)$ | 0.74 |
| Rc | $D_1 = 71.8 - 73.5(Rc)$ | 0.54 |
| **$D(mi/mi^2)$** | | |
| R | $D = 67.7 - 0.0232(R)$ | 0.27 |
| Rr | $D = 84.4 - 202(Rr)$ | 0.76 |
| Rc | $D = 109 - 101(Rc)$ | 0.54 |

TABLE 17

The Effect of Increasing Relief on Basin Slope
and Circularity For Each Lithology
—Symbols Defined in Appendix A

| Regression Equation | $R^2$ | Sum of Squares Variable 1 (%) | Variable 2 (%) |
|---|---|---|---|
| **Mesa Verde Sandstone** | | | |
| Rr = 0.0603 + 0.0002(R) | 0.61 | | |
| Rc = 0.586 - 0.0001(R) | 0.29 | | |
| **Browns Park Sandstone** | | | |
| Rr = 0.587 + 0.0002(R) - 0.109(u) | 0.99 | 28.1 | 71.9 |
| Rc = 0.604 - 0.0007(R) + 0.0257(u) | 0.97 | 99.5 | 0.5 |
| **Mancos Shale** | | | |
| Rr = 0.0551 + 0.0002(R) | 0.52 | | |
| Rc = 0.528 - 0.0000(R) | 0.32 | | |

The Browns Park Sandstone correlations are calculated by multiplying the correlation coefficient ($R^2$) by the sum of squares (%) for the variable of interest. To eliminate variance created by the difference in basin order, the correlation coefficient is multiplied by the sum of squares for Variable 1. The small number of Browns Park Sandstone basins included in the multivariate regression analyses may have caused unrealistic correlation coefficients.

In contrast to the Mesa Verde Sandstone and Mancos Shale drainage basins, the correlation between basin relief and slope for the Browns Park Sandstone field sites is low ($R^2 = 0.28$) (Table 17) and the relationships between basin relief and the other morphologic variables are extremely poor (Table 18). Also, in contrast to the basins in the other lithologies, the inverse relationship between basin relief and circularity for the Browns Park Sandstone field sites is very strong, having an $R^2$ of 0.96. Therefore, as in the case of relief, the correlation between basin circularity and most of the other morphologic variables is low.

Among the Browns Park Sandstone field sites, relief ratio correlates well with several morphologic variables. As basin slope steepens, the number of first-order channels increases whereas the drainage-basin area decreases. As among the Mesa Verde Sandstone basins, relief ratio has a strong intercorrelation with elevation ($R^2 = 1.00$).

density. For the Mesa Verde Sandstone basins, the inverse relationship between basin relief and basin circularity is poor, having an $R^2$ of 0.29. Likewise, the correlation between basin circularity and the other morphologic variables is moderately low.

## Browns Park Sandstone Field Sites

Drainage basins that form on the erosive Browns Park Sandstone are small and gently sloping with stream networks of many closely spaced steep gradient channels (Table 14). Although the average total length of stream channel and total length of first-order stream channels are significantly less than for the drainages on the other lithologies, the Browns Park Sandstone networks' average number of first-order stream channels is greater (Table 15).

The high average number of first-order stream channels and small drainage-basin area result in a higher mean first-order channel frequency and density for the Browns Park Sandstone basins than for basins of the Mesa Verde Sandstone and Mancos Shale. Drainage density also is significantly greater for the Browns Park Sandstone basins. It averages 74.8 miles/mile$^2$ and ranges from 72.4 to 78.0 miles/mile$^2$. Although the Browns Park Sandstone soils have high infiltration and permeability, their erodibility results in a finer drainage network than is found on the other lithologies.

Table 18

The Effect of Topographic Variability on
Drainage-Basin Morphology For the Browns Park Sandstone
-Symbols Defined In Appendix A

| Regression Equation | $R^2$ | Sum of Squares Variable 1 (%) | Variable 2 (%) |
|---|---|---|---|
| **S (ft/ft)** | | | |
| R   S = 0.197 + 0.0001 (R) - 0.0198 (u) | 0.14 | 78.9 | 21.1 |
| Rr   * | * | * | * |
| Rc   S = 0.314 - 0.176 (Rc) - 0.0201 (u) | 0.28 | 88.7 | 11.3 |
| **$\sum_1$ (mi)** | | | |
| R   * | * | * | * |
| Rr   $\sum_1$ = - 11.2 - 24.8 (Rr) + 4.49 (u) | 0.95 | 76.4 | 23.6 |
| Rc   * | * | * | * |
| **$\sum_{1_1}$ (mi)** | | | |
| R   * | * | * | * |
| Rr   $\sum_{1_1}$ = - 5.95 - 15.8 (Rr + 2.52 (u) | 0.97 | 78.7 | 21.3 |
| Rc   * | * | * | * |
| **A (mi²)** | | | |
| R   * | * | * | * |
| Rr   A = - 0.170 - 0.311 (Rr) + 0.0636 (u) | 0.92 | 74.2 | 25.8 |
| Rc   * | * | * | * |
| **$F_1$ (Channels/mi²)** | | | |
| R   * | * | * | * |
| Rr   $F_1$ = 2834 + 3815 (Rr) - 202 (u) | 0.84 | 94.2 | 5.8 |
| Rc   * | * | * | * |
| **$D_1$ (mi/mi²)** | | | |
| R   $D_1$ = 49.0 - 0.0061 (R) - 0.682 (u) | 0.55 | 96.0 | 4.0 |
| Rr   * | * | * | * |
| Rc   $D_1$ = 42.4 + 10.5 (Rc) - 0.806 (u) | 0.64 | 95.6 | 4.4 |
| **D (mi/mi²)** | | | |
| R   D = 104 - 0.0046 (R) - 5.50 (u) | 0.72 | 34.5 | 65.5 |
| Rr   D = 115 - 16.9 (Rr) - 7.54 (u) | 0.68 | 20.6 | 79.4 |
| Rc   D = 98.5 + 8.76 (Rc) - 5.54 (u) | 0.78 | 36.1 | 63.9 |

* Correlation Coefficient Is Less Than 0.10.

Consequently, the relationships between basin slope and the other variables are influenced also by climate and vegetation. The latter influence is apparent in the inverse relationships between basin slope and the total length of channel and total length of first-order channels. Among the Browns Park Sandstone basins, drainage density correlates poorly with all of the topographic variables. Similarly, channel gradient does not correlate well, linearly, with basin relief, circularity, or slope.

## Mancos Shale Field Sites

Drainage basins on the impermeable Mancos Shale are small and circular, and have very gentle topography (Table 14). The Mancos Shale drainage basins have significantly lower average relief and slope than basins of the other lithologies (Table 15). Consequently, average channel gradient is significantly less than on the Mesa Verde and Browns Park Sandstones. Like the stream networks on the Browns Park Sandstone, the Mancos Shale drainages' mean total length of stream channel and total length of first-order stream channels are low, but the average number of first-order channels is relatively high.

The large average number of first-order channels and small drainage-basin area result in a mean first-order channel frequency and density which is significantly higher than that of basins in the Mesa Verde Sandstone and slightly less than that of basins in the Browns Park Sandstone. For

the Mancos Shale field sites, drainage density averages 71.7 miles/mile$^2$ and ranges from 56.2 to 90.3 miles/mile$^2$. It also is significantly greater than the average network density of the Mesa Verde Sandstone basins and slightly less than that of the Browns Park Sandstone basins. The low infiltration capacity and permeability of the Mancos Shale and its soils promote high surface runoff. Consequently, drainage density is high.

Among the Mancos Shale drainage basins, several of the morphologic variables correlate best with basin relief (Table 19). As the topography becomes steeper, total channel length, total first-order channel length, and drainage-basin area increase. On the other hand, the relationships between first-order channel frequency and density and drainage density with basin relief are very weak. The latter correlate better with the climatic and vegetative variables. Channel gradient has a strong direct relationship with basin slope. The Mancos Shale drainage basins have a moderate direct correlation between basin relief and slope ($R^2 = 0.52$) and a low inverse correlation between basin relief and circularity ($R^2 = 0.32$) (Table 17). In addition, except for channel gradient, the relationships between basin slope and circularity with the other morphologic variables are poor.

TABLE 19
The Effect of Topographic Variability on
Drainage-Basin Morphology for the Mancos Shale
-Symbols Defined in Appendix A

| | Regression Equation | $R^2$ |
|---|---|---|
| **S (ft/ft)** | | |
| R | S = 0.0446 + 0.0002 (R) | 0.58 |
| Rr | S = -0.0071 + 0.998 (Rr) | 0.98 |
| Rc | S = -0.0978 + 0.365 (Rc) | 0.46 |
| **$\sum l$ (mi)** | | |
| R | $\sum l$ = 4.52 +0.0136 (R) | 0.46 |
| Rr | $\sum l$ = 9.22 - 0.341 (Rr) | 0.33 |
| Rc | $\sum l$ = 26.9 -32.7 (Rc) | 0.41 |
| **$\sum l_1$ (mi)** | | |
| R | $\sum l_1$ = 2.61 + 0.0081 (R) | 0.49 |
| Rr | $\sum l_1$ = 5.24 + 1.43 (Rr) | 0.33 |
| Rc | $\sum l_1$ = 15.3 - 18.4 (Rc) | 0.38 |
| **A (mi$^2$)** | | |
| R | A = 0.0570 + 0.0002 (R) | 0.49 |
| Rr | A = 0.125 + 0.0930 (Rr) | 0.33 |
| Rc | A = 0.340 - 0.379 (Rc) | 0.21 |
| **$F_1$ (Channels/mi$^2$)** | | |
| R | $F_1$ = 2543 - 1.59 (R) | 0.25 |
| Rr | $F_1$ = 2570 - 5365 (Rr) | 0.17 |
| Rc | $F_1$ = 3440 - 2671 (Rc) | 0.19 |
| **$D_1$ (mi/mi$^2$)** | | |
| R | $D_1$ = 47.0 - 0.0140 (R) | 0.15 |
| Rr | $D_1$ = 48.2 - 55.8 (Rr) | 0.21 |
| Rc | $D_1$ = 60.3 - 33.4 (Rc) | 0.17 |
| **D (mi/mi$^2$)** | | |
| R | D = 80.3 - 0.0250 (R) | 0.14 |
| Rr | D = 84.1 - 116 (Rr) | 0.16 |
| Rc | D = 110 - 69.9 (Rc) | 0.17 |

## Climate and Drainage Basin Morphology

To determine the effect of climate on basin morphology, the morphologic variables were regressed with several climatic and vegetative variables. The latter were chosen so that the effects of precipitation, temperature, and vegetative cover can be considered separately and in combination with one or both of the others. The variables fall into two categories: (1) climatic data, including mean annual precipitation, mean monthly precipitation range, mean annual temperature, mean monthly temperature range, mean annual potential evapotranspiration, and mean annual net precipitation, and (2) vegetative cover data, including percentage of vegetative cover, Thornthwaites P-E Index, mean seasonal net rainfall, and percent mean seasonal rainfall.

The drainage basins at higher elevations, where the climate is cooler and more moist and where vegetative cover is greater, are associated with steeper topography (Table 13). Drainage basin slope is highly correlated with elevation whereas basin relief is highly correlated with vegetative cover. The steep topography of the high elevation sites results in slightly more elongated drainage basins with steeper channel gradients than among the warmer drier sites.

Among the Mesa Verde Sandstone basins, the total length of channel and total length of first-order channels correlate well with the percentage of vegetative cover and

the mean monthly precipitation range (Tables 20 and 21).
However, their respective direct and inverse trends reflect
the influence of basin relief. Drainage-basin area is
determined by the amount of mean annual precipitation and
net precipitation (Table 22), the percentage of vegetative
cover and P-E Index (Table 20), and the percentage of mean
seasonal rainfall (Table 23). As the amount of available
moisture and the vegetative cover increase, the drainage-
basin area increases. The frequency and density of first-
order channels and drainage density correlate best with the
variables which incorporate mean annual temperature
(Figure 9) and potential evapotranspiration (Table 23)
(Figure 10). In addition, they are related inversely to
elevation and mean annual precipitation (Figures 11 and 12)
and directly to the percentage of mean seasonal rainfall
(Figure 13).

Among the Browns Park Sandstone drainage basins,
the total length of channel and total length of first-order
channels are determined largely by mean annual temperature,
precipitation, and net precipitation and mean seasonal net
rainfall (Tables 24-26). Similarly, drainage-basin area and
the frequency of first-order channels correlate well with
the climatic variables as well as those indicating the
potential for vegetation. As available moisture increases,
the frequency of first-order channels increases and channel
length and basin area decrease. The density of first-order
channels and drainage density correlate best with the

## TABLE 20
### The Effect of Vegetative Cover Variability on Drainage-Basin Morphology
### For the Mesa Verde Sandstone - Direct Relationships
### -Symbols Defined in Appendix A

| | Regression Equation | $R^2$ |
|---|---|---|
| **$\sum_1$ (mi)** | | |
| % Veg. Cover | $\sum_1 = -2.13 + 0.318$ (% Veg. Cover) | 0.84 |
| P-E Index | $\sum_1 = 3.46 + 0.0339$ (P.E. Index) | 0.18 |
| M.S. Net Rainfall | $\sum_1 = 13.6 + 0.472$ (M.S. Net Rainfall) | 0.24 |
| **$\sum_{11}$ (mi)** | | |
| % Veg. Cover | $\sum_{11} = -0.747 + 0.170$ (% Veg. Cover) | 0.76 |
| P-E Index | $\sum_{11} = 3.11 + 0.0138$ (P-E Index) | 0.21 |
| M.S. Net Rainfall | $\sum_{11} = 7.01 + 0.166$ (M.S. Net Rainfall) | 0.30 |
| **A ($mi^2$)** | | |
| % Veg. Cover | $A = -0.0652 + 0.0070$ (% Veg. Cover) | 0.80 |
| P-E Index | $A = -0.111 + 0.0016$ (P-E Index) | 0.80 |
| M.S. Net Rainfall | $A = 0.421 + 0.0294$ (M.S. Net Rainfall) | 0.53 |
| **$F_1$ (Channels/$mi^2$)** | | |
| % Veg. Cover | $F_1 = 2209 - 24.4$ (% Veg. Cover) | 0.25 |
| P-E Index | $F_1 = 3195 - 9.84$ (P-E Index) | 0.77 |
| M.S. Net Rainfall | $F_1 = -427 - 231$ (M.S. Net Rainfall) | 0.85 |
| **$D_1$ ($mi/mi^2$)** | | |
| % Veg. Cover | $D_1 = 46.4 - 0.395$ (% Veg. Cover) | 0.14 |
| P-E Index | $D_1 = 69.2 - 0.194$ (P-E Index) | 0.66 |
| M.S. Net Rainfall | $D_1 = -0.867 - 4.37$ (M.S. Net Rainfall) | 0.67 |
| **D ($mi/mi^2$)** | | |
| % Veg. Cover | $D = 73.4 - 0.525$ (% Veg. Cover) | 0.16 |
| P-E Index | $D = 107 - 0.277$ (P-E Index) | 0.70 |
| M.S. Net Rainfall | $D = 7.17 - 6.27$ (M.S. Net Rainfall) | 0.72 |

**TABLE 21**

**The Effect of Vegetative Cover Variability on Drainage-Basin Morphology**
**For the Mesa Verde Sandstone - Inverse Relationships**
**-Symbols Defined in Appendix A**

| | Regression Equation | $R^2$ |
|---|---|---|
| $\sum_1$ (mi) | | |
| % M.S. | | |
| Rainfall | $\sum_1 = 23.3 - 0.212$ (% M.S. Rainfall) | 0.18 |
| M.Mo. T Range | $\sum_1 = 16.9 - 0.154$ (M.Mo.T Range) | 0.31 |
| M.M. PPT Range | $\sum_1 = 69.6 - 66.9$ (M.Mo. PPT Range) | 0.62 |
| $\sum_{11}$ (mi) | | |
| % M.S. | | |
| Rainfall | $\sum_{11} = 10.5 - 0.0758$ (% M.S. Rainfall) | 0.24 |
| M.Mo. T Range | $\sum_{11}\ 7.52 - 0.0390$ (M.Mo.T Range) | 0.33 |
| M.Mo. PPT Range | $\sum_{11}\ 40.4 - 38.9$ (M.Mo. PPT Range) | 0.66 |
| A (mi²) | | |
| %M.S. | | |
| Rainfall | $A = 0.796 - 0.0095$ (% M.S. Rainfall) | 0.71 |
| M.Mo. T. Range | $A = 0.769 - 0.0127$ (M.Mo. T Range) | 0.26 |
| M.Mo. PPT Range | $A = 1.37 - 1.31$ (M.Mo. PPT Range) | 0.46 |
| F₁ (Channels/mi²) | | |
| % M.S. | | |
| Rainfall | $F_1 = -2423 + 59.2$ (% M.S. Rainfall) | 0.72 |
| M.Mo. T. Range | $F_1 = -4024 + 119$ (M.Mo. T Range) | 0.60 |
| M.Mo. PPT Range) | $F_1 = -1851 + 3514$ (M.Mo. PPT Range) | 0.22 |
| D₁ (mi/mi²) | | |
| % M.S. | | |
| Rainfall | $D_1 = -53.2 + 1.35$ (% M.S. Rainfall) | 0.83 |
| M.Mo. T Range | $D_1 = -68.7 + 2.26$ (M. Mo. T Range) | 0.47 |
| M.Mo. PPT Range | $D_1 = 16.1 + 17.1$ (M.Mo. PPT Range) | 0.33 |
| D(mi/mi²) | | |
| % M.S. | | |
| Rainfall | $D = -57.2 + 1.77$ (%M.S. Rainfall) | 0.74 |
| M.Mo. T Range | $D = -88.9 + 3.21$ (M.Mo. T Range) | 0.50 |
| M.Mo. PPT Range | $D = 17.8 + 39.9$ (M.Mo. PPT Range) | 0.32 |

TABLE 22

The Effect of Precipitation Variability on
Drainage-Basin Morphology For the Mesa Verde Sandstone
—Symbols Defined in Appendix A

| | Regression Equation | $R^2$ |
|---|---|---|
| $\sum 1$ (mi) | | |
| M.A. PPT | $\sum 1 = -0.876 + 0.633$ (M.A. PPT) | 0.19 |
| M.A. Net PPT | $\sum 1 = 11.3 + 0.376$ (M.A. Net PPT) | 0.15 |
| $\sum 1_1$ (mi) | | |
| M.A. PPT | $\sum 1_1 = 1.27 + 0.274$ (M.A. PPT) | 0.20 |
| M.A. Net PPT | $\sum 1_1 = 6.24 + 0.143$ (M.A. Net PPT) | 0.25 |
| A (mi$^2$) | | |
| M.A. PPT | $A = -0.309 + 0.0311$ (M.A. PPT) | 0.84 |
| M.A. Net PPT | $A = 0.267 + 0.0198$ (M.A. Net PPT) | 0.76 |
| $F_1$ (Channels/mi$^2$) | | |
| M.A. PPT | $F_1 = 4548 - 198$ (M.A. PPT) | 0.88 |
| M.A. Net | $F_1 = 843 - 137$ (M.A. Net PPT) | 0.95 |
| D(mi/mi$^2$) | | |
| M.A. PPT | $D_1 = 94.7 - 3.84$ (M.A.PPT) | 0.72 |
| M.A. Net PPT | $D_1 = 22.8 - 2.68$ (M.A. Net PPT) | 0.79 |
| D(mi/mi$^2$) | | |
| M.A. PPT | $D = 144 - 5.47$ (M.A. PPT) | 0.77 |
| M.A. Net PPT | $D = 41.4 - 3.80$ (M.A. Net PPT) | 0.84 |

## Table 23
### The Effect of Temperature Variability on Drainage-Basin Morphology For the Mesa Verde Sandstone —Symbols Defined in Appendix A

| | | Regression Equation | $R^2$ |
|---|---|---|---|
| $\sum_1$ (mi) | M.A.T. | $\sum_1 = 32.7 - 0.556$ (M.A.T.) | 0.27 |
| | M.A. Pot.ET | $\sum_1 = 22.0 - 0.607$ (M.A. Pot.ET) | 0.27 |
| $\sum_{l_1}$ (mi) | M.A.T. | $\sum_{l_1} = 11.1 - 0.131$ (M.A.T.) | 0.32 |
| | M.A. Pot.ET | $\sum_{l_1} = 8.89 - 0.157$ (M.A. Pot.ET) | 0.32 |
| A (mi$^2$) | M.A.T. | $A = 1.97 - 0.0434$ (M.A.T.) | 0.57 |
| | M.A. Pot.ET | $A = 1.09 - 0.0450$ (M.A. Pot.ET) | 0.52 |
| $F_1$ (Channels/mi$^2$) | M.A.T. | $F_1 = -13018 + 351$ (M.A.T.) | 0.96 |
| | M.A. Pot.ET | $F_1 = -5986 + 369$ (M.A. Pot.ET) | 0.90 |
| $D_1$ (mi/mi$^2$) | M.A.T. | $D_1 = -256 + 7.06$ (M.A.T.) | 0.85 |
| | M.A. Pot.ET | $D_1 = -114 + 7.36$ (M.A. Pot.ET) | 0.79 |
| D (mi/mi$^2$) | M.A.T. | $D_1 = -351 + 9.93$ (M.A.T.) | 0.89 |
| | M.A. Pot.ET | $D = -150 + 10.3$ (M.A. Pot.ET) | 0.82 |
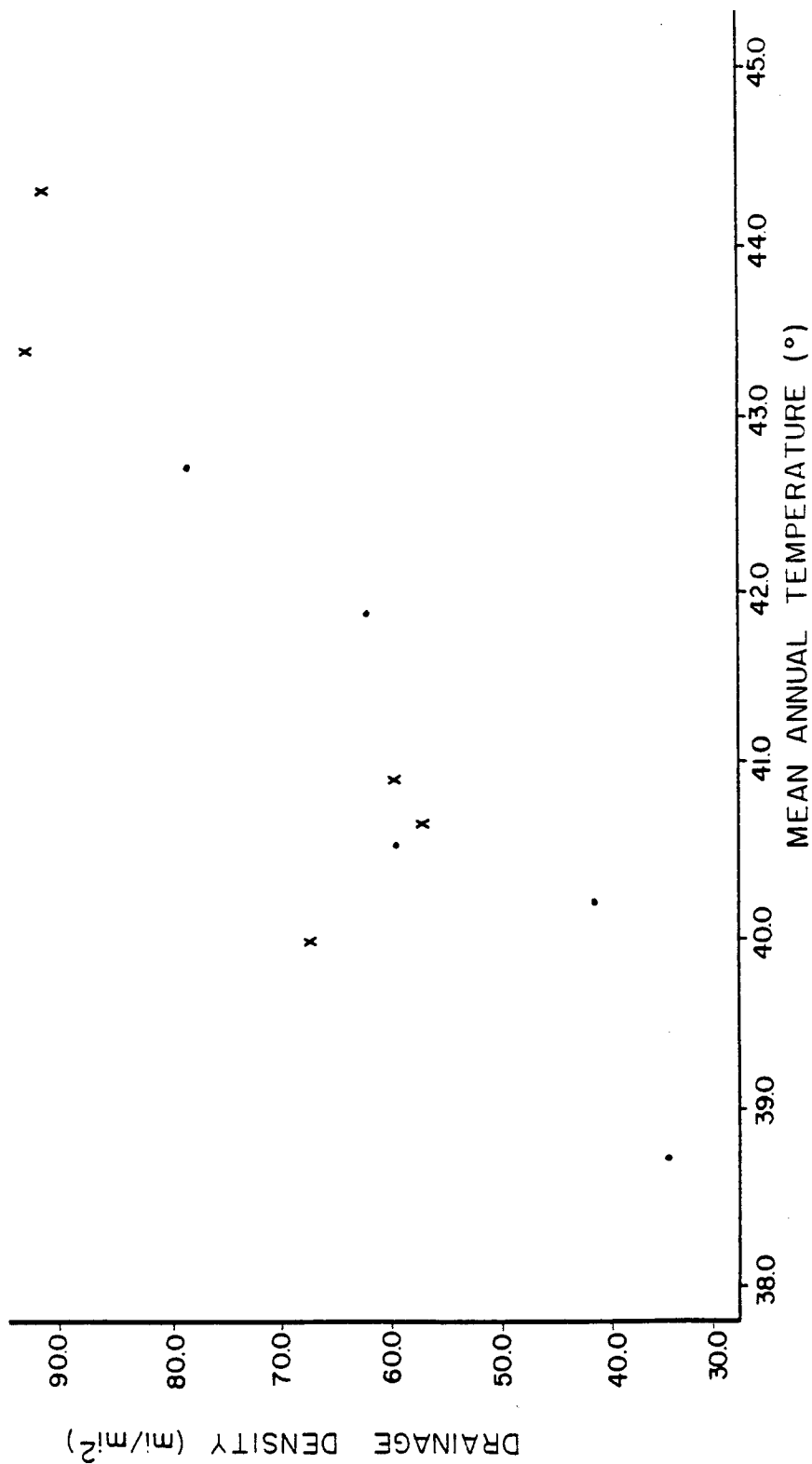
·  MESA VERDE SANDSTONE
x  MANCOS SHALE

FIGURE 9.  A plot of drainage density against mean annual
temperature for the Mesa Verde Sandstone and
Mancos Shale.
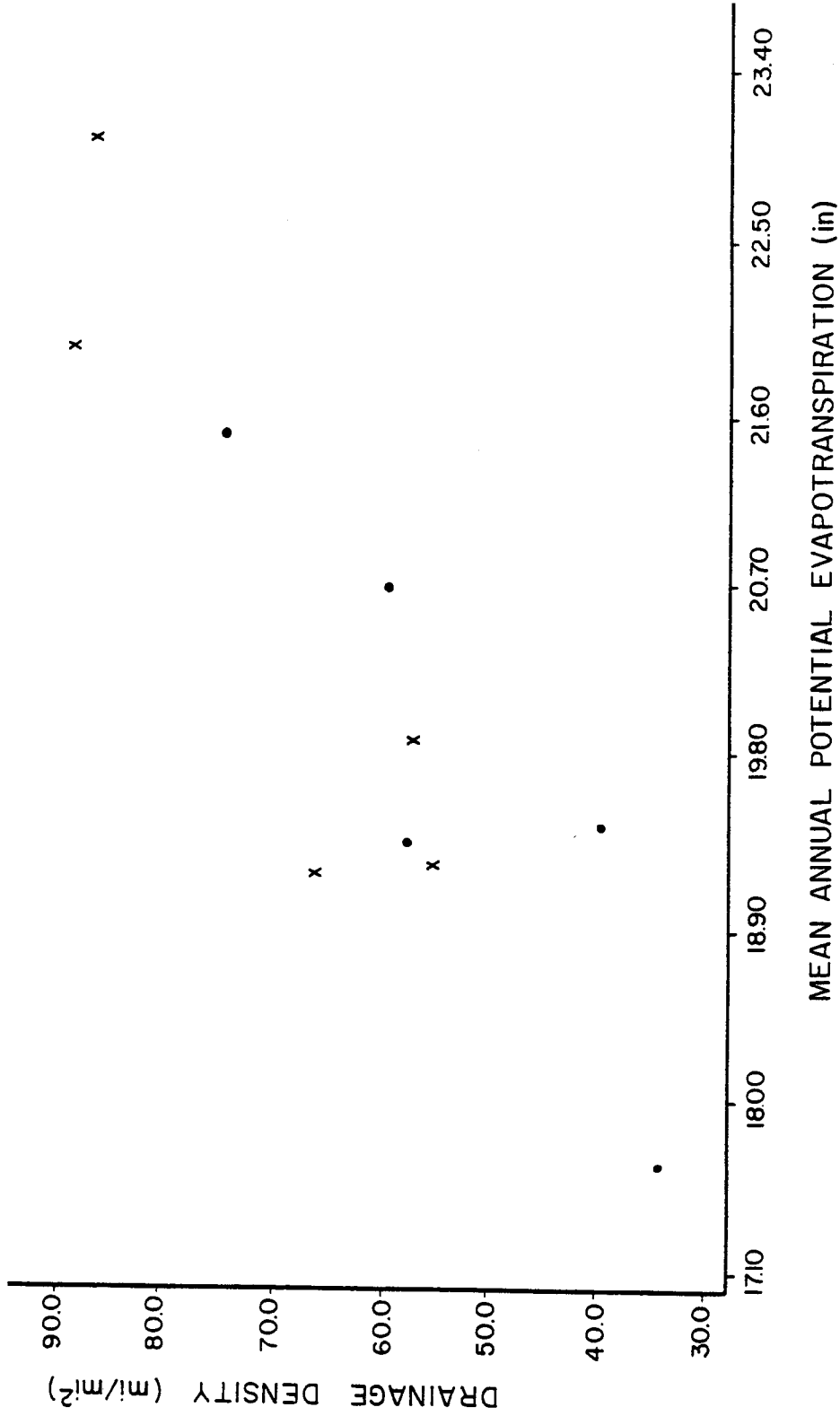
- MESA VERDE SANDSTONE
x MANCOS SHALE

FIGURE 10. A plot of drainage density against mean annual
potential evapotranspiration for the Mesa Verde
Sandstone and Mancos Shale.

FIGURE 11. A plot of drainage density against mean annual precipitation for the Mesa Verde Sandstone and Mancos Shale.

FIGURE 12. A plot of drainage density against mean annual
net precipitation for the Mesa Verde Sandstone
and Mancos Shale.

94
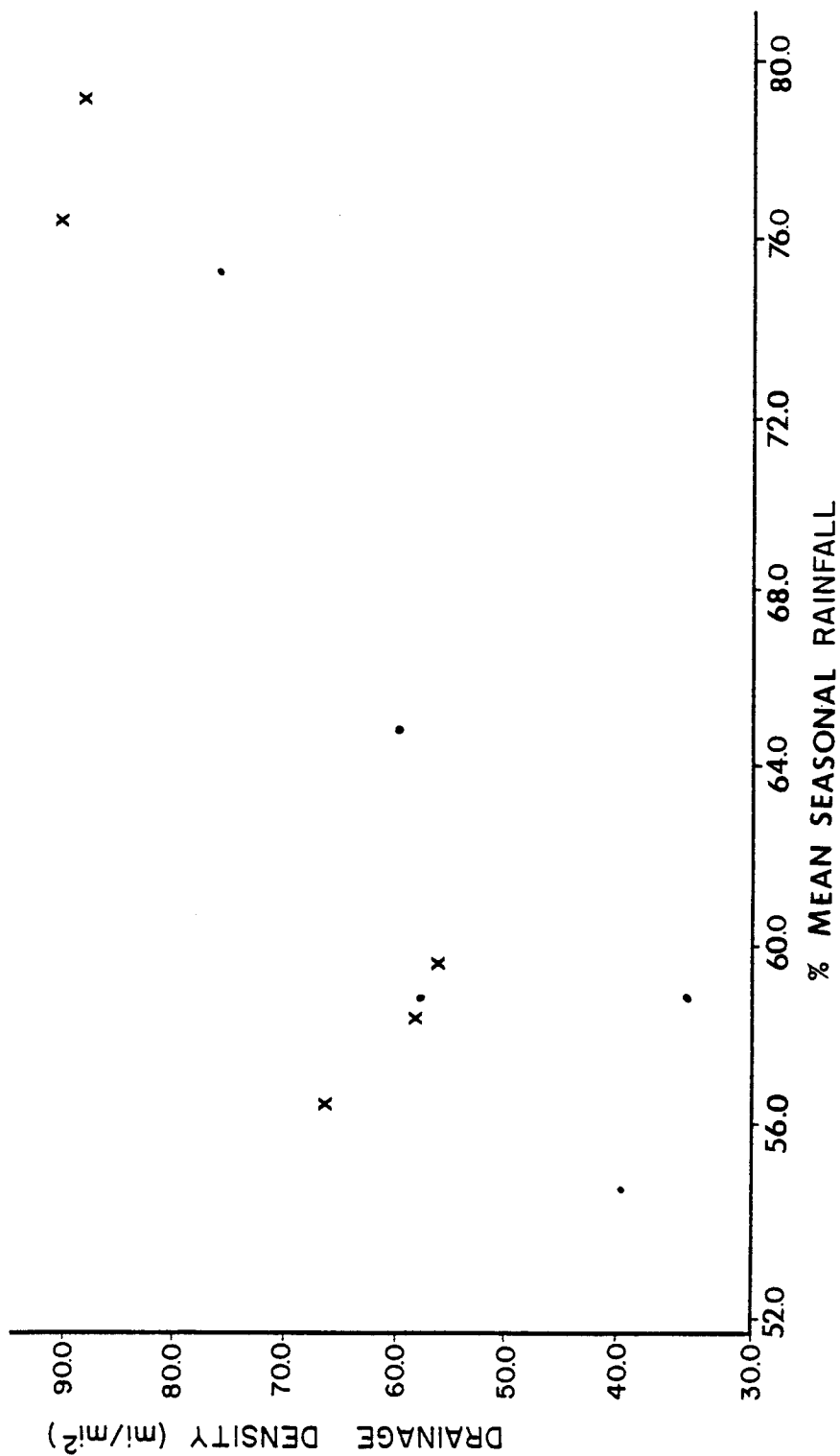


• MESA VERDE SANDSTONE
x MANCOS SHALE

FIGURE 13.   A plot of drainage density against the
percentage of mean seasonal rainfall for the
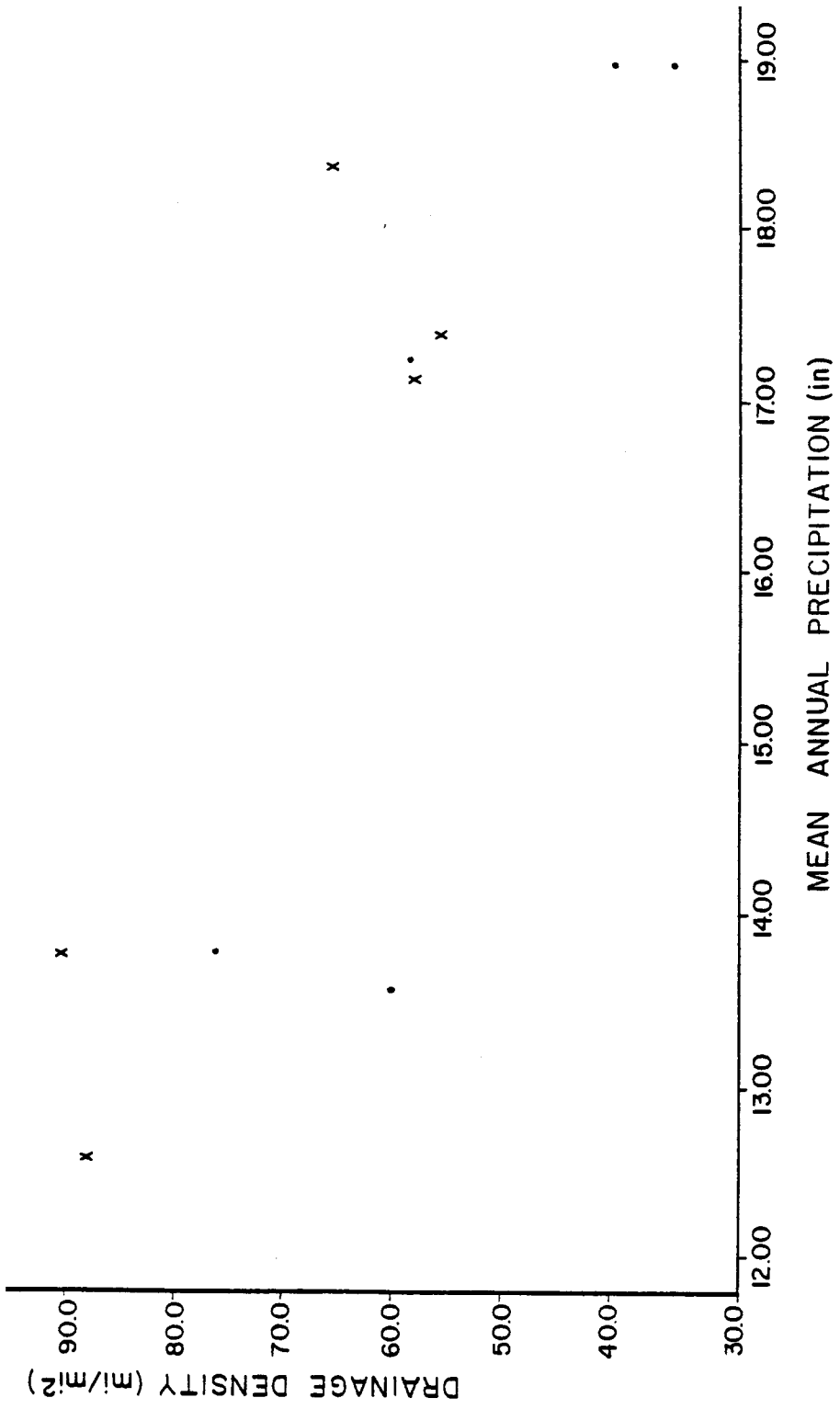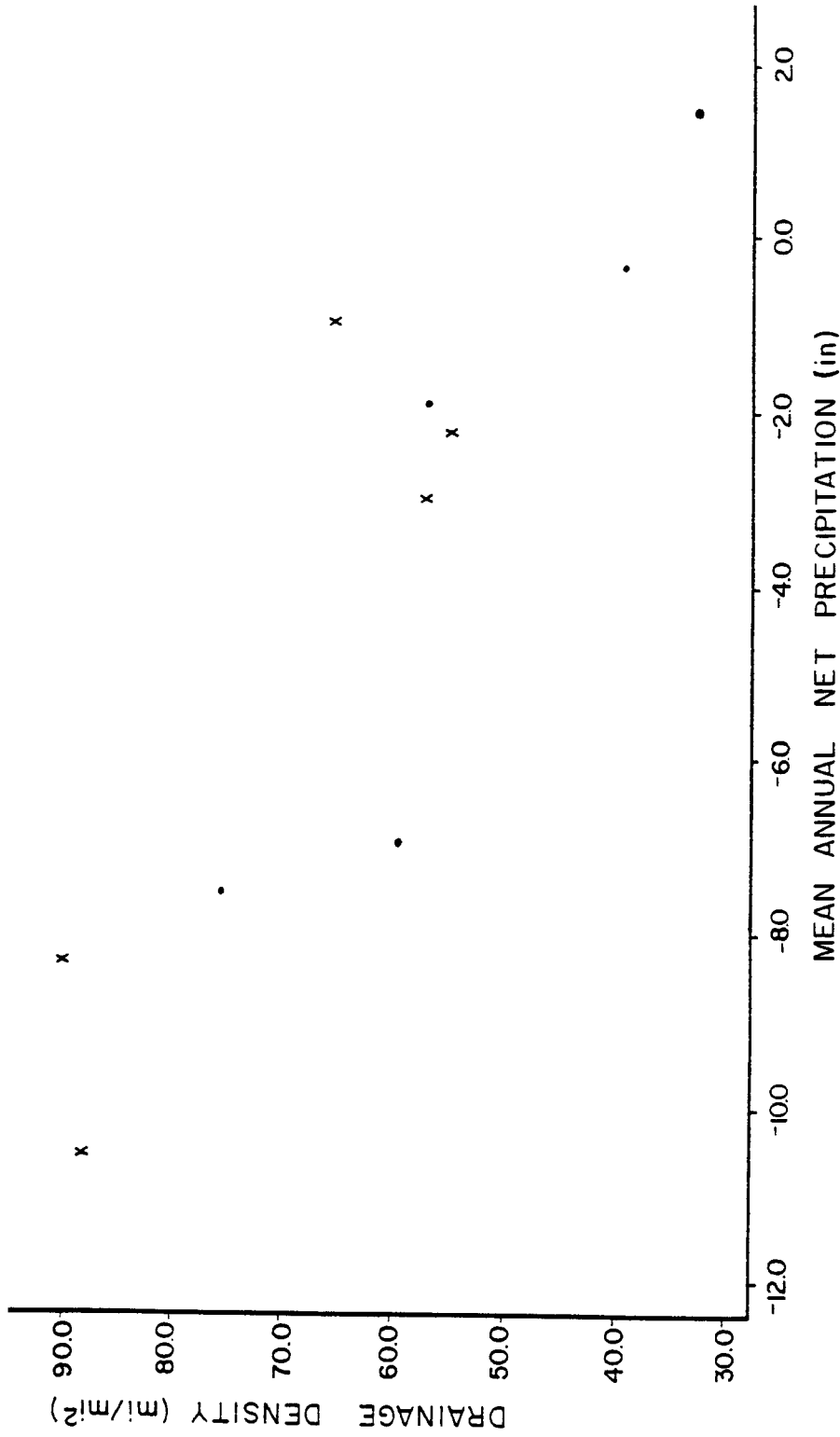Mesa Verde Sandstone and Mancos Shale.

## Table 24
### The Effect of Precipitation Variability on Drainage-Basin Morphology For The Browns Park Sandstone
### —Symbols Defined in Appendix A

| Regression Equation | $R^2$ | Sum of Squares | |
| --- | --- | --- | --- |
| | | Variable 1 (%) | Variable 2 (%) |
| **$\sum_1$ (mi)** | | | |
| M.A. PPT  $\sum_1 = 0.174 - 0.873$ (M.A. PPT) $+ 4.57$ (Order) | 1.00 | 72.1 | 27.9 |
| M.A. Net PPT  $\sum_1 = -15.9 - 0.536$ (M.A. Net PPT) $+ 4.46$ (Order) | 1.00 | 74.6 | 25.4 |
| **$\sum_{11}$ (mi)** | | | |
| M.A. PPT  $\sum_{11} = -0.0068 - 0.509$ (M.A. PPT) $+ 2.68$ (Order) | 1.00 | 71.9 | 28.1 |
| M.A. Net PPT  $\sum_{11} = -9.22 - 0.321$ (M.A. Net PPT) $+ 2.57$ (Order) | 1.00 | 75.4 | 24.6 |
| **A (mi²)** | | | |
| M.A. PPT  $A = 0.0182 - 0.0126$ (M.A. PPT) $+ 0.0611$ (Order) | 1.00 | 73.8 | 26.2 |
| M.A. Net PPT  $A = -0.218 - 0.0074$ (M.A. Net PPT) $+ 0.0606$ (Order) | 0.98 | 75.0 | 25.0 |
| **$F_1$ (Channels/mi²)** | | | |
| M.A. PPT  $F_1 = 905 + 141$ (M.A. PPT) $- 202$ (Order) | 1.00 | 94.2 | 5.8 |
| M.A. Net PPT  $F_1 = 3511 + 85.1$ (M.A. Net PPT) $- 188$ (Order) | 0.98 | 34.0 | 66.0 |
| **$D_1$ (mi/mi²)** | | | |
| M.A. PPT  * | * | * | * |
| M.A. Net PPT  * | * | * | * |
| **D (mi/mi²)** | | | |
| M.A. PPT  $D = 93.1 + 0.443$ (M.A. PPT) $- 5.16$ (Order) | 0.67 | 55.1 | 44.9 |
| M.A. Net PPT  $D = 104 + 0.0679$ (M.A. Net PPT) $- 5.88$ (Order) | 0.64 | 41.5 | 58.5 |

*Correlation Coefficient is less than 0.10.

Table 25

The Effect of Temperature Variability on
Drainage-Basin Morphology For The Browns Park Sandstone
-Symbols Defined in Appendix A

| Regression Equation | $R^2$ | Sum of Squares | |
|---|---|---|---|
| | | Variable 1 (%) | Variable 2 (%) |
| **$\sum l$ (mi)** | | | |
| M.A.T. | | | |
| $\sum l = -65.5 + 1.26$ (M.A.T.) $+ 4.39$ (Order) | 0.98 | 76.7 | 23.3 |
| M.A. Pot.ET | | | |
| $\sum l = -38.1 + 1.12$ (M.A. Pot.ET) $+ 4.71$ (Order) | 0.96 | 70.7 | 29.3 |
| **$\sum l_1$ (mi)** | | | |
| M.A.T. | | | |
| $\sum l_1 = -39.7 + 0.780$ (M.A.T.) $+ 2.50$ (Order) | 0.99 | 78.3 | 21.7 |
| M.A. Pot.ET | | | |
| $\sum l_1 = -22.9 + 0.702$ (M.A. Pot.ET) $+ 2.67$ (Order) | 0.98 | 72.9 | 27.1 |
| **A (mi²)** | | | |
| M.A.T. | | | |
| $A = -0.880 + 0.0167$ (M.A.T.) $+ 0.0610$ (Order) | 0.95 | 75.8 | 24.2 |
| M.A. Pot.ET | | | |
| $A = -0.511 + 0.0143$ (M.A. Pot.ET) $+ 0.0659$ (Order) | 0.93 | 68.8 | 31.2 |
| **$F_1$ (Channels/mi²)** | | | |
| M.A.T. | | | |
| $F_1 = 11299 - 198$ (M.A.T.) $- 182$ (Order) | 0.92 | 95.4 | 4.6 |
| M.A. Pot.ET | | | |
| $F_1 = 6980 - 173$ (M.A. Pot.ET) $- 235$ (Order) | 0.87 | 91.3 | 8.7 |
| **$D_1$ (mi/mi²)** | | | |
| M.A.T. | | | |
| * | * | * | * |
| M.A. Pot.ET | | | |
| * | * | * | * |
| **D (mi/mi²)** | | | |
| M.A.T. | | | |
| $D = 94.7 + 0.333$ (M.A.T.) $- 6.71$ (Order) | 0.65 | 30.2 | 69.8 |
| M.A. Pot.ET | | | |
| $D = 98.4 + 0.583$ (M.A. Pot.ET) $- 7.09$ (Order) | 0.67 | 18.2 | 81.8 |

*Correlation Coefficient is less than 0.10.

Table 26

The Effect of Vegetative Cover Variability on Drainage-Basin Morphology
For the Browns Park Sandstone-Direct Relationships
-Symbols Defined in Appendix A

| Regression Equation | $R^2$ | Sum of Squares Variable 1 (%) | Variable 2 (%) |
|---|---|---|---|
| **$\Sigma_1$ (mi)** | | | |
| % Veg. Cover | * | * | * |
| P-E Index    $\Sigma_1 = -5.76 - 0.0446$ (P-E index) $+ 4.80$ (Order) | 0.99 | 67.1 | 32.9 |
| M.S. Net Rainfall    $\Sigma_1 = -21.2 - 0.770$ (M.S. Net Rainfall) $+ 4.57$ (Order) | 0.98 | 73.0 | 27.0 |
| **$\Sigma_{11}$ (mi)** | | | |
| % Veg. Cover    $\Sigma_{11} = -13.0 - 0.0393$ (% Veg. Cover) $+ 3.83$ (Order) | 0.96 | 11.3 | 88.7 |
| P-E Index    $\Sigma_{11} = -3.79 - 0.0252$ (P-E Index) $+ 2.84$ (Order) | 0.97 | 66.0 | 34.0 |
| M.S. Net Rainfall    $\Sigma_{11} = -12.4 - 0.477$ (M.S. Net Rainfall) $+ 2.61$ (Order) | 0.99 | 74.7 | 25.3 |
| **$A$ (mi$^2$)** | | | |
| % Veg. Cover | * | * | * |
| P-E Index    $A = -0.0563 - 0.0007$ (P-E Index) $+ 0.0634$ (Order) | 1.00 | 70.3 | 29.7 |
| M.S. Net Rainfall    $A = -0.294 - 0.0102$ (M.S. Net Rainfall) $+ 0.0635$ (Order) | 0.95 | 71.9 | 28.1 |
| **$F_1$ (Channels/mi$^2$)** | | | |
| % Veg. Cover    $F_1 = 4535 + 9.31$ (% Veg. Cover) $- 519$ (Order) | 0.81 | 28.5 | 71.5 |
| P-E Index    $F_1 = 1819 + 7.29$ (P-E Index) $- 235$ (Order) | 0.98 | 91.4 | 8.6 |
| M.S. Net Rainfall    $F_1 = 4365 + 120$ (M.S. Net Rainfall) $- 211$ (Order) | 0.91 | 93.4 | 6.6 |
| **$D_1$ (mi/mi$^2$)** | | | |
| % Veg. Cover    $D_1 = 53.4 - 0.0743$ (% Veg. Cover) $- 1.50$ (Order) | 0.74 | 76.0 | 24.0 |
| P-E Index    $D_1 = 40.6 + 0.0247$ (P-E Index) $- 0.577$ (Order) | 0.20 | 94.7 | 5.3 |
| M.S. Net Rainfall | * | * | * |
| **$D$ (mi/mi$^2$)** | | | |
| % Veg. Cover | * | * | * |
| P-E Index    $D = 88.9 + 0.0401$ (P-E Index) $- 4.60$ (Order) | 0.74 | 65.6 | 34.4 |
| M.S. Net Rainfall    $D = 106 - 0.226$ (M.S. Net Rainfall) $- 6.71$ (Order) | 0.65 | 25.5 | 74.5 |

*Correlation Coefficient is less than 0.10.

percentage of mean seasonal rainfall (Table 27). However, as the potential for vegetation increases, the density of channels increases. Most likely, the Browns Park Sandstone field sites did not provide for a sufficient range of climatic and vegetative conditions to determine correctly their influence on the network density variables.

Among the Mancos Shale drainage basins, the total length of stream channels and total length of first-order stream channels do not correlate well with the climatic or vegetative variables. They are related most strongly to basin relief. On the other hand, drainage-basin area is related directly to Thornthwaites P-E Index (Table 28). Also, the frequency and density of first-order channels and drainage density correlate very well directly with the percentage of mean seasonal rainfall (Figure 13) (Table 29). In addition, they are related inversely to elevation and, consequently, reflect mean annual temperature (Figure 9), potential evapotranspiration (Figure 10), precipitation (Figure 11) and net precipitation (Figure 12) and the potential for vegetation (Tables 28-31).

## Nonlinear Relationships

Some of the relationships described previously have better correlations when nonlinear curves are fitted to the

Table 27

The Effect of Vegetative Cover Variability on Drainage-Basin Morphology
For the Browns Park Sandstone-Inverse Relationships
-Symbols Defined in Appendix A

| | Regression Equation | $R^2$ | Sum of Squares | |
| --- | --- | --- | --- | --- |
| | | | Variable 1 (%) | Variable 2 (%) |
| **$\sum_1$ (mi)** | | | | |
| % M.S. Rainfall | $\sum_1$ = - 52.1 + 0.581 (% M.S. Rainfall) + 5.53 (Order) | 0.96 | 45.9 | 54.1 |
| M. Mo. T Range | $\sum_1$ = - 32.6 + 0.334 (M. Mo. T Range) + 4.90 (Order) | 0.93 | 67.9 | 32.1 |
| M. Mo. PPT Range | $\sum_1$ = -26.6 + 2.11 (M. Mo. PPT Range) + 6.61 (Order) | 0.85 | 19.0 | 81.0 |
| **$\sum_{11}$ (mi)** | | | | |
| % M.S. Rainfall | $\sum_{11}$ = - 29.4 + 0.315 (% M.S. Rainfall) + 3.28 (Order) | 0.94 | 43.6 | 56.4 |
| M. Mo. T Range | $\sum_{11}$ = - 19.7 + 0.217 (M. Mo. T Range) + 2.76 (Order) | 0.95 | 70.9 | 29.1 |
| M. Mo. PPT Range | $\sum_{11}$ = - 13.0 - 1.16 (M. Mo. PPT Range) + 3.76 (Order) | 0.84 | 23.3 | 76.7 |
| **A (mi²)** | | | | |
| % M.S. Rainfall | A = - 0.774 + 0.0092 (% M.S. Rainfall) + 0.0736 (Order) | 0.98 | 50.8 | 49.2 |
| M. Mo. T Range | A = - 0.435 + 0.0041 (M. Mo. T Range) + 0.0695 (Order) | 0.90 | 64.7 | 35.3 |
| M. Mo. PPT Range | A = -0.456 + 0.112 (M. Mo. PPT Range) + 0.0941 (Order) | 0.84 | 13.3 | 86.7 |
| **$F_1$ (Channels/mi²)** | | | | |
| % M.S. Rainfall | $F_1$ = 9472 - 96.5 (% M.S. Rainfall) - 351 (Order) | 0.90 | 75.2 | 24.8 |
| M. Mo. T Range | $F_1$ = 6113 - 50.9 (M. Mo. T Range) - 268 (Order) | 0.79 | 87.7 | 12.3 |
| M. Mo. PPT Range | * | * | * | * |
| **$D_1$ (mi/mi²)** | | | | |
| % M.S. Rainfall | $D_1$ = 79.9 - 0.605 (% M.S. Rainfall) - 0.494 (Order) | 0.85 | 97.5 | 2.5 |
| M. Mo. T Range | $D_1$ = 39.9 + 0.443 (M. Mo. T Range) - 3.67 (Order) | 0.64 | 16.2 | 83.8 |
| M. Mo. PPT Range | $D_1$ = 108 - 53 (M. Mo. PPT Range) - 3.84 (Order) | 1.00 | 47.8 | 52.2 |
| **D (mi/mi²)** | | | | |
| % M.S. Rainfall | D = 144 - 0.806 (% M.S. Rainfall) - 4.77 (Order) | 0.83 | 60.2 | 39.8 |
| M. Mo. T Range | * | * | * | * |
| M. Mo. PPT Range | * | * | * | * |

*Correlation Coefficient is less than 0.10.

Table 28

The Effect of Vegetative Cover Variability on Drainage-Basin Morphology
For the Mancos Shale—Direct Relationships
—Symbols Defined In Appendix A

| | Regression Equation | $R^2$ |
|---|---|---|
| **$\sum_1$ (mi)** | | |
| % Veg. Cover | $\sum_1 = 2.44 + 0.219$ (% Veg. Cover) | 0.23 |
| P-E Index | $\sum_1 = -2.40 + 0.0636$ (P-E Index) | 0.35 |
| M.S. Net Rainfall | $\sum_1 = 15.7 + 0.777$ (M.S. Net Rainfall) | 0.16 |
| **$\sum_{11}$ (mi)** | | |
| % Veg. Cover | $\sum_{11} = 1.33 + 0.132$ (% Veg. Cover) | 0.24 |
| P-E Index | $\sum_{11} = -1.48 + 0.0378$ (P-E Index) | 0.37 |
| M.S. Net Rainfall | $\sum_{11} = 9.33 + 0.469$ (M.S. Net Rainfall) | 0.17 |
| **A $(mi^2)$** | | |
| % Veg. Cover | $A = -0.0204 + 0.0050$ (% Veg. Cover) | 0.46 |
| P-E Index | $A = -0.112 + 0.0014$ (P-E Index) | 0.62 |
| M.S. Net Rainfall | $A = 0.294 + 0.0190$ (M.S. Net Rainfall) | 0.36 |
| **$F_1$ $(Channels/mi^2)$** | | |
| % Veg. Cover | $F_1 = 3939 - 63.2$ (% Veg. Cover) | 0.73 |
| P-E Index | $F_1 = 4606 - 14.4$ (P-E Index) | 0.70 |
| M.S. Net Rainfall | $F_1 = 18.6 - 236$ (M.S. Net Rainfall) | 0.57 |
| **$D_1$ $(mi/mi^2)$** | | |
| % Veg. Cover | $D_1 = 63.7 - 0.698$ (% Veg. Cover) | 0.65 |
| P-E Index | $D_1 = 73.1 - 0.170$ (P-E Index) | 0.71 |
| M.S. Net Rainfall | $D_1 = 14.3 - 3.32$ (M.S. Net Rainfall) | 0.81 |
| **D $(mi/mi^2)$** | | |
| % Veg. Cover | $D = 110 - 1.24$ (% Veg. Cover) | 0.65 |
| P-E Index | $D = 126 - 0.298$ (P-E Index) | 0.70 |
| M.S. Net Rainfall | $D = 21.7 - 5.96$ (M.S. Net Rainfall) | 0.84 |

TABLE 29

The Effect of Vegetative Cover Variability on Drainage-Basin Morphology
For the Mancos Shale - Inverse Relationships
-Symbols Defined in Appendix A

| | Regression Equation | $R^2$ |
|---|---|---|
| **$\Sigma_1$ (mi)** | | |
| % M.S. | | |
| Rainfall | $\Sigma_1 = 22.6 - 0.204$ (% M.S. Rainfall) | 0.20 |
| M.Mo.T Range | $\Sigma_1 = 17.8 - 0.188$ (M.Mo. T. Range) | 0.31 |
| M.Mo.PPT Range | $\Sigma_1 = 28.7 - 22.3$ (M.Mo. PPT Range) | 0.15 |
| **$\Sigma_{11}$ (mi)** | | |
| % M.S. | | |
| Rainfall | $\Sigma_{11} = 13.4 - 0.121$ (% M.S. Rainfall) | 0.21 |
| M.Mo.T Range | $\Sigma_{11} = 11.0 - 0.123$ (M.Mo.T Range) | 0.30 |
| M.Mo.PPT Range | $\Sigma_{11} = 17.1 - 13.4$ (M.Mo.PPT Range) | 0.16 |
| **A (mi²)** | | |
| % M.S. | | |
| Rainfall | $A = 0.470 - 0.0051$ (% M.S. Rainfall) | 0.47 |
| M.Mo.T Range | $A = 0.468 - 0.0073$ (M.Mo.T Range) | 0.19 |
| M.Mo.PPT Range | $A = 0.599 - 0.531$ (M.Mo. PPT Range) | 0.33 |
| **$F_1$ (Channels/mi²)** | | |
| % M.S. | | |
| Rainfall | $F_1 = -2274 + 64.7$ (% M.S. Rainfall) | 0.78 |
| M.Mo. T Range | $F_1 = -3749 + 125$ (M.Mo. T Range) | 0.33 |
| M.S. PPT Range | $F_1 = -3325 + 6079$ (M.Mo. PPT Range) | 0.44 |
| **$D_1$ (mi/mi²)** | | |
| % M.S. | | |
| Rainfall | $D_1 = -11.5 + 0.814$ (% M.S. Rainfall) | 0.89 |
| M.Mo. T. Range | $D_1 = -57.7 + 2.18$ (M.Mo. T Range) | 0.71 |
| M.S. PPT Range | $D_1 = -41.0 + 95.1$ (M.Mo. PPT Range) | 0.78 |
| **D (mi/mi²)** | | |
| % M.S. | | |
| Rainfall | $D = -23.2 + 1.44$ (% M.S. Rainfall) | 0.88 |
| M.Mo. T Range | $D = -112 + 4.00$ (M.Mo. T Range) | 0.77 |
| M.Mo.PPT Range | $D = -77.7 + 171$ (M.Mo. PPT Range) | 0.80 |

TABLE 30

The Effect of Temperature Variability on
Drainage-Basin Morphology For the Mancos Shale
—Symbols Defined in Appendix A

| | Regression Equation | $R^2$ |
|---|---|---|
| $\sum l$ (mi) | | |
| M.A.T | $\sum l = 61.2 - 1.25 \ (M.A.T.)$ | 0.23 |
| M.A. Pot.ET | $\sum l = 33.0 - 1.16 \ (M.A.Pot.ET)$ | 0.17 |
| $\sum l_1$ (mi) | | |
| M.A.T | $\sum l_1 = 36.5 - 0.745 \ (M.A.T.)$ | 0.25 |
| M.A.Pot.ET | $\sum l_1 = 19.7 - 0.697 \ (M.A.Pot.ET)$ | 0.19 |
| A (mi$^2$) | | |
| M.A.T | $A = 1.34 - 0.0288 \ (M.A.T)$ | 0.48 |
| M.A.Pot.ET | $A = 0.711 - 0.0280 \ (M.A.Pot.ET)$ | 0.39 |
| $F_1$ (Channels/mi$^2$) | | |
| M.A.T | $F_1 = -12073 + 337 \ (M.A.T)$ | 0.67 |
| M.A.Pot.ET | $F_1 = -5094 + 345 \ (M.A.Pot.ET)$ | 0.60 |
| $D_1$ (mi/mi$^2$) | | |
| M.A.T | $D_1 = -139 + 4.34 \ (M.A.T)$ | 0.81 |
| M.A.Pot.ET | $D_1 = -55.5 + 4.75 \ (M.A.Pot.ET)$ | 0.82 |
| D (mi/mi$^2$) | | |
| M.A.T | $D = -250 + 7.71 \ (M.A.T)$ | 0.81 |
| M.A.Pot.ET | $D = -103 + 8.50 \ (M.A. \ Pot.ET)$ | 0.84 |

3

103

## TABLE 31
### The Effect of Precipitation Variability on
### Drainage-Basin Morphology For the Mancos Shale
### —Symbols Defined in Appendix A

| | Regression Equation | $R^2$ |
|---|---|---|
| $\sum_1$ (mi) | | |
| M.A. PPT | $\sum_1 = -5.99 + 0.954$ (M.A. PPT) | 0.23 |
| M.A. Net PPT | $\sum_1 = 11.9 + 0.539$ (M.A. Net PPT) | 0.21 |
| $\sum_{1_1}$ (mi) | | |
| M.A. PPT | $\sum_{1_1} = -3.68 + 0.571$ (M.A. PPT) | 0.25 |
| M.A. Net PPT | $\sum_{1_1} = 7.01 + 0.323$ (M.A. Net PPT) | 0.22 |
| A (mi$^2$) | | |
| M.A. PPT | $A = -0.216 + 0.0221$ (M.A. PPT) | 0.48 |
| M.A. Net PPT | $A = 0.198 + 0.0127$ (M.A. Net PPT) | 0.44 |
| $F_1$ (Channels/mi$^2$) | | |
| M.A. PPT | $F_1 = 6114 - 259$ (M.A. PPT) | 0.68 |
| M.A. Net PPT | $F_1 = 1232 - 152$ (M.A. Net PPT) | 0.65 |
| $D_1$ (mi/mi$^2$) | | |
| M.A. PPT | $D_1 = 95.2 - 3.33$ (M.A. PPT) | 0.81 |
| M.A. Net PPT | $D_1 = 32.1 - 2.02$ (M.A. Net PPT) | 0.82 |
| D (mi/mi$^2$) | | |
| M.A. PPT | $D = 166 - 5.91$ (M.A. PPT) | 0.81 |
| M.A. Net PPT | $D = 53.7 - 3.59$ (M.A. Net PPT) | 0.83 |

data.  Both exponential (semilog) and power functions (log

log) were tried.  However, the curves of best fit are

approximately linear over the range of values studied.  In

addition, because of the small sample sizes, nonlinear

relationships were not considered in the data analysis.

## Conclusions

The drainage basins that formed on the resistant

Mesa Verde Sandstone are large, circular, and steep.  The

average basin relief and slope and channel gradient are

greater than for drainage basins of the other lithologies.

In addition, the Mesa Verde Sandstone basins have the

greatest channel length, but the least first-order channel

frequency and density and drainage density.  In the Mesa

Verde Sandstone, more area is needed to accumulate flow of

sufficient erosiveness to initiate a channel because of its

high infiltration capacity and permeability.

Conversely, the drainage basins which formed on the

poorly consolidated Browns Park Sandstone and the cohesive,

but impermeable Mancos Shale are small and gently sloping

with very fine textured stream networks.  Although total

channel length is less than on the Mesa Verde Sandstone, the

higher channel frequency and smaller basin area result in a

higher first-order channel density and drainage density.

Among the Mesa Verde Sandstone and Mancos Shale

drainage basins, channel gradient correlates well with basin

slope.  As basin slope increases, channel gradients become

steeper. On the other hand, the total length of channel and total length of first-order channels, are related directly to basin relief. Drainage-basin area, the frequency and density of first-order channels, and drainage density are determined largely by the climatic and vegetative variables. With greater available moisture and vegetative cover, basin area increases and the frequency and density of first order channels and drainage density decrease.

Among the Browns Park Sandstone field sites, the total length of channel, total length of first-order channels, drainage-basin area, and first-order channel frequency correlate strongly with the climatic and vegetative variables. In addition, the latter two correlate well with the relief ratio. With steeper topography and greater available moisture, channel length and frequency increase whereas the basin area decreases. The density of first-order channels correlates best with the percentage of mean seasonal rainfall. Channel gradient and drainage density have poor correlations with both the topographic and climatic variables.

CHAPTER 5

CONCLUSIONS

The development of coal resources throughout northwestern Colorado has had an impact on many stream networks. Changes in basin topography, including basin relief, slope, and shape, channel character, including channel gradient, width, and sinuosity, soil infiltration capacity and permeability, and vegetative type and cover can result from mining and reclamation. Consequently, if a mining company restores the pre-mining drainage contour, the stream system may not be in equilibrium with the new or future conditions. If the stream network is reclaimed with a drainage density that is too low, headcutting, gullying, and excessive erosion may result. On the other hand, if the stream network is reclaimed with a drainage density that is too high, money is wasted on the fashioning of excessive channel length. The operator needs to predict the effects of mining on the drainage-basin morphology and to incorporate them in the reclamation design.

Drainage-basin morphology is determined by lithology and climate and their effects on the amount and intensity of runoff. Lithology effects runoff intensity through infiltration rates and permeability. In addition, resistant lithologies form steeper drainage basins that

enable runoff to have greater potential energy. Climate effects runoff intensity directly through the amount and intensity of precipitation and inversely through vegetative growth. To predict the effects of mining on drainage network morphology, the regression equations determined in this study can be used to evaluate the variability in basin morphometry with changes in topography, climate, and vegetation for the three different rock types.

## The Effects of Increased Runoff Intensity

Mining and reclamation can result in an increase in runoff intensity if the disruption of native soils and substrate cause reduced infiltration and permeability, if the reclaimed topography has steeper basin relief or slope, or if the reclaimed vegetative cover is less than the premining cover. To illustrate the effects of increased runoff intensity on drainage development, hypothetical basins in the Mesa Verde Sandstone, Browns Park Sandstone, and Mancos Shale are reclaimed with 100 feet greater relief. The magnitudes of changes of channel length and frequency, basin area, and drainage density are calculated using the regression equations determined for the field sites earlier in the study (Table 32).

For all three lithologies, as basin relief increases, relief ratio increases (Equations 15, 44, 73). As indicated by the slopes of the regression equations, the rate of basin slope steepening is approximately the same for

Table 32
The Effect of Increasing Basin Relief by 100 feet and Vegetative Cover by 10%
on Drainage-Basin Morphology on each Lithology
—Symbols Defined in Appendix A

Mesa Verde Sandstone Field Sites

| | Increase R $\Delta R = +100$ ft | Increase Rr* $\Delta Rr = +0.02$ | Decrease Rc* $\Delta Rc = -0.01$ | Increase % Veg. Cover $\Delta\% $ Veg. Cover $= +10\%$ | Change in Morphologic Variable |
|---|---|---|---|---|---|
| S | (1) $S = 0.0517 + 0.0001(\Delta R)$ $\Delta S = +0.01$ ft/ft | (8) $S = 0.0131 + 0.774(\Delta Rr)$ $\Delta S = +0.02$ ft/ft | (16) $S = 0.0562 + 0.138(\Delta Rc)$ $\Delta S = -0.00$ ft/ft | ----- | $\Delta S = +0.03$ ft/ft |
| $\sum l$ | (2) $\sum l = 4.47 + 0.0090(\Delta R)$ $\Delta \sum l = +0.90$ mi | (9) $\sum l = 7.43 + 17.2(\Delta Rr)$ $\Delta \sum l = +0.34$ mi | (17) $\sum l = 20.1 - 18.1 (\Delta Rc)$ $\Delta \sum l = +0.18$ mi | (24) $\sum l = 2.13 + 0.318(\Delta\% $ Veg.Cover$)$ $\Delta \sum l = +3.18$ mi | $\Delta \sum l = +4.60$ mi |
| $\sum l_1$ | (3) $\sum l_1 = 2.91 + 0.0046(\Delta R)$ $\Delta \sum l_1 = +0.46$ mi | (10) $\sum l_1 = 4.86 + 6.05(\Delta Rr)$ $\Delta \sum l_1 = +0.12$ mi | (18) $\sum l_1 = 12.8 - 12.6(\Delta Rc)$ $\Delta \sum l_1 = +0.13$ mi | (25) $\sum l_1 = -0.747 + 0.170(\Delta\% $ Veg.Cover$)$ $\Delta \sum l_1 = +1.70$ mi | $\Delta \sum l_1 = +2.41$ mi |
| A | (4) $A = 0.0655 + 0.0002(\Delta R)$ $\Delta A = +0.02$ mi$^2$ | (11) $A = 0.0566 + 0.963(\Delta Rr)$ $\Delta A = +0.02$ mi$^2$ | (19) $A = 0.173 + 0.0581(\Delta Rc)$ $\Delta A = -0.00$ mi/mi$^2$ | (26) $A = -0.0652 + 0.0070(\Delta\% $ Veg.Cover$)$ $\Delta A = +0.07$ mi/mi$^2$ | $\Delta A = +0.11$ mi/mi$^2$ |
| $F_1$ | (5) $F_1 = 1870 - 0.960(\Delta R)$ $\Delta F_1 = -96.0$ Channels/mi$^2$ | (12) $F_1 = 2404 - 7340(\Delta Rr)$ $\Delta F_1 = -146.8$ Channels/mi$^2$ | (20) $F_1 = 2822 - 2819(\Delta Rc)$ $\Delta F_1 = +28.2$ Channels/mi$^2$ | (27) $F_1 = 2209 - 24.4(\Delta\% $ Veg.Cover$)$ $\Delta F_1 = -244.0$ Channels/mi$^2$ | $\Delta F_1 = -458.6$ Channels/mi |
| $D_1$ | (6) $D_1 = 42.2 - 0.0176(\Delta R)$ $\Delta D_1 = -1.8$ mi/mi$^2$ | (13) $D_1 = 53.6 - 145(\Delta Rr)$ $\Delta D_1 = -2.9$ mi/mi$^2$ | (21) $D_1 = 71.8 - 73.5(\Delta Rc)$ $\Delta D_1 = +0.7$ mi/mi$^2$ | (28) $D_1 = 46.4 - 0.395(\Delta\% $ Veg.Cover$)$ $\Delta D_1 = -4.0$ mi/mi$^2$ | $\Delta D_1 = -8.0$ mi/mi$^2$ |
| D | (7) $D = 67.7 - 0.0232(\Delta R)$ $\Delta D = -2.3$ mi/mi$^2$ | (14) $D = 84.4 - 202(\Delta Rr)$ $\Delta D = -4.0$ mi/mi$^2$ | (22) $D = 109 - 101(\Delta Rc)$ $\Delta D = +1.0$ mi/mi$^2$ | (29) $D = 73.4 - 0.525(\Delta\% $ Veg.Cover$)$ $\Delta D = -5.3$ mi/mi$^2$ | $\Delta D = -10.6$ mi/mi$^2$ |

(15) *$Rr = 0.0603 + 0.0002(\Delta R)$    (23) *$Rc = 0.586 - 0.0001(\Delta R)$
$\Delta Rr = +0.02$                          $\Delta Rc = -0.01$

Table 32 (Cont'd)

Browns Park Sandstone Field Sites

| | Increase R $\Delta R=+100$ ft | Increase Rr** $\Delta Rr=+0.02$ | Decrease Rc** $\Delta Rc=-0.07$ | Increase % Veg. Cover $\Delta$% Veg. Cover=+10% | Change in Morphologic Variable |
|---|---|---|---|---|---|
| s | (30) $s = 0.197 + 0.0001(\Delta R)$ $-0.0198(u)$ $\Delta S = +0.01$ ft/ft | (37) * | (45) $s = 0.314 - 0.176(\Delta Rc)$ $-0.0201(u)$ $\Delta S = +0.01$ ft/ft | ———— | $\Delta S = +0.02$ ft/ft |
| $\sum l$ | (31) * | (38) $\sum l = -11.2 - 24.8(\Delta Rr)$ $+4.49(u)$ $\Delta \sum l = -0.50$ mi | (46) * | (53) * | $\Delta \sum l = -0.50$ mi |
| $\sum l_1$ | (32) * | (39) $\sum l_1 = -5.95 - 15.8(\Delta Rr)$ $+2.52(u)$ $\Delta \sum l_1 = -0.32$ mi | (47) * | (54) $\sum l_1 = -13.0 - 0.0393$ $(\Delta$% Veg.Cover)$+3.83(u)$ $\Delta \sum l_1 = -0.39$ mi | $\Delta \sum l_1 = -0.71$ mi |
| A | (33) * | (40) $A = -0.170 - 0.311(\Delta Rr)$ $+0.063(u)$ $\Delta A = -0.01$ mi$^2$ | (48) * | (55) * | $\Delta A = -0.01$ mi$^2$ |
| $F_1$ | (34) * | (41) $F_1 = 2834 + 3815(\Delta Rr)$ $-202(u)$ $\Delta F_1 = +76.3$ Channels/mi$^2$ | (49) * | (56) $F_1 = 4535 + 9.31$ $(\Delta$% Veg.Cover) $-519(u)$ $\Delta F_1 = +93.1$ Channels/mi$^2$ | $\Delta F_1 = +169.4$ Channels/mi$^2$ |
| $D_1$ | (35) $D_1 = 49.0 - 0.0061(\Delta R)$ $-0.682(u)$ $\Delta D_1 = -0.6$ mi/mi | (42) * | (50) $D_1 = 424 + 10.5(\Delta Rc)$ $-0.806(u)$ $\Delta D_1 = -0.8$ mi/mi$^2$ | (57) $D_1 = 53.4 - 0.0743$ $(\Delta$% Veg.Cover) $-1.50(u)$ $\Delta D_1 = -0.7$ mi/mi$^2$ | $\Delta D_1 = -2.1$ mi/mi$^2$ |
| D | (36) $D = 104 - 0.0046(\Delta R)$ $-5.50(u)$ $\Delta D = -0.5$ mi/mi | (43) $D = 115 - 16.9(\Delta Rr)$ $-7.54(u)$ $\Delta D = -0.3$ mi/mi$^2$ | (51) $D = 98.5 + 8.76(\Delta Rc)$ $-5.54(u)$ $\Delta D = -0.6$ mi/mi$^2$ | (58) * | $\Delta D = -1.4$ mi/mi$^2$ |

(44) **Rr $= 0.587 + 0.0002(\Delta R)$ $-0.109(u)$ $\Delta Rr = +0.02$

(52) **Rc $= 0.604 - 0.0007(\Delta R)$ $+0.0257(u)$ $\Delta Rc = -0.07$

*Correlation Coefficient is less than 0.10.

Table 32 (Cont'd)

Mancos Shale Field Sites

| | Increase R $\Delta R = +100$ ft | Increase Rr* $\Delta Rr = +0.02$ | Decrease Rc* $\Delta Rc = -0.01$ | Increase % Veg. Cover $\Delta$% Veg. Cover $= +10$% | Change in Morphologic Variable |
|---|---|---|---|---|---|
| S | (59) $S = 0.0446 + 0.0002(\Delta R)$ $\Delta S = +0.02$ ft/ft | (66) $S = -0.0071 + 0.998(\Delta Rr)$ $\Delta S = +0.02$ ft/ft | (74) $S = -0.0978 + 0.365(\Delta Rc)$ $\Delta S = +0.00$ ft/ft | ---------- | $\Delta S = +0.04$ ft/ft |
| $\Sigma l$ | (60) $\Sigma l = 4.52 + 0.0136(\Delta R)$ $\Delta \Sigma l = +1.36$ mi | (67) $\Sigma l = 9.22 - 0.341(\Delta Rr)$ $\Delta \Sigma l = 0.01$ mi | (75) $\Sigma l = 26.9 - 32.7(\Delta Rc)$ $\Delta \Sigma l = +0.00$ mi | (82) $\Sigma l = 2.44 + 0.219(\Delta$% Veg.Cover) $\Delta \Sigma l = +2.19$ mi | $\Delta \Sigma l = +3.54$ mi |
| $\Sigma l_1$ | (61) $\Sigma l_1 = 2.61 + 0.0081(\Delta R)$ $\Delta \Sigma l_1 = +0.81$ mi | (68) $\Sigma l_1 = 5.24 + 1.43(\Delta Rr)$ $\Delta \Sigma l_1 = +0.03$ mi | (76) $\Sigma l_1 = 15.3 - 18.4(\Delta Rc)$ $\Delta \Sigma l_1 = -0.00$ mi | (83) $\Sigma l_1 = 1.33 + 0.132(\Delta$% Veg.Cover) $\Delta \Sigma l_1 = +1.32$ mi | $\Delta \Sigma l_1 = +2.16$ mi |
| A | (62) $A = 0.0570 + 0.0002(\Delta R)$ $\Delta A = +0.02$ mi² | (69) $A = 0.125 + 0.0930(\Delta Rr)$ $\Delta A = +0.00$ mi² | (77) $A = 0.340 - 0.379(\Delta Rc)$ $\Delta A = +0.00$ mi² | (84) $A = -0.0204 + 0.0050(\Delta$% Veg.Cover) $\Delta A = +0.05$ mi² | $\Delta A = +0.07$ mi² |
| $F_1$ | (63) $F_1 = 2543 - 1.59(\Delta R)$ $\Delta F_1 = -159.0$ Channels/mi² | (70) $F_1 = 2570 - 5365(\Delta Rr)$ $\Delta F_1 = -107.3$ Channels/mi² | (78) $F_1 = 3440 - 2671(\Delta Rc)$ $\Delta F_1 = +0.0$ Channels/mi² | (85) $F_1 = 3939 - 63.2(\Delta$% Veg.Cover) $\Delta F_1 = -632.0$ Channels/mi² | $\Delta F_1 = -898.3$ Channels/mi² |
| $D_1$ | (64) $D_1 = 47.0 - 0.0140(\Delta R)$ $\Delta D_1 = -1.4$ mi/mi² | (71) $D_1 = 48.2 - 55.8(\Delta Rr)$ $\Delta D_1 = -1.1$ mi/mi² | (79) $D_1 = 60.3 - 33.4(\Delta Rc)$ $\Delta D_1 = +0.0$ mi/mi² | (86) $D_1 = 63.7 - 0.698(\Delta$% Veg.Cover) $\Delta D_1 = -7.0$ mi/mi² | $\Delta D_1 = -9.5$ mi/mi² |
| D | (65) $D = 80.3 - 0.0250(\Delta R)$ $\Delta D = -2.5$ mi/mi² | (72) $D = 84.1 - 116(\Delta Rr)$ $\Delta D = -2.3$ mi/mi² (73) $*Rr = 0.0551 + 0.0002(\Delta R)$ $\Delta Rr = +0.02$ | (80) $D = 110 - 69.9(\Delta Rc)$ $\Delta D = +0.0$ mi/mi² (81) $*Rc = 0.528 - 0.000(\Delta R)$ $\Delta *Rc = -0.00$ | (87) $D = 110 - 1.24(\Delta$% Veg.Cover) $\Delta D = -12.4$ mi/mi² | $\Delta D = -17.2$ mi/mi² |

the Mesa Verde Sandstone, Browns Park Sandstone, and Mancos Shale. As basin relief and slope increase, channel gradients also become steeper (Equations 1, 8, 30, 59, 66).

The higher gradients and steeper topography cause runoff to have greater potential energy. This increase in runoff intensity results in the development of more elongated and parallel streams and, therefore, narrower drainage basins (Equations 23, 52, 81). In the Mesa Verde Sandstone drainage basins, channel lengthening is approximately equal among the first-order and higher order channels (Equations 2, 3, 9, 10). Conversely, in the Mancos Shale drainage basins, lengthening is predominantly among the first-order tributaries (Equations 60, 61, 67, 68).

Although more circular basins have a characteristic dendritic drainage pattern with less runoff being concentrated into a single channel, elongated basins often have many small order streams draining into a large low gradient trunk stream. With decreasing basin circularity, drainages on the Mesa Verde Sandstone increase their total channel length, primarily, through the elongation and formation of new first-order channels (Equations 17, 18).

Among all of the basins, the density of first-order channels and drainage density are inversely related to basin relief and slope (Equations 6, 7, 13, 14, 35, 36, 43, 64, 65, 71, 72). This result disagrees with other geomorphologists' observations that steep watersheds are subject to more intense rates of erosion and develop finer

networks than basins of low relief (Strahler, 1956; Schumm, 1956; Chorley and Morgan, 1962). However, in this study, steeper topography is directly correlated with elevation. Consequently, the decrease in network density reflects the increase of vegetative cover not the changes in topography.

In summary, if mining results in an increase in runoff intensity, the mine operator can expect the development of more elongate and parallel streams and, therefore, narrower drainage basins. Channel length may increase, primarily, through the elongation and formation of new first-order tributatries, as well as, lengthening among the higher order channels. More intense rates of erosion also may cause drainage density to increase.

**The Effects of Decreased Runoff Intensity**

Mining and reclamation also can result in decreased runoff intensity. Increased infiltration and permeability of reclaimed spoils, gentler post-mining topography, or enhanced vegetative cover will lower the amount and intensity of runoff. To illustrate the effects of decreased runoff intenstity on drainage development, the hypothetical basins in the Mesa Verde Sandstone, Browns Park Sandstone, and Mancos Shale are reclaimed with ten percent greater vegetative cover. Again, the magnitudes of changes in the morphologic variables are calculated using the regression equations determined for the field sites earlier in the study (Table 32).

Increasing mean annual precipitation and net
precipitation and decreasing mean annual temperature and
potential evapotranspiration are associated with greater
vegetative cover. Vegetation modifies runoff intensity and
increases surface resistance. The ability of vegetation to
inhibit channel formation and elongation causes the total
length of first-order channels, among the Browns Park
Sandstone basins, to decrease with increasing vegetative
cover (Equation 54). Similarly, among the Mesa Verde
Sandstone and Mancos Shale basins, greater vegetative cover
enables greater drainage-basin area (Equations 26, 84) and
causes the frequency and density of first-order channels and
drainage density to decrease (Equations 27, 28, 29, 85, 86,
87). As indicated by the rates of the regression equations,
the increase in vegetative cover is more effective on the
Mancos Shale. Among the Browns Park Sandstone basins,
drainage density has a poor relationship with vegetative
cover (Equation 58). Most likely, the range of climatic and
vegetative conditions among the Browns Park Sandstone field
sites was inadequate to determine their relationships with
drainage density.

Among the Mesa Verde Sandstone and Mancos Shale
field sites, vegetative cover is sufficiently dense to cause
a decrease in drainage density with increasing precipitation
and decreasing temperature (Figures 9-13). This result
agrees with the previously described relationships between
drainage density and the climatic zones of the United

States. Over the range of mean annual precipitation studied, 9.34 to 22.73 inches, and at 50°F mean annual temperature, Schumm (1965) found drainage density increased, peaked and then decreased (Figure 2). The peak corresponds to a transition in vegetation from desert shrubs to grass. Among the field sites, mean annual temperatures are less than 50°F and, consequently, the transition in vegetation probably occurs at a lower mean annual precipitation. Therefore, only an inverse relationship between drainage density and mean annual precipitation is observed (Tables 22, 31).

In summary, if mining results in a decrease in runoff intensity, the mine operator can expect the development of larger drainage basins with shorter and fewer stream channels. In addition, the total drainage density and the density of first-order channels of the post-mining stream network may be less than for the premining network.

## Combined Effects of Change

The total effects of increased runoff intensity (R, Rr, Rc) and decreased runoff intensity (% Veg. Cover) are presented in the last column of Table 32 for the three lithologies. On the Mesa Verde Sandstone and Mancos Shale, channel length and drainage area increase. Although the channel lengthening is primarily among the first-order tributaries, the frequency of first-order channels decreases substantially. The significant increase in drainage area

results in a decrease in the density of first-order channels and drainage density. On the Browns Park Sandstone, channel length and drainage area decrease slightly and the frequency of first-order channels and drainage density also decrease slightly.

## Limitations of the Method

In addition to compensating for changes in landscape and vegetation, as presented in this study, the mine operator needs to account for changes in infiltration capacity, permeability, and erodibility of the native soil and substrate caused by mining. Also, when headwater bedrock-controlled tributaries are replaced by drainages incised into unconsolidated spoils, channel hydraulics must be adjusted in cooperation with changes in the post-mining drainage-basin morphology.

The study focuses only on small ephemeral stream systems for which snow melt is very important to the drainage development and vegetative cover. Also, the small sample sizes detract from the statistical analysis and cause, in the case of the Browns Park Standstone basins, unrealistic relationships.

Finally, the method is limited by the inherent instability of semiarid landscapes. In semiarid regions, drainage systems erode and aggrade in response to the dynamic nature of their environment. No reclamation methodology can result in the design of a stream system which will be static over the long term.

# LITERATURE CITED

Abrahams, A. D., 1972, Drainage Densities and Sediment
     Yields in Eastern Australia:  Australian Geog.
     Studies, V. 10, pp. 19-41.

Baker, F. S., 1944, Mountain Climates of the Western United
     States:  Ecol. Monographs, V. 14, pp. 233-254.

Bass, N. W., Eby, J. B., and Campbell, M. R., 1955, Geology
     and Mineral Fuels of Parts of Routt and Moffat
     Counties, Colorado:  U.S. Geol. Survey Bull. 1027-D,
     pp. 143-250.

Bennett, O. L., Doss, B. D., Ashley, D. A., Kilmer, V. J.,
     and Richardson, E. C., 1964, Effects of Soil Moisture
     Regime on Yield, Nutrient Content, and Evapotranspira-
     tion for Three Annual Forage Species:  Agronomy
     Journal, V. 56, pp. 195-198.

Buffler, R. T., 1967, The Browns Park Formation and Its
     Relationship to the Late Tertiary Geologic History of
     the Elkhead Region, Northwestern Colorado - South
     Central Wyoming:  Ph.D., University of California,
     Berkeley, California, 175 pages.

Carlston, C. W., 1963, Drainage Density and Streamflow:
     U.S. Geol. Survey Prof. Paper 442-C, pp. 1-8.

Carlston, C. W., 1966, The Effect of Climate on Drainage
     Density and Stream Flow:  Bull. Int. Assoc. of
     Scientific Hydrol., V. 12, pp. 62-69.

Chorley, R. J., 1957, Climate and Morphometry:  Journal of
     Geol., V. 65, pp. 628-638.

Chorley, R. J., and Morgan, M. A., 1962, Comparison of
     Morphometric Features, Unaka Mountains, Tennessee and
     North Carolina and Dartmoor, England:  Geol. Society
     of America Bull., V. 73, pp. 17-34.

Eccker, S. L., 1984, The Effect of Lithology and Climate on
     the Morphology of Drainage Basins in Northwestern
     Colorado - Appendix B:  M.S., Colorado State
     University, Fort Collins, Colorado, 169 pages.

Fisher, D. J., Erdmann, C. E., Reeside, J. B., Jr., 1896, Cretaceous and Tertiary Formations of the Book Cliffs, Carbon, Emery, and Grand Counties, Utah and Garfield and Mesa Counties, Colorado: U.S. Geol. Survey Prof. Paper 332, pp. 1-80.

Fok, Y., 1971, Law of Stream Relief in Horton's Stream Morphological System: Water Resources Research, V. 7, pp. 201-203.

Gifford, G. F., 1982, Rainfall Simulator Studies - 1981: Amax Belle Ayr Permit to Mine Application, Wyoming Dept. of Envir. Quality Land Quality Division, Cheyenne, Wyoming, 18 pages.

Gregory, K. J., 1976, Drainage Networks and Climate in: E. Derbyshire's Geomorphology and Climate, John Wiley and Sons, New York, Ch. 10, pp. 289-314.

Gregory, K. J., and Gardiner, V., 1974, Drainage Density and Climate: Zeitschrift Fur Geomorphologie, V. 19, pp. 287-298.

Gregory, K. J., and Walling, D. E., 1968, The Variation of Drainage Density Within a Catchment: Bull. Int. Assoc. of Scientific Hydrol., V. 13, pp. 61-68.

Gregory, K. J., and Walling, D. E., 1973: Drainage Basin Form and Process, John Wiley and Sons, New York, 458 pages.

Hamon, W. R., 1963, Estimating Potential Evapo-transpiration: American Society of Civil Engineers Trans., Paper No. 3415, V. 128, Part I, pp. 324-342.

Hansen, W. R., 1975, The Geologic Story of the Uinta Mountains: U.S. Geol. Survey Bull. 1291, 144 pages.

Heil, R. D., 1976, Characterization Studies of Major Soils Found in Proposed Oil Shale and Coal Development Areas of Northwestern Colorado: EMRIA Report No. 23, U.S. Dept. of Agric. Bureau of Land Management, Colorado State University, Fort Collins, Colorado, 220 pages.

Heil, R. D., Romine, D. S., Moreland, D. C., Dansdill, R. K., Montgomery, R. H., and Cipra, J. E., 1977, Soils of Colorado: Colorado State University Experiment Station, Fort Collins, Colorado Bull. 566S, 40 pages.

Henry, A. J., 1919, Increase of Precipitation with Altitude: Monthly Weather Review, V. 47, pp. 33-41.

Horton, R. E., 1945, Erosional Development of Streams and their Drainage Basins; Hydrophysical Approach to Quantitative Morphology: U.S. Geol. Survey Bull., V. 56, pp. 275-370.

Katiyar, V. S., 1982, Rainfall and Runoff Relationships in a Small Himalayan Watershed: Ph.D., Colorado State University, Fort Collins, Colorado, 106 pages.

Kohler, M. A., 1958, Meteorological Aspects of Evaporation Phenomena: Trans. Int. Assoc. of Science and Hydrol., V. III, pp. 421-436.

Langbein, W. B., and Schumm, S. A., 1958, Yield of Sediment in Relation to Mean Annual Precipitation: Trans. American Geophys. Un., V. 39, pp. 1077-1084.

Leopold, L. B., 1951, Rainfall Frequency: An Aspect of Climatic Variation: Trans. American Geophys. Un., V. 32, pp. 347-357.

Lillesand, T. M., and Diefer, R. W., 1979: Remote Sensing and Image Interpretation, John Wiley and Sons, New York, 612 pages.

Marlatt, W. E., 1971, Environmental Inventory of a Portion of Piceance Basin in Rio Blanco County, Colorado: Colorado State University Environmental Research Center, Fort Collins, Colorado, Ch. VI, pp. 1-14.

Maxwell, J. C., 1961, Quantitative Geomorphology of the San Dimas Experimental Forest, California: Ph.D., Columbia University, New York, New York, 114 pages.

McGinnies, W. G., Parker, K. W., and Glendening, G. E., 1944: Southwestern Range Ecology, Colorado State University Library, Fort Collins, Colorado, 211 pages.

Melton, M. A., 1957, An Analysis of the Relations Among Elements of Climate, Surface Properties and Geomorphology: Office of Naval Research Project NR 389-042, Technical Report No. 11, Columbia University, New York, 40 pages.

Melton, M. A., 1958, Correlation Structure of Morphometric Properties of Drainage Systems and their Controlling Agents: Journal of Geol., V. 66, pp. 442-460.

Miller, V. C., 1953, A Quantitative Geomorphic Study of Drainage Basin Characteristics in the Clinch Mountain Area Virginia and Tennessee: Technical Report No. 3, Columbia University, New York, 65 pages.

Morgan, R. P., 1976, The Role of Climate in the Denudation
    System: A Case Study from West Malaysia in:
    E. Derbyshire's Geomorphology and Climate, John Wiley
    and Sons, New York, Ch. 11, pp. 317-343.

Morisawa, M. E., 1959, Relation of Quantitative
    Geomorphology to Stream Flow in Representative
    Watersheds of the Appalachian Plateau Province:
    Office of Naval Research Project NR 389-042, Technical
    Report No. 20, Columbia University, New York,
    18 pages.

Reeside, J. B., Jr., 1924, Upper Cretaceous and Tertiary
    Formations of the Western Part of the San Juan Basin
    of Colorado and New Mexico: U.S. Geol. Survey Prof.
    Paper 134, pp. 1-70.

Richter, B. D., 1982, Precipitation Analysis for the
    Piceance Basin, Northwestern Colorado: M.S., Colorado
    State University, Fort Collins, Colorado, 178 pages.

Robbins, W. W., 1917, Native Vegetation and Climate of
    Colorado in their Relation to Agriculture: Colorado
    Agric. Experiment Station Bull. 224, pp. 1-56.

Rosenberg, N. J., 1974: Microclimate the Biological
    Environment, John Wiley and Sons, New York, p. 159.

Russler, B. H. and Spreen, W. C., 1947, Topographically
    Adjusted Normal Isohyetal Maps for Western Colorado:
    U.S. Weather Bureau Technical Paper No. 4, 27 pages.

Schumm, S. A., 1956, Evolution of Drainage Systems at Perth
    Amboy, New Jersey: Geol. Society of America Bull.,
    V. 67, pp. 597-646.

Schumm, S. A., 1961, The Effect of Sediment Characteristics
    on Erosion and Deposition in Ephemeral Stream
    Channels: U.S. Geol. Survey Prof. Paper 352C, pp. 31-
    70.

Schumm, S. A., 1965, Quaternary Paleohydrology in: The
    Quaternary of the United States, ed. H. E. Wright and
    D. G. Frey, Princeton University Press, Princeton, New
    Jersey, pp. 783-794.

Schumm, S. A., 1975, Geomorphic Implications of Climatic
    Changes in: Introduction to Fluvial Processes, ed.
    R. J. Chorley, Methuen and Co., Ltd., Bungay, Suffolk,
    pp. 202-211.

Sears, J. D., Hunt, C. B., and Hendricks, T. A., 1941,
    Transgressive and Regressive Cretaceous Deposits in
    Southern San Juan Basin, New Mexico: U.S. Geol.
    Survey Prof. Paper 193-F, pp. 101-121.

Seginer, I., 1966, Gully Development and Sediment Yield: Journal of Hydrol., V. 4, pp. 236-253.

Siemer, E. G., and Heermann, D. F., 1970, Climatological Data for Gunnison Colorado and the Mountain Meadow Research Ranch: Colorado State University Experiment Station, Report No. 850, pp. 1-16.

Smith, G. E., 1930, Notes on Rainfall and Evaporation: Monthly Weather Review, V. 58, pp. 253-254.

Sotiriadis, L., and Astaras, Th., 1977, A Comparison of Drainage Densities as Computed from Topographic Maps, Aerial Photographs, and Field Survey: Annales Géologiques Des Pays Hélleniques, V. 28, pp. 145-159.

Steele, T. D., Bauer, D. P., Wentz, D. A., and Warner, J. W., 1979, The Yampa River Basin, Colorado and Wyoming -- A Preview to Expanded Coal-Resource Development and its Impacts on Regional Water Resources: U.S. Geol. Survey Water Resource Investigations 78-126, 133 pages.

Stoddart, D. R., 1969, Climatic Geomorphology: Review and Reassessment: Progress in Geol., V. 1, pp. 159-222.

Strahler, A. N., 1952, Hypsometric (Area-Altitude) Analysis of Erosional Topography: American Geol. Society Bull., V. 63, pp. 1117-1142.

Strahler, A. N., 1956, The Nature of Induced Erosion and Aggradation in: W. L. Thomas' Man's Role in Changing the Face of the Earth, University of Chicago Press, Chicago, Illinois, pp. 621-638.

Tew, R. K., 1969, Water Use, Adaptability and Chemical Composition of Grasses Seeded at High Elevations: Journal of Range Management, V. 22, pp. 280-283.

Thornthwaite, C. W., 1931, The Climates of North America According to a New Classification: Geog. Review, V. 21, pp. 633-655.

Tiedeman, J. A., 1978, Phyto-Edaphic Classification of the Piceance Basin: Ph.D., Colorado State University, Fort Collins, Colorado, 281 pages.

Tweto, O., 1975, Preliminary Geologic Map of East Half of Vernal 1° by 2° Quadrangle, Colorado: U.S. Geol. Survey Open-File Report 75-588, Scale 1:250,000, 8 pages, 1 pl.

Tweto, O., 1976, Geologic Map of Craig 1° by 2° Quadrangle, Northwestern Colorado: U.S. Geol. Survey Misc. Investigations Series Map MI-972, Scale 1:250,000, 1 pl.

U.S. Dept. of the Interior, 1977, Supplement to the Northwest Colorado Coal Regional Environmental Statement FES 77-1, Ch. 2, pp. 2-63.

Welder, G. E., and McGreevey L. J., 1966, Groundwater Reconnaissance of the Great Divide and Washakie Basins and Some Adjacent Areas, Southwestern Wyoming: U.S. Geol. Survey Hydrol. Investigations Atlas HA-219, 10 pages., 3 Sheets.

Wilson, W. T., 1954, Analysis of Winter Precipitation Observations in the Cooperative Snow Investigations: Monthly Weather Review, V. 82, pp. 183-199.

Wilson, L., 1971, Drainage Density, Length Ratios, and Lithology in a Glaciated Area of Southern Connecticut: Geol. Society of America Bull. V. 82, pp. 2955-2956.

Wymore, I. F., 1974, Water Requirements for Stabilization of Spent Shale: Ph.D., Colorado State University, Fort Collins, Colorado, 137 pages.

# APPENDIX A

## LEGEND FOR TABLES

A               Drainage Basin Area ($mi^2$).

$\alpha$        Level of Significance of the Test.

$A_c$           Area of a Circle with the Same Perimeter as the Drainage Basin.

D               Drainage Density:

$$D = \frac{\Sigma l}{A} \quad (mi/mi^2) \quad (Horton, 1945).$$

$D_1$           Density of First Order Stream Channels:

$$D_1 = \frac{\Sigma l_1}{A} \quad (mi/mi^2) \quad (Melton, 1957).$$

d               Longest Dimension of the Drainage Basin Parallel to the Principle Drainage Line (ft).

F               Stream Channel Frequency:

$$F = \frac{N}{A} \quad (Channels/mi^2) \quad (Horton, 1945).$$

$F_1$           Frequency of First-Order Stream Channels:

$$F_1 = \frac{N_1}{A} \quad (Channels/mi^2) \quad (Melton, 1957).$$

$\Sigma l$      Total Length of Stream Channel (mi).

$\Sigma l_1$    Total Length of First-Order Stream Channel (mi).

122

$\dfrac{\sum l_1}{\sum l_{2-5}}$ — Ratio of First-Order Stream Channel Length to Higher Order Stream Channel Length.

M — M = % Silt-Clay in Channel Bed Samples x
$$M = \frac{\text{\% Silt-Clay in Channel Bed Samples x Channel Width + \% Silt-Clay in Channel Bank Samples x (2)Channel Depth}}{\text{Channel Width x (2)Channel Depth}}$$

(Schumm, 1961).

M.A. Pot. ET — Mean Annual Potential Evapotranspiration (in).

M.A. Net PPT — Mean Annual Net Precipitation:

M.A. Net PPT = M.A. PPT - M.A. Pot. ET (in).

M.A. PPT — Mean Annual Precipitation (in).

M.A. T — Mean Annual Temperature (°).

M.Mo. PPT Range — Mean Monthly Precipitation Range (in).

M.Mo. T Range — Mean Monthly Temperature Range (°).

M.S. Pot. ET — Mean Seasonal Potential Evapotranspiration (in).

M.S. Net Rainfall — Mean Seasonal Net Precipitation Falling as Rain:

M.S. Net Rainfall = M.S. Rainfall - M.S. Pot. ET (in).

M.S. Rainfall — Mean Seasonal Precipitation Falling as Rain (in).

$N_1$ — Number of First-Order Stream Channels Within the Drainage Basin.

P-E Index      Thornthwaite's Precipitation Effectiveness Index:

$$I = 10 \sum_{12} \frac{P}{E}$$

(Thornthwaite, 1931).

% M.S. Rainfall      Percent of Mean Seasonal Precipitation Falling as Rain.

% Veg. Cover      Percent of Drainage Basin Covered by Crown Cover of Foliage.

R      Total Basin Relief (ft).

$R^2$      Correlation Coefficient.

$R_c$      Drainage Basin Circularity:

$$Rc = \frac{A}{A_c} \quad \text{(Miller, 1953).}$$

$R_r$      Relief Ratio:

$$Rr = \frac{R}{d} \quad \text{(Schumm, 1956).}$$

S      Stream Channel Gradient (ft/ft).

u      Stream Channel Order

(Horton, 1945 and Strahler, 1952).